May, 2008

Branching Ratios and Polarization in $B \to VV, VA, AA$ Decays

Hai-Yang Cheng[1] **and Kwei-Chou Yang**[2]

[1] Institute of Physics, Academia Sinica
Taipei, Taiwan 115, Republic of China

[2] Department of Physics, Chung Yuan Christian University
Chung-Li, Taiwan 320, Republic of China

Abstract

We present a detailed study of charmless two-body B decays into final states involving two vector mesons (VV) or two axial-vector mesons (AA) or one vector and one axial-vector meson (VA), within the framework of QCD factorization, where A is either a $^3P_1$ or $^1P_1$ axial-vector meson. The main results are as follows. (i) In the presence of NLO nonfactorizable corrections, effective Wilson coefficients a_i^h are helicity dependent. For some penguin-dominated modes, the constructive (destructive) interference in the negative-helicity (longitudinal-helicity) amplitude of the $\overline{B} \to VV$ decay will render the former comparable to the latter and push up the transverse polarization. (ii) In QCD factorization, the transverse polarization fraction can be large for penguin-dominated charmless VV modes by allowing for sizable penguin annihilation contributions. (iii) Using the measured $\bar{K}^{*0}\rho^-$ channel as an input, we predict the branching ratios and polarization fractions for other $\overline{B} \to \bar{K}^*\rho$ decays. (iv) The smallness of the axial-vector decay constant of the $^1P_1$ axial vector meson can be tested by measuring various $b_1\rho$ modes to see if $\Gamma(\overline{B}^0 \to b_1^-\rho^+) \ll \Gamma(\overline{B}^0 \to b_1^+\rho^-)$ and $\Gamma(B^- \to b_1^-\rho^0) \ll \Gamma(B^- \to b_1^0\rho^-)$. (v) For the penguin-dominated modes a_1K^* and b_1K^*, it is found that the former are dominated by transverse polarization amplitudes, whereas the latter are governed by longitudinal polarization states. (vi) The rates of $B \to K_1(1270)K^*$ and $K_1(1400)K^*$ are generally very small. The decay modes $K_1^-K^{*+}$ and $K_1^+K^{*-}$ are of particular interest as they are the only AV modes which receive contributions solely from weak annihilation. (vii) For tree-dominated $B \to AA$ decays, the $a_1^+a_1^-$, $a_1^-a_1^0$, $a_1^-b_1^+$, $a_1^-b_1^0$, $b_1^+\rho^-$ and $b_1^0\rho^-$ modes have sizable branching ratios, of order $(20 \sim 40) \times 10^{-6}$. (viii) There are many penguin-dominated $B \to AA$ decays within the reach of B factories: $K_1(1270)(a_1, b_1^\pm)$, $K_1(1400)(b_1, a_1^\pm)$, $K_1(1270)(f_1(1285), f_1(1420))$ and $K_1(1400)(f_1(1420), h_1(1170))$.

I. INTRODUCTION

Recently we have studied the charmless two-body B decays involving an axial-vector meson A and a pseudoscalar meson P in the final state [1, 2]. There are two distinct types of axial-vector mesons, namely, ${}^3P_1$ and ${}^1P_1$. We have studied their light-cone distribution amplitudes using the QCD sum rule method. Owing to the G-parity, the chiral-even two-parton light-cone distribution amplitudes of the ${}^3P_1$ (${}^1P_1$) mesons are symmetric (antisymmetric) under the exchange of quark and anti-quark momentum fractions in the SU(3) limit. For chiral-odd light-cone distribution amplitudes, it is the other way around. In this work, we will generalize our previous study to charmless VA and AA modes. Moreover, we will use this chance to re-examine $B \to VV$ decays.

The charmless decays $B \to VV, VA, AA$ are expected to have rich physics as they have three polarization states. Through polarization studies, these channels can shed light on the underlying helicity structure of the decay mechanism. Experimentally, $B \to K^*\phi$ decays have been studied with full angular analysis and hence can provide information on polarization fractions and relative strong phases among various helicity amplitudes. Historically, it was the observation of large transverse polarization in $B \to K^*\phi$ decays that had triggered a burst of theoretical and experimental interest in the study of charmless $B \to VV$ decays. BaBar and Belle have observed that $f_L \sim 1/2$ and $f_\parallel \sim f_\perp \sim 1/4$ in the $K^*\phi$ channels [3, 4], where $f_L, f_\perp$ and $f_\parallel$ are the longitudinal, perpendicular, and parallel polarization fractions, respectively. The transverse polarization fraction $f_T = f_\parallel + f_\perp \sim 1/2$ is found to be of the same order magnitude as the longitudinal one f_L in the penguin-dominated $K^*\phi$ and $K^*\rho$ modes (except the decay $B^- \to K^{*-}\rho^0$). While the naive expectation of $f_\parallel \sim f_\perp$ is borne out by experiment, the observed large f_T is in contradiction to the naive anticipation of a small transverse polarization of order $f_T \sim m_V^2/m_B^2$. This has promoted many to explore the possibility of new physics in penguin-dominated $B \to VV$ decays. If so, the new physics effects should also manifest themselves in penguin-dominated VA and AA modes.

The analysis of charmless $B \to VV$ decays within the framework of QCD factorization [5, 6] was first performed by us [7] followed by many others [8, 9, 10, 11, 12, 13]. In these studies, NLO corrections to the helicity-dependent coefficients a_i^h such as vertex corrections, penguin contributions and hard spectator scattering were calculated. However, most of the early results do not agree with each other due to the incorrect projection on the polarization states. Recently, Beneke, Rohrer and Yang [13] have used the correct light-cone projection operators and computed complete NLO corrections to a_i^h and weak annihilation amplitudes. We will follow their work closely in the study of $B \to VV$ decays.

The generalization of the analysis of $B \to VV$ decays to VA and AA modes is highly nontrivial. First of all, while the ${}^3P_1$ meson behaves similarly to the vector meson, this is not the case for the ${}^1P_1$ meson. For the latter, its decay constant vanishes in the SU(3) limit and its chiral-even two-parton light-cone distribution amplitude (LCDA) is anti-symmetric under the exchange of quark and anti-quark momentum fractions in the SU(3) limit due to the G parity, contrary to the symmetric behavior for the ${}^3P_1$ meson. Second, there are two mixing effects for axial-vector mesons: one is the mixing between ${}^3P_1$ and ${}^1P_1$ states, e.g., K_{1A} and K_{1B} and the other is the mixing among ${}^3P_1$ or ${}^1P_1$ states themselves. In this work we will derive the longitudinal and transverse projectors

for axial-vector mesons and work out the hard spectator scattering and annihilation contributions to VA and AA decays.

Since the resolution of the $K^*\phi$ polarization anomaly may call for new physics beyond the standard model, this issue has received much attention in the past years. However, there are two crucial points that have been often overlooked in the literature. First, a reliable estimate of polarization fractions cannot be achieved unless the decay rate is correctly reproduced. Second, all the existing calculations except [7, 8, 12, 13] assume that the effective Wilson coefficients a_i^h are helicity independent. This leads to the scaling law: $f_T \sim \mathcal{O}(m_V^2/m_B^2)$. Calculations based on naive factorization often predict too small $B \to K^*\phi$ and $B \to K^*\rho$ rates by a factor of $2 \sim 3$. Obviously, it does not make sense at all to compare theory with experiment for $f_{L,T}$ at this stage as the definition of polarization fractions depends on the partial rate and hence the prediction can be easily off by a factor of $2 \sim 3$. The first task is to have some mechanism to bring up the rates. While the QCD factorization and pQCD [14] approaches rely on penguin annihilation, soft-collinear effective theory invokes charming penguin [15] and the final-state interaction model considers final-state rescattering of intermediate charm states [16, 17, 18]. Once the measured rate is reproduced, then it becomes sensible to ask what is the effect of this mechanism on polarization fractions. Next, it is important to consider NLO corrections to various helicity coefficients a_i^h, such as vertex corrections, penguin and hard spectator scattering contributions. It turns out that in some of $\overline{B} \to VV$ decays, e.g. $\overline{B} \to \bar{K}^*\phi, \bar{K}^{*0}\rho^0$, NLO nonfactorizable corrections will render negative-helicity amplitude comparable to the longitudinal one and hence will bring up the transverse polarization. Therefore, any serious solution to the polarization puzzle should take into account NLO effects on a_i^h.

There have been a few studies of charmless $B \to AV$ and $B \to AA$ decays in the literature [19, 20, 21]. Except for [19] done in QCD factorization, the analysis in other two references was carried out in the framework of generalized factorization in which the nonfactorizable effects are described by the parameter $N_c^{\rm eff}$, the effective number of colors. It has been claimed in [21] that most of $B \to AV$ decays are suppressed and $\Gamma(B \to AV) < \Gamma(B \to AP)$. This seems to be in contradiction to the naive anticipation that AV modes will have larger rates because of the existence of three polarization states for the vector meson. One of the main motivations for this work is to examine if the claim of [21] holds.

The present paper is organized as follows. In Sec. II we summarize all the input parameters relevant to the present work, such as the mixing angles, decay constants, form factors and light-cone distribution amplitudes for ${}^3P_1$ and ${}^1P_1$ axial-vector mesons and their Gegenbauer moments. We then apply QCD factorization in Sec. III to study $B \to VV, VA, AA$ decays and derive the relevant spectator interaction and annihilation terms. Results and discussions are presented in Sec. IV. Sec. V contains our conclusions. Flavor operators and the factorizable amplitudes of selective $B \to AV$ and AA decays are summarized in Appendices A and B, respectively. In Appendix C we give an explicit evaluation of the annihilation amplitude for the decay $B \to VA$. Since annihilation and hard spectator scattering amplitudes involve end-point divergences X_A^h, we give explicit expressions of them for various VV, VA and AA modes in terms of X_A^h in Appendices D and E.

II. INPUT PARAMETERS

In this section we shall briefly discuss and summarize all the input parameters relevant to the present work, such as the mixing angles, decay constants, form factors and light-cone distribution amplitudes for vector and axial-vector mesons.

A. Mixing angles

Mixing angles of the axial-vector mesons have been discussed in [22] and [1]. Here we recapitulate the main points. For axial-vector mesons there are two mixing angles of interest: one is the mixing between $^3P_1$ and $^1P_1$ states, e.g., K_{1A} and K_{1B} and the other is the mixing among $^3P_1$ or $^1P_1$ states themselves, for example, the $^3P_1$ states $f_1(1285)$ and $f_1(1420)$ have mixing due to SU(3) breaking effects.

The non-strange axial vector mesons, for example, the neutral $a_1(1260)$ and $b_1(1235)$ cannot have mixing because of the opposite C-parities. In the isospin limit, charged $a_1(1260)$ and $b_1(1235)$ also cannot have mixing because of the opposite G-parities. On the contrary, the strange partners of $a_1(1260)$ and $b_1(1235)$, namely, K_{1A} and K_{1B}, respectively, are not mass eigenstates and they are mixed together due to the strange and non-strange light quark mass difference. We write

$$\begin{aligned} K_1(1270) &= K_{1A}\sin\theta_{K_1} + K_{1B}\cos\theta_{K_1}, \\ K_1(1400) &= K_{1A}\cos\theta_{K_1} - K_{1B}\sin\theta_{K_1}. \end{aligned} \tag{2.1}$$

Various experimental information yields $\theta_{K_1} \approx \pm 37^\circ$ and $\pm 58^\circ$ (see e.g. [23]). The sign of θ_{K_1} is intimately related to the relative phase of the K_{1A} and K_{1B} states. We choose the phase convention such that the decay constants of K_{1A} and K_{1B} are of the same sign, while the $B \to K_{1A}$ and $B \to K_{1B}$ form factors are opposite in sign. In this convention for K_{1A} and K_{1B}, the mixing angle θ_{K_1} is favored to be negative as implied by the experimental measurement of the ratio of $K_1\gamma$ production in B decays [1, 24].

Just like the $\eta - \eta'$ mixing in the pseudoscalar sector, the 1^1P_1 states $h_1(1170)$ and $h_1(1380)$ may be mixed in terms of the pure octet h_8 and singlet h_1,

$$|h_1(1170)\rangle = |h_1\rangle\cos\theta_{^1P_1} + |h_8\rangle\sin\theta_{^1P_1}, \quad |h_1(1380)\rangle = -|h_1\rangle\sin\theta_{^1P_1} + |h_8\rangle\cos\theta_{^1P_1}\,, \tag{2.2}$$

and likewise the 1^3P_1 states $f_1(1285)$ and $f_1(1420)$ have mixing via

$$|f_1(1285)\rangle = |f_1\rangle\cos\theta_{^3P_1} + |f_8\rangle\sin\theta_{^3P_1}, \quad |f_1(1420)\rangle = -|f_1\rangle\sin\theta_{^3P_1} + |f_8\rangle\cos\theta_{^3P_1}\,. \tag{2.3}$$

Using the Gell-Mann-Okubo mass formula [25, 26], we found that the mixing angles $\theta_{^1P_1}$ and $\theta_{^3P_1}$ depend on the angle θ_{K_1} and are given by [1]

$$\begin{aligned} \theta_{^1P_1} = 25.2^\circ, \qquad \theta_{^3P_1} = 27.9^\circ, \quad \text{for } \theta_{K_1} = -37^\circ, \\ \theta_{^1P_1} \simeq 0^\circ, \qquad \theta_{^3P_1} = 53.2^\circ, \quad \text{for } \theta_{K_1} = -58^\circ. \end{aligned} \tag{2.4}$$

B. Decay constants and form factors

Decay constants of vector and axial-vector mesons are defined as

$$\begin{aligned}\langle V(p,\epsilon)|\bar{q}_2\gamma_\mu q_1|0\rangle &= -if_V m_V \epsilon^*_\mu,\\ \langle {}^{3(1)}P_1(p,\epsilon)|\bar{q}_2\gamma_\mu\gamma_5 q_1|0\rangle &= if_{^3P_1(^1P_1)} m_{^3P_1(^1P_1)}\epsilon^*_\mu.\end{aligned} \tag{2.5}$$

Transverse decay constants are defined via the tensor current by

$$\begin{aligned}\langle {}^{3(1)}P_1(p,\epsilon)|\bar{q}_2\sigma_{\mu\nu}\gamma_5 q_1|0\rangle &= f^\perp_{^{3(1)}P_1}(\epsilon^*_\mu p^\nu - \epsilon^*_\nu p^\mu),\\ \langle V(p,\epsilon)|\bar{q}_2\sigma_{\mu\nu} q_1|0\rangle &= -f^\perp_V(\epsilon^*_\mu p^\nu - \epsilon^*_\nu p^\mu).\end{aligned} \tag{2.6}$$

The decay constants $f_{^1P_1}$ of the $^1P_1$ non-strange neutral mesons $b_1^0(1235), h_1(1170), h_1(1380)$ vanish due to charge conjugation invariance. Likewise, the decay constant f_{b_1} of the charged b_1 vanishes owing to its even G-parity valid in the isospin limit. In general, the decay constants $f_{^1P_1}$ and $f^\perp_{^3P_1}$ are zero in the SU(3) limit. As discussed in [1], they are related to $f^\perp_{^1P_1}$ and $f_{^3P_1}$, respectively, via

$$f_{^1P_1} = f^\perp_{^1P_1}(\mu) a_0^{\parallel,{}^1P_1}(\mu), \qquad f^\perp_{^3P_1}(\mu) = f_{^3P_1} a_0^{\perp,{}^3P_1}(\mu), \tag{2.7}$$

where $a_0^{\parallel,{}^{1,3}P_1}$ are the zeroth Gegenbauer moment of $\Phi_\parallel^{{}^{1,3}P_1}$ to be defined later. Since we will assume isospin symmetry in practical calculations, this means that $f_{^1P_1} = 0$ for the b_1 and h_1 mesons and $f^\perp_{^3P_1} = 0$ for a_1 and f_1 mesons. Note that since $f_{^1P_1}$ and $f^\perp_{^3P_1}$ are G-parity violating quantities, their signs have to be flipped from particle to antiparticle due to the G-parity, for example, $f_{K^+_{1B}} = -f_{K^-_{1B}}$. In the present work, the G-parity violating parameters, e.g. $a_1^K, a_1^{\parallel,K_{1A}}, a_{0,2}^{\perp,K_{1A}}, a_1^{\perp,K_{1B}}$ and $a_{0,2}^{\parallel,K_{1B}}$, are considered for mesons containing a strange quark.

For the decay constants $f^q_{f_1(1285)}$ and $f^q_{f_1(1420)}$ for 1^3P_1 states defined by

$$\begin{aligned}\langle 0|\bar{q}\gamma_\mu\gamma_5 q|f_1(1285)(P,\lambda)\rangle &= -im_{f_1(1285)} f^q_{f_1(1285)}\epsilon^{(\lambda)}_\mu,\\ \langle 0|\bar{q}\gamma_\mu\gamma_5 q|f_1(1420)(P,\lambda)\rangle &= -im_{f_1(1420)} f^q_{f_1(1420)}\epsilon^{(\lambda)}_\mu,\end{aligned} \tag{2.8}$$

and the tensor decay constants for 1^1P_1 states defined by

$$\begin{aligned}\langle 0|\bar{q}\sigma_{\mu\nu} q|h_1(1170)(P,\lambda)\rangle &= if^{\perp,q}_{h_1(1170)}\,\epsilon_{\mu\nu\alpha\beta}\epsilon^\alpha_{(\lambda)}P^\beta,\\ \langle 0|\bar{q}\sigma_{\mu\nu} q|h_1(1380)(P,\lambda)\rangle &= if^{\perp,q}_{h_1(1380)}\,\epsilon_{\mu\nu\alpha\beta}\epsilon^\alpha_{(\lambda)}P^\beta,\end{aligned} \tag{2.9}$$

the reader is referred to [1, 22] for details.

Form factors for the $\overline{B}\to A$ and $\overline{B}\to V$ transitions read as

$$\begin{aligned}\langle A(p,\lambda)|A_\mu|\overline{B}(p_B)\rangle &= i\frac{2}{m_B - m_A}\varepsilon_{\mu\nu\alpha\beta}\epsilon^{*\nu}_{(\lambda)}p_B^\alpha p^\beta A^{BA}(q^2),\\ \langle A(p,\lambda)|V_\mu|\overline{B}(p_B)\rangle &= -\Big\{(m_B - m_A)\epsilon^{(\lambda)*}_\mu V_1^{BA}(q^2) - (\epsilon^{(\lambda)*}\cdot p_B)(p_B+p)_\mu\frac{V_2^{BA}(q^2)}{m_B - m_A}\\ &\quad -2m_A\frac{\epsilon^{(\lambda)*}\cdot p_B}{q^2}q^\mu\left[V_3^{BA}(q^2) - V_0^{BA}(q^2)\right]\Big\},\\ \langle V(p,\lambda)|V_\mu|\overline{B}(p_B)\rangle &= -i\frac{2}{m_B + m_V}\varepsilon_{\mu\nu\alpha\beta}\epsilon^{*\nu}_{(\lambda)}p_B^\alpha p^\beta V^{BV}(q^2),\\ \langle V(p,\lambda)|A_\mu|\overline{B}(p_B)\rangle &= (m_B + m_V)\epsilon^{(\lambda)*}_\mu A_1^{BV}(q^2) - (\epsilon^{(\lambda)*}\cdot p_B)(p_B+p)_\mu\frac{A_2^{BV}(q^2)}{m_B + m_V}\\ &\quad -2m_V\frac{\epsilon^{(\lambda)*}\cdot p_B}{q^2}q^\mu\left[A_3^{BV}(q^2) - A_0^{BV}(q^2)\right],\end{aligned} \tag{2.10}$$

TABLE I: Form factors for $B \to a_1, b_1, K_{1A}, K_{1B}$ transitions obtained in the covariant light-front model [27] are fitted to the 3-parameter form Eq. (2.12) except for the form factor V_2 denoted by * for which the fit formula Eq. (2.13) is used.

F	$F(0)$	a	b	F	$F(0)$	a	b
A^{Ba_1}	0.25	1.51	0.64	A^{Bb_1}	-0.10	1.92	1.62
$V_0^{Ba_1}$	0.13	1.71	1.23	$V_0^{Bb_1}$	-0.39	1.41	0.66
$V_1^{Ba_1}$	0.37	0.29	0.14	$V_1^{Bb_1}$	0.18	1.03	0.32
$V_2^{Ba_1}$	0.18	1.14	0.49	$V_2^{Bb_1}$	0.03^*	2.13^*	2.39^*
$A^{BK_{1A}}$	0.26	1.47	0.59	$A^{BK_{1B}}$	-0.11	1.88	1.53
$V_0^{BK_{1A}}$	0.14	1.62	1.14	$V_0^{BK_{1B}}$	-0.41	1.40	0.64
$V_1^{BK_{1A}}$	0.39	0.21	0.16	$V_1^{BK_{1B}}$	-0.19	0.96	0.30
$V_2^{BK_{1A}}$	0.17	1.02	0.45	$V_2^{BK_{1B}}$	0.05^*	1.78^*	2.12^*

where $q = p_B - p$, $V_3^{BA}(0) = V_0^{BA}(0)$ and

$$\begin{aligned} V_3^{BA}(q^2) &= \frac{m_B - m_A}{2m_A} V_1^{BA}(q^2) - \frac{m_B + m_A}{2m_A} V_2^{BA}(q^2), \\ A_3^{BV}(q^2) &= \frac{m_B + m_V}{2m_V} A_1^{BV}(q^2) - \frac{m_B - m_V}{2m_V} A_2^{BV}(q^2). \end{aligned} \tag{2.11}$$

Form factors for $B \to a_1(1260), b_1(1235), K_{1A}, K_{1B}$ transitions have been calculated in the relativistic covariant light-front quark model (LFQM) (Table I) [27], the light-cone sum rule (LCSR) method (Table II) [28], and the pQCD approach [29]. Various $B \to A$ form factors also can be obatined in the Isgur-Scora-Grinstein-Wise (ISGW) model [30, 31] based on the nonrelativistic constituent quark picture. However, as pointed out in [1], the predicted form factor $V_0^{Ba_1}(0) \approx 1.0$ in the ISGW2 model [31] is too big and will lead to too large rates for $\overline{B}^0 \to a_1^{\pm}\pi^{\mp}$ and the wrong pattern $\mathcal{B}(\overline{B}^0 \to a_1^+\pi^-) \gg \mathcal{B}(\overline{B}^0 \to a_1^-\pi^+)$, in contradiction to the experimental result $\mathcal{B}(\overline{B}^0 \to a_1^+\pi^-) \sim \frac{1}{2}\mathcal{B}(\overline{B}^0 \to a_1^-\pi^+)$. This may imply that relativistic effects in heavy-to-light transitions at maximum recoil that have been neglected in the ISGW model should be taken into account in order to get realistic form factors.

It should be stressed that in the convention of the present work and LCSR, the decay constants of $^1P_1$ and $^3P_1$ axial-vector mesons are of the same sign, while form factors $V_i^{B\to^1P_1}$ and $V_i^{B\to^3P_1}$ have opposite signs. The sign convention is the other way around in the LFQM and pQCD calculations. Therefore, as explained in [1], we put additional minus signs to the $B \to {}^1P_1$ form factors in Table I.

The momentum dependence of the form factors calculated in the light-front quark model and the LCSR approach is parametrized in the three-parameter form:

$$F(q^2) = \frac{F(0)}{1 - a\,q^2/m_B^2 + b\,q^4/m_B^4} \tag{2.12}$$

In the LFQM we use a different parametrization for the form factor $V_2(q^2)$ in some transitions [27]

$$F(q^2) = \frac{F(0)}{(1 - q^2/m_B^2)[1 - a\,q^2/m_B^2 + b\,q^4/m_B^4]}. \tag{2.13}$$

TABLE II: Same as Table I but in the light-cone sum rule model [28].

F	$F(0)$	a	b	F	$F(0)$	a	b
A^{Ba_1}	0.30 ± 0.05	1.64	0.986	A^{Bb_1}	-0.16 ± 0.03	1.69	0.910
$V_0^{Ba_1}$	0.30 ± 0.05	1.77	0.926	$V_0^{Bb_1}$	-0.39 ± 0.07	1.22	0.426
$V_1^{Ba_1}$	0.60 ± 0.11	0.645	0.250	$V_1^{Bb_1}$	-0.32 ± 0.06	0.748	0.063
$V_2^{Ba_1}$	0.26 ± 0.05	1.48	1.00	$V_2^{Bb_1}$	-0.06 ± 0.01	0.539	1.76
$A^{BK_{1A}}$	0.27 ± 0.05	1.60	0.974	$A^{BK_{1B}}$	$-0.22^{+0.06}_{-0.04}$	1.72	0.912
$V_0^{BK_{1A}}$	0.22 ± 0.04	2.40	1.78	$V_0^{BK_{1B}}$	$-0.45^{+0.12}_{-0.08}$	1.34	0.690
$V_1^{BK_{1A}}$	0.56 ± 0.11	0.635	0.211	$V_1^{BK_{1B}}$	$-0.48^{+0.13}_{-0.08}$	0.729	0.074
$V_2^{BK_{1A}}$	0.25 ± 0.05	1.51	1.18	$V_2^{BK_{1B}}$	$-0.10^{+0.03}_{-0.02}$	0.919	0.855
A^{Bf_1}	0.18 ± 0.03	1.63	0.900	A^{Bh_1}	-0.10 ± 0.02	1.54	0.848
$V_0^{Bf_1}$	0.18 ± 0.03	1.81	0.880	$V_0^{Bh_1}$	-0.24 ± 0.04	1.16	0.294
$V_1^{Bf_1}$	0.37 ± 0.07	0.640	0.153	$V_1^{Bh_1}$	-0.21 ± 0.04	0.612	0.078
$V_2^{Bf_1}$	0.16 ± 0.03	1.47	0.956	$V_2^{Bh_1}$	-0.04 ± 0.01	0.500	1.63
A^{Bf_8}	0.13 ± 0.02	1.64	0.919	A^{Bh_8}	-0.08 ± 0.02	1.56	0.827
$V_0^{Bf_8}$	0.12 ± 0.02	1.84	0.749	$V_0^{Bh_8}$	-0.18 ± 0.03	1.22	0.609
$V_1^{Bf_8}$	0.26 ± 0.05	0.644	0.209	$V_1^{Bh_8}$	-0.18 ± 0.03	0.623	0.094
$V_2^{Bf_8}$	0.11 ± 0.02	1.49	1.09	$V_2^{Bh_8}$	-0.03 ± 0.01	0.529	1.53

For $B \to \rho, K^*, \omega$ form factors, we shall use the results in [32] obtained from light-cone sum rules.

C. Light-cone distribution amplitudes

The light-cone distribution amplitudes (LCDAs) relevant for the present study are defined as [22, 33]

$$\begin{aligned}\langle V(P,\lambda)|\bar{q}_1(y)\gamma_\mu q_2(x)|0\rangle &= -if_V m_V \int_0^1 du\, e^{i(u\,py+\bar{u}px)} \left\{ p_\mu \frac{\epsilon^{*(\lambda)}z}{pz}\,\Phi_\parallel(u) + \varepsilon_{\perp\mu}^{*(\lambda)}\, g_\perp^{(v)}(u) \right. \\ &\left. -\frac{1}{2} z_\mu \frac{\epsilon^{*(\lambda)}z}{(pz)^2} m_V^2\, g_3(u) \right\}, \qquad (2.14)\\ \langle V(P,\lambda)|\bar{q}_1(y)\gamma_\mu\gamma_5 q_2(x)|0\rangle &= if_V \left(1 - \frac{f_V^\perp}{f_V}\frac{m_{q_1}+m_{q_2}}{m_V}\right) m_V\, \varepsilon_{\mu\nu\rho\sigma}\, \epsilon_{(\lambda)}^{*\nu} p^\rho z^\sigma \\ &\times \int_0^1 du\, e^{i(u\,py+\bar{u}\,px)}\, \frac{g_\perp^{(a)}(u)}{4}, \qquad (2.15)\end{aligned}$$

$$\begin{aligned}\langle V(P,\lambda)|\bar{q}_1(y)\sigma_{\mu\nu} q_2(x)|0\rangle = -f_V^\perp \int_0^1 du\, e^{i(u\,py+\bar{u}\,px)} &\left\{ (\varepsilon_{\perp\mu}^{*(\lambda)} p_\nu - \varepsilon_{\perp\nu}^{*(\lambda)} p_\mu)\Phi_\perp(u) \right. \\ &\left. + \frac{m_A^2\, \epsilon^{*(\lambda)}z}{(pz)^2}\,(p_\mu z_\nu - p_\nu z_\mu)\, h_\parallel^{(t)}(u) \right.\end{aligned}$$

$$+\frac{1}{2}(\varepsilon_{\perp\mu}^{*(\lambda)} z_\nu - \varepsilon_{\perp\nu}^{*(\lambda)} z_\mu)\frac{m_V^2}{p\cdot z} h_3(u)\Bigg\}, \tag{2.16}$$

$$\langle V(P,\lambda)|\bar{q}_1(y) q_2(x)|0\rangle = -f_V^\perp\left(1-\frac{f_V}{f_V^\perp}\frac{m_{q_1}+m_{q_2}}{m_V}\right) m_V^2\,(\epsilon^{*(\lambda)} z)\int_0^1 du\, e^{i(u\,py+\bar{u}\,px)}\,\frac{h_\parallel^{(s)}(u)}{2}\,, \tag{2.17}$$

for the vector meson, and

$$\begin{aligned}\langle A(P,\lambda)|\bar{q}_1(y)\gamma_\mu\gamma_5 q_2(x)|0\rangle &= i f_A m_A\int_0^1 du\, e^{i(u\,py+\bar{u}px)}\Bigg\{p_\mu\,\frac{\epsilon^{*(\lambda)} z}{pz}\,\Phi_\parallel(u) + \varepsilon_{\perp\mu}^{*(\lambda)}\, g_\perp^{(a)}(u)\\ &\quad -\frac{1}{2} z_\mu\frac{\epsilon^{*(\lambda)} z}{(pz)^2} m_A^2 g_3(u)\Bigg\},\end{aligned} \tag{2.18}$$

$$\langle A(P,\lambda)|\bar{q}_1(y)\gamma_\mu q_2(x)|0\rangle = -i f_A m_A\,\varepsilon_{\mu\nu\rho\sigma}\,\epsilon_{(\lambda)}^{*\nu} p^\rho z^\sigma\int_0^1 du\, e^{i(u\,py+\bar{u}\,px)}\,\frac{g_\perp^{(v)}(u)}{4}, \tag{2.19}$$

$$\begin{aligned}\langle A(P,\lambda)|\bar{q}_1(y)\sigma_{\mu\nu}\gamma_5 q_2(x)|0\rangle = f_A^\perp\int_0^1 du\, e^{i(u\,py+\bar{u}\,px)}\Bigg\{&(\varepsilon_{\perp\mu}^{*(\lambda)} p_\nu - \varepsilon_{\perp\nu}^{*(\lambda)} p_\mu)\Phi_\perp(u)\\ &+\frac{m_A^2\,\epsilon^{*(\lambda)} z}{(pz)^2}\,(p_\mu z_\nu - p_\nu z_\mu)\,h_\parallel^{(t)}(u)\\ &+\frac{1}{2}(\varepsilon_{\perp\mu}^{*(\lambda)} z_\nu - \varepsilon_{\perp\nu}^{*(\lambda)} z_\mu)\frac{m_A^2}{pz} h_3(u)\Bigg\},\end{aligned} \tag{2.20}$$

$$\langle A(P,\lambda)|\bar{q}_1(y)\gamma_5 q_2(x)|0\rangle = f_A^\perp m_A^2(\epsilon^{*(\lambda)} z)\int_0^1 du\, e^{i(u\,py+\bar{u}\,px)}\,\frac{h_\parallel^{(p)}(u)}{2}\,, \tag{2.21}$$

for the axial-vector meson, where $z = y - x$ with $z^2 = 0$ and we have introduced the light-like vector $p_\mu = P_\mu - m_{V(A)}^2 z_\mu/(2Pz)$ with the meson momentum $P^2 = m_{V(A)}^2$. Here $\Phi_\parallel, \Phi_\perp$ are twist-2 LCDAs, $g_\perp^{(a)}, g_\perp^{(v)}, h_\parallel^{(t)}, h_\parallel^{(p)}$ twist-3 ones, and g_3, h_3 twist-4. In the definitions of LCDAs, the longitudinal and transverse *projections* of polarization vectors $\epsilon_\mu^{*(\lambda)}$ along the $z-$direction for the (axial-)vector meson are given by [33]

$$\varepsilon_{\parallel\,\mu}^{*(\lambda)} \equiv \frac{\epsilon^{*(\lambda)} z}{pz}\left(p_\mu - \frac{m_{V(A)}^2}{2pz}\, z_\mu\right), \qquad \varepsilon_{\perp\,\mu}^{*(\lambda)} = \epsilon_\mu^{*(\lambda)} - \varepsilon_{\parallel\,\mu}^{*(\lambda)}\,. \tag{2.22}$$

One should distinguish the above projectors from the *exactly* longitudinal and transverse polarization vectors of the (axial-)vector meson, which are independent of the coordinate variable $z = y - x$, defined as

$$\epsilon^{*(0)\mu} = \frac{E}{m_{V(A)}}\left[\left(1-\frac{m_{V(A)}^2}{4E^2}\right)n_-^\mu - \frac{m_{V(A)}^2}{4E^2} n_+^\mu\right], \quad \epsilon_\perp^{*(\lambda)\mu} \equiv \left(\epsilon^{*(\lambda)\mu} - \frac{\epsilon^{*(\lambda)} n_+}{2}\, n_-^\mu - \frac{\epsilon^{*(\lambda)} n_-}{2}\, n_+^\mu\right)\delta_{\lambda,\pm 1}\,, \tag{2.23}$$

where we have defined two light-like vectors $n_\pm^\mu$ with $n_-^\mu \equiv (1,0,0,-1)$, and $n_+^\mu \equiv (1,0,0,1)$ and assumed that the meson moves along the n_-^μ direction.

In the QCDF calculation, the LCDAs of the vector meson appear in the following way [34]

$$\langle V(P,\lambda)|\bar{q}_{1\,\alpha}(y)\, q_{2\,\delta}(x)|0\rangle = -\frac{i}{4}\int_0^1 du\, e^{i(u\,py+\bar{u}px)}$$

$$\times\left\{f_V m_V\left(\not p\,\frac{\epsilon^{*(\lambda)}z}{pz}\,\Phi_\parallel(u)+\not\epsilon_\perp^{*(\lambda)}\,g_\perp^{(v)}(u)+\varepsilon_{\mu\nu\rho\sigma}\,\epsilon_{(\lambda)}^{*\mu}p^\rho z^\sigma\,\gamma^\nu\gamma_5\,\frac{g_\perp^{(a)}(u)}{4}\right)\right.$$
$$+f_V^\perp\left(\not\epsilon_\perp^{*(\lambda)}\;\not p\,\Phi_\perp(u)-i\frac{m_V^2(\epsilon^{*(\lambda)}z)}{(p\cdot z)^2}\sigma_{\mu\nu}p^\mu z^\nu h_\parallel^{(t)}(u)-im_V^2(\epsilon^{*(\lambda)}z)\frac{h_\parallel^{(s)}(u)}{2}\right)$$
$$\left.+\mathcal{O}[(x-y)^2]\right\}_{\delta\alpha}. \tag{2.24}$$

Here, all the components of the parton should be taken into account in the calculation before the collinear approximation is applied, so that one can assign the momenta

$$k_1^\mu=uEn_-^\mu+k_\perp^\mu+\frac{k_\perp^2}{4uE}n_+^\mu\,,\qquad k_2^\mu=\bar uEn_-^\mu-k_\perp^\mu+\frac{k_\perp^2}{4\bar uE}n_+^\mu\,, \tag{2.25}$$

to the quark and antiquark, respectively, in an energetic light final-state meson with the momentum P^μ and mass m, satisfying the relation $P^\mu=En_-^\mu+m^2n_+^\mu/(4E)\simeq En_-^\mu$. To obtain the light-cone projection operator of the meson in the momentum space, we apply the following substitution in the calculation

$$z^\mu\to-i\frac{\partial}{\partial k_{1\,\mu}}\simeq-i\left(\frac{n_+^\mu}{2E}\frac{\partial}{\partial u}+\frac{\partial}{\partial k_{\perp\,\mu}}\right), \tag{2.26}$$

where terms of order $k_\perp^2$ have been omitted. Moreover, to perform the calculation in the momentum space, we need to express Eq. (2.24) in terms of z-independent variables, P and $\epsilon^{*(\lambda)}$, instead of p and $\varepsilon^{*(\lambda)}$. Consequently, the light-cone projection operator of the meson in the momentum space, including twist-3 two-parton distribution amplitudes, reads

$$M_{\delta\alpha}=M_{\delta\alpha\parallel}+M_{\delta\alpha\perp}\,, \tag{2.27}$$

where $M_{\delta\alpha\parallel}$ and $M_{\delta\alpha\perp}$ are the longitudinal and transverse projectors, respectively.

For the vector meson, the longitudinal projector reads [34]

$$M_\parallel^V = -i\frac{f_V}{4}\,\frac{m_V(\epsilon_{(\lambda)}^*n_+)}{2}\;\not n_-\,\Phi_\parallel(u)-i\frac{f_V^\perp m_V}{4}\,\frac{m_V(\epsilon_{(\lambda)}^*n_+)}{2E}\left\{-\frac{i}{2}\,\sigma_{\mu\nu}\,n_-^\mu n_+^\nu\,h_\parallel^{(t)}(u)\right.$$
$$\left.-iE\int_0^u dv\,(\Phi_\perp(v)-h_\parallel^{(t)}(v))\;\sigma_{\mu\nu}n_-^\mu\,\frac{\partial}{\partial k_{\perp\nu}}+\frac{h_\parallel'^{(s)}(u)}{2}\right\}\Bigg|_{k=up}+\mathcal{O}\left[\left(\frac{m_V}{E}\right)^2\right], \tag{2.28}$$

and the transverse projector has the form

$$M_\perp^V = -i\frac{f_V^\perp}{4}E\;\not\epsilon_\perp^{*(\lambda)}\;\not n_-\,\Phi_\perp(u)$$
$$-i\frac{f_Vm_V}{4}\left\{\not\epsilon_\perp^{*(\lambda)}\,g_\perp^{(v)}(u)-E\int_0^u dv\,(\Phi_\parallel(v)-g_\perp^{(v)}(v))\;\not n_-\,\epsilon_{\perp\mu}^{*(\lambda)}\,\frac{\partial}{\partial k_{\perp\mu}}\right.$$
$$\left.+i\varepsilon_{\mu\nu\rho\sigma}\,\gamma^\mu\epsilon_\perp^{*(\lambda)\nu}\,n_-^\rho\gamma_5\left[n_+^\sigma\,\frac{g_\perp'^{(a)}(u)}{8}-E\,\frac{g_\perp^{(a)}(u)}{4}\,\frac{\partial}{\partial k_{\perp\sigma}}\right]\right\}\Bigg|_{k=up}+\mathcal{O}\left[\left(\frac{m_V}{E}\right)^2\right], \tag{2.29}$$

where $k_\perp$ is the transverse momentum of the q_1 quark in the vector meson. For the axial-vector meson, the longitudinal projector is given by

$$M_\parallel^A = -i\frac{f_A}{4}\,\frac{m_A(\epsilon_{(\lambda)}^*n_+)}{2}\;\not n_-\gamma_5\,\Phi_\parallel(u)+i\frac{f_A^\perp m_A}{4}\,\frac{m_A(\epsilon_{(\lambda)}^*n_+)}{2E}\left\{-\frac{i}{2}\,\sigma_{\mu\nu}\gamma_5\,n_-^\mu n_+^\nu\,h_\parallel^{(t)}(u)\right.$$
$$\left.-iE\int_0^u dv\,(\Phi_\perp(v)-h_\parallel^{(t)}(v))\;\sigma_{\mu\nu}\gamma_5n_-^\mu\,\frac{\partial}{\partial k_{\perp\nu}}+\gamma_5\frac{h_\parallel'^{(p)}(u)}{2}\right\}\Bigg|_{k=up}+\mathcal{O}\left[\left(\frac{m_A}{E}\right)^2\right], \tag{2.30}$$

and the transverse projector given by

$$
\begin{aligned}
M_\perp^A \;=\; & i\frac{f_A^\perp}{4} E \not\epsilon_\perp^{*(\lambda)} \not{n}_- \gamma_5 \, \Phi_\perp(u) \\
& -i\frac{f_A m_A}{4} \Bigg\{ \not\epsilon_\perp^{*(\lambda)} \gamma_5 \, g_\perp^{(a)}(u) - E \int_0^u dv \, (\Phi_\parallel(v) - g_\perp^{(a)}(v)) \not{n}_- \gamma_5 \, \epsilon_{\perp\mu}^{*(\lambda)} \frac{\partial}{\partial k_{\perp\mu}} \\
& + i\varepsilon_{\mu\nu\rho\sigma} \gamma^\mu \epsilon_\perp^{*(\lambda)\nu} \, n_-^\rho \left[n_+^\sigma \frac{g_\perp^{\prime(v)}(u)}{8} - E \, \frac{g_\perp^{(v)}(u)}{4} \frac{\partial}{\partial k_{\perp\sigma}} \right] \Bigg\} \Bigg|_{k=up} + \mathcal{O}\left[\left(\frac{m_A}{E} \right)^2 \right]. \quad (2.31)
\end{aligned}
$$

In the present study, we choose the coordinate systems in the Jackson convention; that is, in the $\overline{B}$ rest frame, one of the vector or axial-vector mesons is moving along the z axis of the coordinate system and the other along the $-z$ axis, while the x axes of both daughter particles are parallel [35]

$$
\begin{aligned}
& \epsilon_1^{\mu(0)} = (p_c, 0, 0, E_1)/m_1, \qquad \epsilon_2^{\mu(0)} = (p_c, 0, 0, -E_2)/m_2, \\
& \epsilon_1^{\mu(\pm1)} = \frac{1}{\sqrt{2}}(0, \mp1, -i, 0), \qquad \epsilon_2^{\mu(\pm1)} = \frac{1}{\sqrt{2}}(0, \mp1, +i, 0), \quad (2.32)
\end{aligned}
$$

where p_c is the center mass momentum of the final state meson and $\epsilon_1^{*(\pm1)} \cdot \epsilon_2^{*(\pm1)} = -\delta_{\pm1,\pm1}$. In the large energy limit, if the A meson moves along the n_-^μ direction, we will have $\epsilon_A^{*(\lambda)} \cdot n_+ = 2E_A/m_A \, \delta_{\lambda,0}$ and $\epsilon_A^{*(\lambda)} \cdot n_- = 0$. Note that if the coordinate systems are in the Jacob-Wick convention where the y axes of both decay particles are parallel, the transverse polarization vectors of the second meson will become $\epsilon_2^\mu(\pm1) = (0, \pm1, -i, 0)/\sqrt{2}$ and $\epsilon_1^{*(\pm1)} \cdot \epsilon_2^{*(\pm1)} = \delta_{\pm1,\pm1}$. In general, the QCDF amplitudes can be reduced to the form of $\int_0^1 du \, \mathrm{tr}(M^A \ldots)$.

To obtain the projector on the transverse polarization states in the helicity basis, one can insert $\epsilon_\perp^* = \epsilon_\mp^*$ to obtain

$$
\begin{aligned}
M_\mp^V(u) \;=\; & -i\frac{f_V^\perp}{4} E \not\epsilon_\mp^{*(\lambda)} \not{n}_- \Phi_\perp^V(u) \\
& -i\frac{f_V m_V}{8} \Bigg\{ \not\epsilon_\mp^{*(\lambda)} (1-\gamma_5) \left(g_\perp^{(v)}(u) \pm \frac{g_\perp^{\prime(a)}(u)}{4} \right) + \not\epsilon_\mp^{*(\lambda)} (1+\gamma_5) \left(g_\perp^{(v)}(u) \mp \frac{g_\perp^{\prime(a)}(u)}{4} \right) \\
& -E \not{n}_- (1-\gamma_5) \left(\int_0^u dv (\Phi_\parallel(v) - g_\perp^{(v)}(v)) \mp \frac{g_\perp^{(a)}(u)}{4} \right) \epsilon_{\mp\nu}^* \frac{\partial}{\partial k_{\perp\nu}} \\
& -E \not{n}_- (1+\gamma_5) \left(\int_0^u dv (\Phi_\parallel(v) - g_\perp^{(v)}(v)) \pm \frac{g_\perp^{(a)}(u)}{4} \right) \epsilon_{\mp\nu}^* \frac{\partial}{\partial k_{\perp\nu}} \Bigg\} \Bigg|_{k_\perp=0} + \mathcal{O}\left[\left(\frac{m_V}{E} \right)^2 \right], \\
& \quad (2.33)
\end{aligned}
$$

and

$$
\begin{aligned}
M_\mp^A(u) \;=\; & i\frac{f_A^\perp}{4} E \not\epsilon_\mp^{*(\lambda)} \not{n}_- \gamma_5 \Phi_\perp^A(u) \\
& -i\frac{f_A m_A}{8} \Bigg\{ - \not\epsilon_\mp^{*(\lambda)} (1-\gamma_5) \left(g_\perp^{(a)}(u) \pm \frac{g_\perp^{\prime(v)}(u)}{4} \right) + \not\epsilon_\mp^{*(\lambda)} (1+\gamma_5) \left(g_\perp^{(a)}(u) \mp \frac{g_\perp^{\prime(v)}(u)}{4} \right) \\
& +E \not{n}_- (1-\gamma_5) \left(\int_0^u dv (\Phi_\parallel(v) - g_\perp^{(a)}(v)) \mp \frac{g_\perp^{(v)}(u)}{4} \right) \epsilon_{\mp\nu}^* \frac{\partial}{\partial k_{\perp\nu}}
\end{aligned}
$$

$$-E\,\not{n}_-(1+\gamma_5)\left(\int_0^u dv(\Phi_\parallel(v)-g_\perp^{(a)}(v))\pm\frac{g_\perp^{(v)}(u)}{4}\right)\epsilon^*_{\mp\nu}\frac{\partial}{\partial k_{\perp\nu}}\Bigg\}\Bigg|_{k_\perp=0}+\mathcal{O}\left[\left(\frac{m_A}{E}\right)^2\right]. \tag{2.34}$$

Applying equations of motion to LCDAs, one can obtain the following Wandzura-Wilczek relations in which twist-3 LCDAs are related to the twist-2 ones [33] via

$$g_\perp^{(v)}(u) = \frac{1}{2}\left[\int_0^u\frac{\Phi_\parallel(v)}{\bar v}\,dv+\int_u^1\frac{\Phi_\parallel(v)}{v}\,dv\right]+\dots, \tag{2.35}$$

$$g_\perp^{(a)}(u) = 2\left[\bar u\int_0^u\frac{\Phi_\parallel(v)}{\bar v}\,dv+u\int_u^1\frac{\Phi_\parallel(v)}{v}\,dv\right]+\dots, \tag{2.36}$$

$$h_\parallel^{(t)}(u) = (2u-1)\left[\int_0^u\frac{\Phi_\perp(v)}{\bar v}\,dv-\int_u^1\frac{\Phi_\perp(v)}{v}\,dv\right]+\dots, \tag{2.37}$$

$$h_\parallel^{(s)}(u) = 2\left[\bar u\int_0^u\frac{\Phi_\perp(v)}{\bar v}\,dv+u\int_u^1\frac{\Phi_\perp(v)}{v}\,dv\right]+\dots, \tag{2.38}$$

for vector mesons, and

$$g_\perp^{(a)}(u) = \frac{1}{2}\left[\int_0^u\frac{\Phi_\parallel(v)}{\bar v}\,dv+\int_u^1\frac{\Phi_\parallel(v)}{v}\,dv\right]+\dots, \tag{2.39}$$

$$g_\perp^{(v)}(u) = 2\left[\bar u\int_0^u\frac{\Phi_\parallel(v)}{\bar v}\,dv+u\int_u^1\frac{\Phi_\parallel(v)}{v}\,dv\right]+\dots, \tag{2.40}$$

$$h_\parallel^{(t)}(u) = (2u-1)\left[\int_0^u\frac{\Phi_\perp(v)}{\bar v}\,dv-\int_u^1\frac{\Phi_\perp(v)}{v}\,dv\right]+\dots, \tag{2.41}$$

$$h_\parallel^{(p)}(u) = 2\left[\bar u\int_0^u\frac{\Phi_\perp(v)}{\bar v}\,dv+u\int_u^1\frac{\Phi_\perp(v)}{v}\,dv\right]+\dots, \tag{2.42}$$

for axial-vector mesons, where the ellipses denote additional contributions from three-particle distribution amplitudes containing gluons and terms proportional to light quark masses, which we do not consider here and below. Eqs. (2.35)-(2.42) further give us

$$\begin{aligned}
&\frac{g_\perp^{\prime(a)}(v)}{4}+g_\perp^{(v)}(v)=\int_v^1\frac{\Phi_\parallel(u)}{u}du\equiv\Phi_+(v)\,,\\
&\frac{g_\perp^{\prime(a)}(v)}{4}-g_\perp^{(v)}(v)=-\int_0^v\frac{\Phi_\parallel(u)}{\bar u}du\equiv-\Phi_-(v)\,,\\
&h_\parallel^{\prime(s)}(v)=-2\left[\int_0^v\frac{\Phi_\perp(u)}{\bar u}du-\int_v^1\frac{\Phi_\perp(u)}{u}du\right]\equiv-2\Phi_v(v),\\
&\int_0^v du(\Phi_\perp(u)-h_\parallel^{(t)}(u))=v\bar v\left[\int_0^v\frac{\Phi_\perp(u)}{\bar u}du-\int_v^1\frac{\Phi_\perp(u)}{u}du\right]=v\bar v\Phi_v(v),\\
&\int_0^v du(\Phi_\parallel(u)-g_\perp^{(v)}(u))=\frac{1}{2}\left[\bar v\int_0^v\frac{\Phi_\parallel(u)}{\bar u}du-v\int_v^1\frac{\Phi_\parallel(u)}{u}du\right]=\frac{1}{2}\Big(\bar v\Phi_-(v)-v\Phi_+(v)\Big),
\end{aligned} \tag{2.43}$$

for vector mesons, and

$$\frac{g_\perp^{\prime(v)}(v)}{4}+g_\perp^{(a)}(v)=\int_v^1\frac{\Phi_\parallel(u)}{u}du\equiv\Phi_+(v)\,,$$

$$
\begin{aligned}
&\frac{g_\perp'^{(v)}(v)}{4} - g_\perp^{(a)}(v) = -\int_0^v \frac{\Phi_\parallel(u)}{\bar{u}} du \equiv -\Phi_-(v)\,,\\
&h_\parallel'^{(p)}(v) = -2\left[\int_0^v \frac{\Phi_\perp(u)}{\bar{u}} du - \int_v^1 \frac{\Phi_\perp(u)}{u} du\right] \equiv -2\Phi_a(v),\\
&\int_0^v du(\Phi_\perp(u) - h_\parallel^{(t)}(u)) = v\bar{v}\left[\int_0^v \frac{\Phi_\perp(u)}{\bar{u}} du - \int_v^1 \frac{\Phi_\perp(u)}{u} du\right] = v\bar{v}\Phi_a(v), \qquad (2.44)\\
&\int_0^v du(\Phi_\parallel(u) - g_\perp^{(a)}(u)) = \frac{1}{2}\left[\bar{v}\int_0^v \frac{\Phi_\parallel(u)}{\bar{u}} du - v\int_v^1 \frac{\Phi_\parallel(u)}{u} du\right] = \frac{1}{2}\Big(\bar{v}\Phi_-(v) - v\Phi_+(v)\Big),
\end{aligned}
$$

for axial-vector mesons.

After applying the Wandzura-Wilczek relations, the transverse helicity projectors (2.33) and (2.34) can be simplified to

$$
\begin{aligned}
M_\mp^V(u) \;=\; & -i\frac{f_V^\perp}{4} E \not{\epsilon}_\mp^{*(\lambda)} \not{n}_- \Phi_\perp^V(u)\\
& -i\frac{f_V m_V}{8}\Bigg\{\epsilon_{\mp\nu}^{*(\lambda)}\Phi_+(u)\left[\gamma^\nu(1\mp\gamma_5) + uE\not{n}_-(1\mp\gamma_5)\frac{\partial}{\partial k_{\perp\nu}}\right]\\
& \quad +\epsilon_{\mp\nu}^{*(\lambda)}\Phi_-(u)\left[\gamma^\nu(1\pm\gamma_5) - \bar{u}E\not{n}_-(1\pm\gamma_5)\frac{\partial}{\partial k_{\perp\nu}}\right]\Bigg\}\Bigg|_{k_\perp=0} + \mathcal{O}\left[\left(\frac{m_V}{E}\right)^2\right],
\end{aligned}
\qquad (2.45)
$$

and

$$
\begin{aligned}
M_\mp^A(u) \;=\; & i\frac{f_A^\perp}{4} E \not{\epsilon}_\mp^{*(\lambda)} \not{n}_-\gamma_5 \Phi_\perp^A(u)\\
& -i\frac{f_A m_A}{8}\Bigg\{\epsilon_{\mp\nu}^{*(\lambda)}\Phi_+(u)\left[\gamma^\nu(1\mp\gamma_5) + uE\not{n}_-(1\mp\gamma_5)\frac{\partial}{\partial k_{\perp\nu}}\right]\gamma_5\\
& \quad +\epsilon_{\mp\nu}^{*(\lambda)}\Phi_-(u)\left[\gamma^\nu(1\pm\gamma_5) - \bar{u}E\not{n}_-(1\pm\gamma_5)\frac{\partial}{\partial k_{\perp\nu}}\right]\gamma_5\Bigg\}\Bigg|_{k_\perp=0} + \mathcal{O}\left[\left(\frac{m_A}{E}\right)^2\right].
\end{aligned}
\qquad (2.46)
$$

From Eqs. (2.28)-(2.31) and (2.35)-(2.44), we see that Φ_+ and Φ_- project onto transversely polarized vector or axial-vector mesons in which quark and antiquark flips helicity, respectively, while $\Phi_{v(a)}$ projects onto longitudinally polarized vector (axial-vector) mesons in which either the quark or antiquark flips helicity.

We next specify the LCDAs for vector and axial-vector mesons. The general expressions of LCDAs are

$$
\Phi_V(x,\mu) = 6x(1-x)\left[1 + \sum_{n=1}^{\infty} a_n^V(\mu) C_n^{3/2}(2x-1)\right], \qquad (2.47)
$$

and

$$
\Phi_v(x,\mu) = 3\left[2x - 1 + \sum_{n=1}^{\infty} a_n^{\perp,V}(\mu) P_{n+1}(2x-1)\right], \qquad (2.48)
$$

for the vector meson, where $P_n(x)$ are the Legendre polynomials. The normalization of LCDAs is

$$
\int_0^1 dx \Phi_V(x) = 1, \qquad \int_0^1 dx \Phi_v(x) = 0. \qquad (2.49)
$$

The explicit expressions of the LCDAs of axial-vector mesons have been discussed in details in [1, 22]. We use

$$\begin{aligned}
\Phi_\perp^{^1P_1}(u) &= 6u\bar{u}\left\{1+3a_1^{\perp,^1P_1}(2u-1)+a_2^{\perp,^1P_1}\frac{3}{2}\Big[5(2u-1)^2-1\Big]\right\},\\
\Phi_\parallel^{^1P_1}(u) &= 6u\bar{u}\left\{a_0^{\parallel,^1P_1}+3a_1^{\parallel,^1P_1}(2u-1)+a_2^{\parallel,^1P_1}\frac{3}{2}\Big[5(2u-1)^2-1\Big]\right\},\\
\Phi_a^{^1P_1}(u) &= 3\left[(2u-1)+\sum_{n=1}^{\infty}a_n^{\perp,^1P_1}(\mu)P_{n+1}(2u-1)\right],
\end{aligned} \tag{2.50}$$

for $^1P_1$ mesons, and

$$\begin{aligned}
\Phi_\parallel^{^3P_1}(u) &= 6u\bar{u}\left\{1+3a_1^{\parallel,^3P_1}(2u-1)+a_2^{\parallel,^3P_1}\frac{3}{2}\Big[5(2u-1)^2-1\Big]\right\},\\
\Phi_\perp^{^3P_1}(u) &= 6u\bar{u}\left\{a_0^{\perp,^3P_1}+3a_1^{\perp,^3P_1}(2u-1)+a_2^{\perp,^3P_1}\frac{3}{2}\Big[5(2u-1)^2-1\Big]\right\},\\
\Phi_a^{^3P_1}(u) &= 3\left[a_0^{\perp,^3P_1}(2u-1)+\sum_{n=1}^{\infty}a_n^{\perp,^3P_1}(\mu)P_{n+1}(2u-1)\right],
\end{aligned} \tag{2.51}$$

for $^3P_1$ mesons. The normalization conditions are

$$\begin{aligned}
&\int_0^1 dx\Phi_\parallel^{^1P_1}(x)=a_0^{\parallel,^1P_1}, \qquad \int_0^1 dx\Phi_\parallel^{^3P_1}(x)=1,\\
&\int_0^1 dx\Phi_\perp^{^1P_1}(x)=1, \qquad \int_0^1 dx\Phi_\parallel^{^3P_1}(x)=a_0^{\perp,^3P_1},\\
&\int_0^1 dx\Phi_a^{^1P_1}(x)=\int_0^1 dx\Phi_a^{^3P_1}(x)=0.
\end{aligned} \tag{2.52}$$

It should be stressed that the LCDAs $\Phi_\parallel^{^1P_1}$ and $\Phi_\perp^{^3P_1}$ are defined with the decay constants $f_{^1P_1}^\perp$ and $f_{^3P_1}$, respectively, even though their corresponding normalizations are $f_{^1P_1}$ and $f_{^3P_1}^\perp$. As stressed in [1], if we employ the decay constants $f_{^1P_1}$ and $f_{^3P_1}^\perp$ to define the the LCDAs $\Phi_\parallel^{^1P_1}$ and $\Phi_\perp^{^3P_1}$, they will have the form

$$\begin{aligned}
\Phi_\parallel^{^1P_1}(u) &= f_{^1P_1}6u\bar{u}\left\{1+\mu_{^1P_1}\sum_{i=1}^{2}a_i^{\parallel,^1P_1}C_i^{3/2}(2u-1)\right\},\\
\Phi_\perp^{^3P_1}(u) &= f_{^3P_1}^\perp 6u\bar{u}\left\{1+\mu_{^3P_1}\sum_{i=1}^{2}a_i^{\perp,^3P_1}C_i^{3/2}(2u-1)\right\},
\end{aligned} \tag{2.53}$$

where $\mu_{^1P_1}=1/a_0^{\parallel,^1P_1}$ and $\mu_{^3P_1}=1/a_0^{\perp,^3P_1}$ which become infinite in the SU(3) limit. Therefore, it is most convenient to use Eq. (2.50) for the LCDA $\Phi_\parallel^{^1P_1}$ and (2.51) for the LCDA $\Phi_\parallel^{^3P_1}$ which amount to treating the decay constant of $^1P_1$ as $f_{^1P_1}^\perp$ and the tensor decay constant of $^3P_1$ as $f_{^3P_1}$. Of course, this does not mean that $f_{^1P_1}$ ($f_{^3P_1}^\perp$) is equal to $f_{^1P_1}^\perp$ ($f_{^3P_1}$).

For the B meson, we use the light-cone projector [34]

$$M_{\beta\alpha}^B=-\frac{if_Bm_B}{4}\left\{\frac{1+\not{v}}{2}\left[\Phi_1^B(\omega)\not{n}_+ +\Phi_2^B(\omega)\Big(\not{n}_- -l_+\gamma_\perp^\nu\frac{\partial}{\partial l_\perp^\nu}\Big)\right]\gamma_5\right\}_{\alpha\beta}. \tag{2.54}$$

The integral of the B meson wave function is parameterized as [5]

$$\int_0^1\frac{d\rho}{1-\rho}\Phi_1^B(\rho)\equiv\frac{m_B}{\lambda_B}, \tag{2.55}$$

where $1-\rho$ is the momentum fraction carried by the light spectator quark in the B meson.

D. A summary of input quantities

It is useful to summarize all the input quantities we have used in this work.

For the CKM matrix elements, we use the Wolfenstein parameters $A = 0.807 \pm 0.018$, $\lambda = 0.2265 \pm 0.0008$, $\bar{\rho} = 0.141^{+0.029}_{-0.017}$ and $\bar{\eta} = 0.343 \pm 0.016$ [36]. The corresponding three unitarity angles are $\alpha = (90.7^{+4.5}_{-1.9})^\circ$, $\beta = (21.7 \pm 0.017)^\circ$ and $\gamma = (67.6^{+2.8}_{-4.5})^\circ$.

For the running quark masses we shall use [25, 37]

$$\begin{aligned}
&m_b(m_b) = 4.2\,\text{GeV}, && m_b(2.1\,\text{GeV}) = 4.94\,\text{GeV}, && m_b(1\,\text{GeV}) = 6.34\,\text{GeV},\\
&m_c(m_b) = 0.91\,\text{GeV}, && m_c(2.1\,\text{GeV}) = 1.06\,\text{GeV}, && m_c(1\,\text{GeV}) = 1.32\,\text{GeV},\\
&m_s(2.1\,\text{GeV}) = 95\,\text{MeV}, && m_s(1\,\text{GeV}) = 118\,\text{MeV}, &&\\
&m_d(2.1\,\text{GeV}) = 5.0\,\text{MeV}, && m_u(2.1\,\text{GeV}) = 2.2\,\text{MeV}. &&
\end{aligned} \tag{2.56}$$

Among the quarks, the strange quark gives the major theoretical uncertainty to the decay amplitude. Hence, we will only consider the uncertainty in the strange quark mass given by $m_s(2.1\,\text{GeV}) = 95 \pm 20$ MeV. Notice that for the one-loop penguin contribution, the relevant quark mass is the pole mass rather than the current one [38]. Since the penguin loop correction is governed by the ratio of the pole masses squared $s_i \equiv (m_i^{\rm pole}/m_b^{\rm pole})^2$ [see Eqs. (3.18) and (3.20) below] and since the pole mass is meaningful only for heavy quarks, we only need to consider the ratio of c and b quark pole masses given by $s_c = (0.3)^2$.

The strong coupling constants employed in the present work are

$$\alpha_s(4.2\,\text{GeV}) = 0.221, \quad \alpha_s(2.1\,\text{GeV}) = 0.293, \quad \alpha_s(1.45\,\text{GeV}) = 0.359, \quad \alpha_s(1\,\text{GeV}) = 0.495\,. \tag{2.57}$$

For longitudinal and transverse decay constants of the vector mesons, we use (in units of MeV)

$$\begin{aligned}
&f_\rho = 216 \pm 3, && f_\omega = 187 \pm 5, && f_{K^*} = 220 \pm 5, && f_\phi = 215 \pm 5,\\
&f_\rho^\perp = 165 \pm 9, && f_\omega^\perp = 151 \pm 9, && f_{K^*}^\perp = 185 \pm 10, && f_\phi^\perp = 186 \pm 9\,,
\end{aligned} \tag{2.58}$$

where the values of f_V and $f_V^\perp(1\text{GeV})$ are taken from [39].

The decay constants $f_{^3P_1}$ for a_1, f_1, f_8 [1] and $f_{^1P_1}^\perp(1\,\text{GeV})$ for b_1, h_1, h_8 obtained from QCD sum rule methods are listed in [22]. For the decay constants of K_{1A} and K_{1B} we use

$$f_{K_{1A}} = 250 \pm 13\ \text{MeV}, \qquad f_{K_{1B}} = a_0^{\parallel,K_{1B}} f_{K_{1B}}^\perp \approx -28\ \text{MeV}, \tag{2.59}$$

where uses of $f_{K_{1B}}^\perp = 190 \pm 10$ MeV [22] and the value of $a_0^{\parallel,K_{1B}}$ from Table III have been made. Therefore,

$$\begin{aligned}
f_{K_1(1270)} &= -184 \pm 11\ \text{MeV}\,, \quad f_{K_1(1400)} = 177 \pm 12\ \text{MeV}\,, && \text{for } \theta_{K_1} = -37^\circ,\\
f_{K_1(1270)} &= -234 \pm 15\ \text{MeV}, \quad f_{K_1(1400)} = 100 \pm 12\ \text{MeV}\,, && \text{for } \theta_{K_1} = -58^\circ.
\end{aligned} \tag{2.60}$$

[1] Recall that f_8 and f_1 are SU(3)-octet and -singlet states.

TABLE III: Gegenbauer moments of $\Phi_\perp$ and $\Phi_\parallel$ for 1^3P_1 and 1^1P_1 mesons, respectively, where $a_0^{\perp,K_{1A}}$ and $a_0^{\parallel,K_{1B}}$ are updated from the $B\to K_1\gamma$ analysis [24], and $a_1^{\parallel,K_{1A}}, a_2^{\perp,K_{1A}}, a_2^{\parallel,K_{1B}}$, and $a_1^{\perp,K_{1B}}$ are then obtained from Eq. (141) in [22]. The scale dependence of Gegenbauer moments is referred to Eq. (2.57).

μ	$a_2^{\parallel,a_1(1260)}$	$a_2^{\parallel,f_1^{^3P_1}}$	$a_2^{\parallel,f_8^{^3P_1}}$	$a_2^{\parallel,K_{1A}}$	$a_1^{\parallel,K_{1A}}$	
1 GeV	-0.02 ± 0.02	-0.04 ± 0.03	-0.07 ± 0.04	-0.05 ± 0.03	$-0.30^{+0.26}_{-0.00}$	
2.2 GeV	-0.01 ± 0.01	-0.03 ± 0.02	-0.05 ± 0.03	-0.04 ± 0.02	$-0.24^{+0.21}_{-0.00}$	
μ	$a_1^{\perp,a_1(1260)}$	$a_1^{\perp,f_1^{^3P_1}}$	$a_1^{\perp,f_8^{^3P_1}}$	$a_1^{\perp,K_{1A}}$	$a_0^{\perp,K_{1A}}$	$a_2^{\perp,K_{1A}}$
1 GeV	-1.04 ± 0.34	-1.06 ± 0.36	-1.11 ± 0.31	-1.08 ± 0.48	$0.26^{+0.03}_{-0.22}$	0.02 ± 0.21
2.2 GeV	-0.81 ± 0.26	-0.82 ± 0.28	-0.86 ± 0.24	-0.84 ± 0.37	$0.24^{+0.03}_{-0.21}$	0.01 ± 0.15
μ	$a_1^{\parallel,b_1(1235)}$	$a_1^{\parallel,h_1^{^1P_1}}$	$a_1^{\parallel,h_8^{^1P_1}}$	$a_1^{\parallel,K_{1B}}$	$a_0^{\parallel,K_{1B}}$	$a_2^{\parallel,K_{1B}}$
1 GeV	-1.95 ± 0.35	-2.00 ± 0.35	-1.95 ± 0.35	-1.95 ± 0.45	-0.15 ± 0.15	$0.09^{+0.16}_{-0.18}$
2.2 GeV	-1.56 ± 0.28	-1.60 ± 0.28	-1.56 ± 0.28	-1.56 ± 0.36	-0.15 ± 0.15	$0.06^{+0.11}_{-0.13}$
μ	$a_2^{\perp,b_1(1235)}$	$a_2^{\perp,h_1^{^1P_1}}$	$a_2^{\perp,h_8^{^1P_1}}$	$a_2^{\perp,K_{1B}}$	$a_1^{\perp,K_{1B}}$	
1 GeV	0.03 ± 0.19	0.18 ± 0.22	0.14 ± 0.22	-0.02 ± 0.22	$0.30^{+0.00}_{-0.31}$	
2.2 GeV	0.02 ± 0.14	0.14 ± 0.17	0.11 ± 0.17	-0.02 ± 0.17	$0.25^{+0.00}_{-0.26}$	

The Gegenbauer moments $a_i^{(\perp),V}$ and $a_i^{\parallel\,(\perp),A}$ have been studied using the QCD sum rule method. Here we employ the most recent updated values evaluated at $\mu=1$ GeV [40]

$$a_1^{K^*}=0.03\pm0.02,\quad a_1^{\perp,K^*}=0.04\pm0.03,\quad a_2^{K^*}=0.11\pm0.09,\quad a_2^{\perp,K^*}=0.10\pm0.08,$$
$$a_2^{\rho,\omega}=0.15\pm0.07,\quad a_2^{\perp,\rho,\omega}=0.14\pm0.06,\quad a_2^{\phi}=0.18\pm0.08,\quad a_2^{\perp,\phi}=0.14\pm0.07. \quad (2.61)$$

Note that $a_1^V=0$, $a_1^{\perp,V}$=0 for $V=\rho,\omega,\phi$. The Gegenbauer moments $a_i^{\parallel\,(\perp),A}$ for axial-vector mesons are summarized in Table III. This table is taken from [22] with some updates on the Gegenbauer moments $a_0^{\perp,K_{1A}}$, $a_0^{\parallel,K_{1B}}$, $a_1^{\parallel,K_{1A}}, a_2^{\perp,K_{1A}}, a_2^{\parallel,K_{1B}}$, $a_1^{\perp,K_{1B}}$, $a_1^{\perp,a_1}$ and $a_1^{\perp,f_1^{^3P_1}}$. As stressed before, the values of the G-parity violating Gegenbauer moments (e.g. $a_1^K, a_1^{\parallel,K_{1A}}, a_{0,2}^{\perp,K_{1A}}, a_1^{\perp,K_{1B}}$ and $a_{0,2}^{\parallel,K_{1B}}$) are displayed for the mesons containing a strange quark. Their signs are flipped for the mesons containing a $\bar{s}$ quark. In general, $\Phi_K(1-x)=\Phi_{\bar{K}}(x)$.

For the B meson, we shall use $\lambda_B(1\ \mathrm{GeV}) = (250 \pm 100)$ MeV for its wave function and $f_B = 210 \pm 20$ MeV for its decay constant.

The Wilson coefficients $c_i(\mu)$ at various scales, $\mu = 4.4$ GeV, 2.1 GeV, 1.45 GeV and 1 GeV are taken from [41]. For the renormalization scale of the decay amplitude, we choose $\mu = m_b(m_b)$. However, as will be discussed below, the hard spectator and annihilation contributions will be evaluated at the hard-collinear scale $\mu_h = \sqrt{\mu\Lambda_h}$ with $\Lambda_h \approx 500$ MeV.

III. $B \to VA, AA$ DECAYS IN QCD FACTORIZATION

Within the framework of QCD factorization [5], the effective Hamiltonian matrix elements are written in the form

$$\langle M_1 M_2|\mathcal{H}_{\rm eff}|\overline{B}\rangle = \frac{G_F}{\sqrt{2}} \sum_{p=u,c} \lambda_p \langle M_1 M_2|\mathcal{T}_{\mathcal{A}}{}^{h,p} + \mathcal{T}_{\mathcal{B}}{}^{h,p}|\overline{B}\rangle\,, \tag{3.1}$$

where $\lambda_p \equiv V_{pb}V_{pq}^*$ with $q = d, s$, and the superscript h denotes the helicity of the final-state meson. $\mathcal{T}_{\mathcal{A}}{}^{h,p}$ describes contributions from naive factorization, vertex corrections, penguin contractions and spectator scattering expressed in terms of the flavor operators $a_i^{p,h}$, while $\mathcal{T}_{\mathcal{B}}$ contains annihilation topology amplitudes characterized by the annihilation operators $b_i^{p,h}$.

The flavor operators $a_i^{p,h}$ are basically the Wilson coefficients in conjunction with short-distance nonfactorizable corrections such as vertex corrections and hard spectator interactions. In general, they have the expressions [5, 6]

$$\begin{aligned} a_i^{p,h}(M_1M_2) \;=\; & \left(c_i + \frac{c_{i\pm1}}{N_c}\right) N_i^h(M_2) \int_0^1 \Phi^{M_2,h}(x)dx \\ & + \frac{c_{i\pm1}}{N_c}\,\frac{C_F\alpha_s}{4\pi}\Big[V_i^h(M_2) + \frac{4\pi^2}{N_c} H_i^h(M_1M_2)\Big] + P_i^{h,p}(M_2), \end{aligned} \tag{3.2}$$

where $i = 1, \cdots, 10$, the upper (lower) signs apply when i is odd (even), c_i are the Wilson coefficients, $C_F = (N_c^2-1)/(2N_c)$ with $N_c = 3$, M_2 is the emitted meson and M_1 shares the same spectator quark with the B meson. The quantities $V_i^h(M_2)$ account for vertex corrections, $H_i^h(M_1M_2)$ for hard spectator interactions with a hard gluon exchange between the emitted meson and the spectator quark of the B meson and $P_i(M_2)$ for penguin contractions. The LCDA $\Phi^{M,h}$ in the first term of Eq. (3.2) is $\Phi_\parallel^M$ for $h = 0$ and $\Phi_\perp^M$ for $h = \pm$. The expression of the quantities $N_i^h(M_2)$ reads

$$N_i^h(M_2) = \begin{cases} 0, & i = 6, 8, \\ 1, & \text{else.} \end{cases} \tag{3.3}$$

<u>*Vertex corrections*</u>

The vertex corrections are given by

$$V_i^0(M_2) = \begin{cases} \displaystyle\int_0^1 dx\, \Phi_\parallel^{M_2}(x) \Big[12\ln\frac{m_b}{\mu} - 18 + g(x)\Big], & (i = 1\text{–}4, 9, 10) \\ \displaystyle\int_0^1 dx\, \Phi_\parallel^{M_2}(x) \Big[-12\ln\frac{m_b}{\mu} + 6 - g(1-x)\Big], & (i = 5, 7) \\ \displaystyle\int_0^1 dx\, \Phi_{m_2}(x) \Big[-6 + h(x)\Big], & (i = 6, 8) \end{cases} \tag{3.4}$$

$$V_i^{\pm}(M_2) = \begin{cases} \displaystyle\int_0^1 dx\, \Phi_{\pm}^{M_2}(x) \Big[12 \ln \frac{m_b}{\mu} - 18 + g_T(x) \Big], & (i = 1\text{–}4, 9, 10) \\ \displaystyle\int_0^1 dx\, \Phi_{\mp}^{M_2}(x) \Big[-12 \ln \frac{m_b}{\mu} + 6 - g_T(1-x) \Big], & (i = 5, 7) \\ 0, & (i = 6, 8) \end{cases} \tag{3.5}$$

with

$$\begin{aligned} g(x) &= 3\left(\frac{1-2x}{1-x} \ln x - i\pi \right) \\ &\quad + \Big[2\mathrm{Li}_2(x) - \ln^2 x + \frac{2 \ln x}{1-x} - (3 + 2i\pi) \ln x - (x \leftrightarrow 1-x) \Big], \\ h(x) &= 2\mathrm{Li}_2(x) - \ln^2 x - (1 + 2i\pi) \ln x - (x \leftrightarrow 1-x), \\ g_T(x) &= g(x) + \frac{\ln x}{\bar{x}}, \end{aligned} \tag{3.6}$$

where $\bar{x} = 1 - x$, $\Phi_{\parallel}^M$ is a twist-2 light-cone distribution amplitude of the meson M, Φ_m (for the longitudinal component), and $\Phi_{\pm}$ (for transverse components) are twist-3 ones. Specifically, $\Phi_m = \Phi_v$ for $M = V$ and $\Phi_m = \Phi_a$ for $M = A$.

Hard spectator terms

$H_i^h(M_1 M_2)$ arise from hard spectator interactions with a hard gluon exchange between the emitted meson and the spectator quark of the $\overline{B}$ meson. $H_i^0(M_1 M_2)$ have the expressions:

$$H_i^0(M_1 M_2) = \frac{i f_B f_{M_1} f_{M_2}}{X_0^{(\overline{B} M_1, M_2)}} \frac{m_B}{\lambda_B} \int_0^1 du dv \left(\frac{\Phi_{\parallel}^{M_1}(u) \Phi_{\parallel}^{M_2}(v)}{\bar{u}\bar{v}} \pm r_\chi^{M_1} \frac{\Phi_{m_1}(u) \Phi_{\parallel}^{M_2}(v)}{\bar{u} v} \right), \tag{3.7}$$

for $i = 1 - 4, 9, 10$,

$$H_i^0(M_1 M_2) = -\frac{i f_B f_{M_1} f_{M_2}}{X_0^{(\overline{B} M_1, M_2)}} \frac{m_B}{\lambda_B} \int_0^1 du dv \left(\frac{\Phi_{\parallel}^{M_1}(u) \Phi_{\parallel}^{M_2}(v)}{\bar{u} v} \pm r_\chi^{M_1} \frac{\Phi_{m_1}(u) \Phi_{\parallel}^{M_2}(v)}{\bar{u}\bar{v}} \right), \tag{3.8}$$

for $i = 5, 7$, and $H_i^0(M_1 M_2) = 0$ for $i = 6, 8$, where the upper (lower) signs apply when $M_1 = V$ ($M_1 = A$). The transverse hard spectator terms $H_i^{\pm}(M_1 M_2)$ read

$$H_i^-(M_1 M_2) = \eta^-(M_1 M_2) \frac{2 i f_B f_{M_1}^{\perp} f_{M_2} m_{M_2}}{m_B X_-^{(\overline{B} M_1, M_2)}} \frac{m_B}{\lambda_B} \int_0^1 du dv \frac{\Phi_{\perp}^{M_1}(u) \Phi_-^{M_2}(v)}{\bar{u}^2 v}, \tag{3.9}$$

$$H_i^+(M_1 M_2) = \eta^+(M_1 M_2) \frac{2 i f_B f_{M_1} f_{M_2} m_{M_1} m_{M_2}}{m_B^2 X_+^{(\overline{B} M_1, M_2)}} \frac{m_B}{\lambda_B} \int_0^1 du dv \frac{(\bar{u} - v) \Phi_+^{M_1}(u) \Phi_+^{M_2}(v)}{\bar{u}^2 \bar{v}^2}, \tag{3.10}$$

for $i = 1 - 4, 9, 10$, and

$$H_i^-(M_1 M_2) = \sigma^-(M_1 M_2) \frac{2 i f_B f_{M_1}^{\perp} f_{M_2} m_{M_2}}{m_B X_-^{(\overline{B} M_1, M_2)}} \frac{m_B}{\lambda_B} \int_0^1 du dv \frac{\Phi_{\perp}^{M_1}(u) \Phi_+^{M_2}(v)}{\bar{u}^2 \bar{v}}, \tag{3.11}$$

$$H_i^+(M_1 M_2) = \sigma^+(M_1 M_2) \frac{2 i f_B f_{M_1} f_{M_2} m_{M_1} m_{M_2}}{m_B^2 X_+^{(\overline{B} M_1, M_2)}} \frac{m_B}{\lambda_B} \int_0^1 du dv \frac{(u - v) \Phi_+^{M_1}(u) \Phi_-^{M_2}(v)}{\bar{u}^2 v^2}, \tag{3.12}$$

for $i = 5, 7$, and

$$H_i^-(M_1M_2) \;=\; \sigma^-(M_1M_2)\frac{if_Bf_{M_1}f_{M_2}m_{M_2}}{m_BX_-^{(\overline{B}M_1,M_2)}}\frac{m_Bm_{M_1}}{m_{M_2}^2}\;\frac{m_B}{\lambda_B}\int_0^1 dudv\;\frac{\Phi_+^{M_1}(u)\Phi_\perp^{M_2}(v)}{v\bar{u}\bar{v}}, \quad (3.13)$$

$$H_i^+(M_1M_2) \;=\; 0, \quad (3.14)$$

for $i = 6, 8$, where

$$\begin{aligned}
\eta^-(M_1M_2) \;&=\; \begin{cases} +1; & \text{for } M_1M_2 = VV, VA, \\ -1; & \text{for } M_1M_2 = AV, AA, \end{cases} \\
\sigma^-(M_1M_2) \;&=\; \begin{cases} +1; & \text{for } M_1M_2 = VA, AV, \\ -1; & \text{for } M_1M_2 = VV, AA, \end{cases} \\
\sigma^+(M_1M_2) \;&=\; \begin{cases} +1; & \text{for } M_1M_2 = VA, AA, \\ -1; & \text{for } M_1M_2 = VV, AV, \end{cases}
\end{aligned} \quad (3.15)$$

and $\eta^+(M_1M_2) = -1$. To write down Eq. (3.13), we have factored out the $r_\chi^{M_2}$ term so that $a_6^\pm$ will contribute to the decay amplitude in the product of $r_\chi^{M_2}a_6^\pm \propto r_\chi^{M_2}H_6^\pm$. Two remarks are in order: (i) We have checked explicitly that the hard spectator terms depend on the B meson wave function $\Phi_1^B(\rho)$, but not on $\Phi_2^B(\rho)$. (ii) Since Beneke *et al.* [13] adopted the Jacob convention for transverse polarization states, they have $\epsilon_1^* \cdot \epsilon_2^* = 1$. As a consequence, their expressions for the parameters $\eta^\pm$, $\sigma^\pm$ and the decay amplitudes $X_\pm^{(\overline{B}V_1,V_2)}$ defined below have signs opposite to ours. Nevertheless, the expressions for $H_i^\pm(M_1M_2)$ are independent of the choice for transverse polarization vectors.

The helicity dependent factorizable amplitudes defined by

$$X^{(\overline{B}M_1,M_2)} = \langle M_2(p_2,\epsilon_2^*)|J_\mu|0\rangle\langle M_1(p_1,\epsilon_1^*)|J^\mu|B\rangle \quad (3.16)$$

have the expressions

$$\begin{aligned}
X_0^{(\overline{B}V_1,M_2)} \;&=\; \frac{if_{M_2}}{2m_{V_1}}\left[(m_B^2 - m_{V_1}^2 - m_{M_2}^2)(m_B + m_{V_1})A_1^{BV_1}(q^2) - \frac{4m_B^2p_c^2}{m_B + m_{V_1}}A_2^{BV_1}(q^2)\right], \\
X_0^{(\overline{B}A_1,M_2)} \;&=\; \frac{if_{M_2}}{2m_{A_1}}\left[(m_B^2 - m_{A_1}^2 - m_{M_2}^2)(m_B - m_{A_1})V_1^{BA_1}(q^2) - \frac{4m_B^2p_c^2}{m_B - m_{A_1}}V_2^{BA_1}(q^2)\right], \\
X_\pm^{(\overline{B}V_1,M_2)} \;&=\; -if_{M_2}m_Bm_{M_2}\left[\left(1 + \frac{m_{V_1}}{m_B}\right)A_1^{BV_1}(q^2) \mp \frac{2p_c}{m_B + m_{V_1}}V^{BV_1}(q^2)\right], \\
X_\pm^{(\overline{B}A_1,M_2)} \;&=\; -if_{M_2}m_Bm_{M_2}\left[\left(1 - \frac{m_{A_1}}{m_B}\right)V_1^{BA_1}(q^2) \mp \frac{2p_c}{m_B - m_{A_1}}A^{BA_1}(q^2)\right],
\end{aligned} \quad (3.17)$$

where $M_2 = V_2, A_2$ and p_c is the c.m. momentum.

Penguin terms

At order α_s, corrections from penguin contractions are present only for $i = 4, 6$. For $i = 4$ we obtain

$$\begin{aligned}
P_4^{h,p}(M_2) \;=\; \frac{C_F\alpha_s}{4\pi N_c}\Bigg\{ & c_1\Big[G_{M_2}^h(s_p) + g_{M_2}\Big] + c_3\Big[G_{M_2}^h(s_s) + G_{M_2}^h(1) + 2g_{M_2}\Big] \\
& + (c_4 + c_6)\sum_{i=u}^{b}\Big[G_{M_2}^h(s_i) + g'_{M_2}\Big] - 2c_{8g}^{\rm eff}G_g^h\Bigg\},
\end{aligned} \quad (3.18)$$

where $s_i = m_i^2/m_b^2$ and the function $G^h_{M_2}(s)$ is given by

$$\begin{aligned} G^h_{M_2}(s) &= 4\int_0^1 du\,\Phi^{M_2,h}(u)\int_0^1 dx\,x\bar{x}\ln[s-\bar{u}x\bar{x}-i\epsilon], \\ g_{M_2} &= \left(\frac{4}{3}\ln\frac{m_b}{\mu}+\frac{2}{3}\right)\int_0^1\Phi^{M_2,h}(x)dx, \\ g'_{M_2} &= \frac{4}{3}\ln\frac{m_b}{\mu}\int_0^1\Phi^{M_2,h}(x)dx, \end{aligned} \tag{3.19}$$

with $\Phi^{M_2,0}=\Phi^{M_2}_{\parallel}$, $\Phi^{M_2,\pm}=\Phi^{M_2}_{\pm}$. For $i=6$, the result for the penguin contribution is

$$P^{h,p}_6(M_2)=\frac{C_F\alpha_s}{4\pi N_c}\left\{c_1\hat{G}^h_{M_2}(s_p)+c_3\Big[\hat{G}^h_{M_2}(s_s)+\hat{G}^h_{M_2}(1)\Big]+(c_4+c_6)\sum_{i=u}^{b}\hat{G}^h_{M_2}(s_i)\right\}. \tag{3.20}$$

In analogy with (3.19), the function $\hat{G}_{M_2}(s)$ is defined as

$$\begin{aligned} \hat{G}^0_{M_2}(s) &= 4\int_0^1 du\,\Phi_{m_2}(u)\int_0^1 dx\,x\bar{x}\ln[s-\bar{u}x\bar{x}-i\epsilon], \\ \hat{G}^{\pm}_{M_2}(s) &= 0\,. \end{aligned} \tag{3.21}$$

Therefore, the transverse penguin contractions vanish for $i=6,8$: $P^{\pm,p}_{6,8}=0$. Note that we have factored out the $r^{M_2}_\chi$ term in Eq. (3.20) so that when the vertex correction $V_{6,8}$ is neglected, a^0_6 will contribute to the decay amplitude in the product $r^{M_2}_\chi a^0_6\approx r^{M_2}_\chi P^0_6$.

For $i=8,10$ we find

$$P^{h,p}_8(M_2)=\frac{\alpha_{\rm em}}{9\pi N_c}\,(c_1+N_c c_2)\,\hat{G}^h_{M_2}(s_p)\,, \tag{3.22}$$

$$P^{h,p}_{10}(M_2)=\frac{\alpha_{\rm em}}{9\pi N_c}\left\{(c_1+N_c c_2)\Big[G^h_{M_2}(s_p)+2g_{M_2}\Big]-3c^{\rm eff}_\gamma G^h_g\right\}. \tag{3.23}$$

For $i=7,9$,

$$P^{-,p}_{7,9}(M_2)=-\frac{\alpha_{\rm em}}{3\pi}C^{\rm eff}_{7\gamma}\frac{m_B m_b}{m^2_{M_2}}+\frac{2\alpha_{\rm em}}{27\pi}(c_1+N_c c_2)\left[\delta_{pc}\ln\frac{m_c^2}{\mu^2}+\delta_{pu}\ln\frac{\nu^2}{\mu^2}+1\right], \tag{3.24}$$

if $M_2=\rho^0,\omega,\phi$, otherwise $P^{-,p}_{7,9}(M_2)=0$. Here the first term is an electromagnetic penguin contribution to the transverse helicity amplitude enhanced by a factor of $m_B m_b/m^2_{M_2}$, as first pointed out in [42]. Note that the quark loop contains an ultraviolet divergence for both transverse and longitudinal components which must be subtracted in accordance with the scheme used to define the Wilson coefficients. The scale and scheme dependence after subtraction is required to cancel the scale and scheme dependence of the electroweak penguin coefficients. Therefore, the scale μ in the above equation is the same as the one appearing in the expressions for the penguin corrections, e.g. Eq. (3.19). On the other hand, the scale ν is referred to the scale of the decay constant $f_{M_2}(\nu)$ as the operator $\bar{q}\gamma^\mu q$ has a non-vanishing anomalous dimension in the presence of electromagnetic interactions [6]. The ν dependence of Eq. (3.24) is compensated by that of $f_{M_2}(\nu)$.

The relevant integrals for the dipole operators $O_{g,\gamma}$ are

$$\begin{aligned} G^0_g &= \int_0^1 du\,\frac{\Phi^{M_2}_\parallel(u)}{\bar{u}}\,, \\ G^\pm_g &= \int_0^1\frac{du}{\bar{u}}\left[\frac{1}{2}\Big(\bar{u}\Phi^{M_2}_-(u)-u\Phi^{M_2}_+(u)\Big)-\bar{u}\Phi^{M_2}_\pm(u)+\frac{1}{2}\Big(\bar{u}\Phi^{M_2}_-(u)+u\Phi^{M_2}_+(u)\Big)\right]. \end{aligned} \tag{3.25}$$

Using Eq. (2.44), $G_g^{\pm}$ can be further reduced to

$$\begin{aligned} G_g^+ &= \int_0^1 du \Big[\Phi_-^{M_2}(u) - \Phi_+^{M_2}(u)\Big] = 0, \\ G_g^- &= 0. \end{aligned} \tag{3.26}$$

Hence, $G_g^{\pm}$ in Eq. (3.25) are actually equal to zero. It was first pointed out by Kagan [11] that the dipole operators Q_{8g} and $Q_{7\gamma}$ do not contribute to the transverse penguin amplitudes at $\mathcal{O}(\alpha_s)$ due to angular momentum conservation.

Annihilation topologies

The weak annihilation contributions to the decay $\overline{B} \to M_1 M_2$ can be described in terms of the building blocks $b_i^{p,h}$ and $b_{i,\rm EW}^{p,h}$

$$\frac{G_F}{\sqrt{2}} \sum_{p=u,c} \lambda_p \langle M_1 M_2 | \mathcal{T}_{\mathcal{B}}^{h,p} | \overline{B}^0 \rangle = i \frac{G_F}{\sqrt{2}} \sum_{p=u,c} \lambda_p f_B f_{M_1} f_{M_2} \sum_i (d_i b_i^{p,h} + d_i' b_{i,\rm EW}^{p,h}). \tag{3.27}$$

The building blocks have the expressions

$$\begin{aligned} b_1 &= \frac{C_F}{N_c^2} c_1 A_1^i, \qquad b_3 = \frac{C_F}{N_c^2}\Big[c_3 A_1^i + c_5 (A_3^i + A_3^f) + N_c c_6 A_3^f\Big], \\ b_2 &= \frac{C_F}{N_c^2} c_2 A_1^i, \qquad b_4 = \frac{C_F}{N_c^2}\Big[c_4 A_1^i + c_6 A_2^f\Big], \\ b_{3,\rm EW} &= \frac{C_F}{N_c^2}\Big[c_9 A_1^i + c_7 (A_3^i + A_3^f) + N_c c_8 A_3^i\Big], \\ b_{4,\rm EW} &= \frac{C_F}{N_c^2}\Big[c_{10} A_1^i + c_8 A_2^i\Big], \end{aligned} \tag{3.28}$$

where for simplicity we have omitted the superscripts p and h in above expressions. The subscripts 1,2,3 of $A_n^{i,f}$ denote the annihilation amplitudes induced from $(V-A)(V-A)$, $(V-A)(V+A)$ and $(S-P)(S+P)$ operators, respectively, and the superscripts i and f refer to gluon emission from the initial and final-state quarks, respectively. Following [6] we choose the convention that M_1 contains an antiquark from the weak vertex and M_2 contains a quark from the weak vertex. The explicit expressions of weak annihilation amplitudes are:

$$\begin{aligned} A_1^{i,0}(M_1 M_2) &= \pi \alpha_s \int_0^1 du\, dv \left\{ C^{M_1 M_2}\, \Phi_\parallel^{M_1}(v) \Phi_\parallel^{M_2}(v) \left[\frac{1}{u(1-\bar{u}v)} + \frac{1}{u\bar{v}^2}\right] \right. \\ &\qquad \left. - D^{M_1 M_2}\, r_\chi^{M_1} r_\chi^{M_2}\, \Phi_{m_1}(u)\, \Phi_{m_2}(v) \frac{2}{u\bar{v}} \right\}, \end{aligned} \tag{3.29}$$

$$A_1^{i,-}(M_1 M_2) = -\pi \alpha_s \frac{2 m_{M_1} m_{M_2}}{m_B^2} \int_0^1 du\, dv \left\{ \Phi_-^{M_1}(u)\, \Phi_-^{M_2}(v) \left[\frac{\bar{u}+\bar{v}}{u^2 \bar{v}^2} + \frac{1}{(1-\bar{u}v)^2}\right] \right\}, \tag{3.30}$$

$$A_1^{i,+}(M_1 M_2) = -\pi \alpha_s \frac{2 m_{M_1} m_{M_2}}{m_B^2} \int_0^1 du\, dv \left\{ \Phi_+^{M_1}(u)\, \Phi_+^{M_2}(v) \left[\frac{2}{u\bar{v}^3} - \frac{v}{(1-\bar{u}v)^2} - \frac{v}{\bar{v}^2(1-\bar{u}v)}\right] \right\}, \tag{3.31}$$

$$A_2^{i,0}(M_1 M_2) = \pi \alpha_s \int_0^1 du\, dv \left\{ C^{M_1 M_2}\, \Phi_\parallel^{M_1}(v) \Phi_\parallel^{M_2}(v) \left[\frac{1}{\bar{v}(1-\bar{u}v)} + \frac{1}{u^2 \bar{v}}\right] \right.$$

$$-D^{M_1M_2}\, r_\chi^{M_1} r_\chi^{M_2}\, \Phi_{m_1}(u)\, \Phi_{m_2}(v) \frac{2}{u\bar{v}} \Bigg\}, \tag{3.32}$$

$$A_2^{i,-}(M_1M_2) \;=\; -\pi\alpha_s \frac{2m_{M_1}m_{M_2}}{m_B^2} \int_0^1 du\, dv \left\{ C^{M_1M_2}\, \Phi_+^{M_1}(u)\, \Phi_+^{M_2}(v) \times \left[\frac{u+v}{u^2\bar{v}^2} + \frac{1}{(1-\bar{u}v)^2} \right] \right\}, \tag{3.33}$$

$$A_2^{i,+}(M_1M_2) \;=\; -\pi\alpha_s \frac{2m_{M_1}m_{M_2}}{m_B^2} \int_0^1 du\, dv \left\{ C^{M_1M_2}\, \Phi_-^{M_1}(u)\, \Phi_-^{M_2}(v) \times \left[\frac{2}{u^3\bar{v}} - \frac{\bar{u}}{(1-\bar{u}v)^2} - \frac{\bar{u}}{u^2(1-\bar{u}v)} \right] \right\}, \tag{3.34}$$

$$A_3^{i,0}(M_1M_2) \;=\; \pi\alpha_s \int_0^1 du\, dv \left\{ C^{M_1M_2}\, r_\chi^{M_1} \Phi_{m_1}(v) \Phi_\parallel^{M_2}(v)\, \frac{2\bar{u}}{u\bar{v}(1-\bar{u}v)} + D^{M_1M_2}\, r_\chi^{M_2}\, \Phi_\parallel^{M_1}(v)\, \Phi_{m_2}(v) \frac{2v}{u\bar{v}(1-\bar{u}v)} \right\}, \tag{3.35}$$

$$A_3^{i,-}(M_1M_2) \;=\; -\pi\alpha_s \int_0^1 du\, dv \left\{ -C^{M_1M_2} \frac{m_{M_2}}{m_{M_1}} r_\chi^{M_1}\, \Phi_\perp^{M_1}(u)\, \Phi_-^{M_2}(v) \frac{2}{u\bar{v}(1-\bar{u}v)} + D^{M_1M_2} \frac{m_{M_1}}{m_{M_2}} r_\chi^{M_2}\, \Phi_+^{M_1}(u)\, \Phi_\perp^{M_2}(v) \frac{2}{u\bar{v}(1-\bar{u}v)} \right\}, \tag{3.36}$$

$$A_3^{f,0}(M_1M_2) \;=\; \pi\alpha_s \int_0^1 du\, dv \left\{ C^{M_1M_2}\, r_\chi^{M_1}\, \Phi_{m_1}(u) \Phi_\parallel^{M_2}(v)\, \frac{2(1+\bar{v})}{u\bar{v}^2} - D^{M_1M_2}\, r_\chi^{M_2}\, \Phi_\parallel^{M_1}(u)\, \Phi_{m_2}(v) \frac{2(1+u)}{u^2\bar{v}} \right\}, \tag{3.37}$$

$$A_3^{f,-}(M_1M_2) \;=\; -\pi\alpha_s \int_0^1 du\, dv \left\{ C^{M_1M_2}\, \frac{m_{M_2}}{m_{M_1}} r_\chi^{M_1}\, \Phi_\perp^{M_1}(u)\, \Phi_-^{M_2}(v) \frac{2}{u^2\bar{v}} + D^{M_1M_2}\, \frac{m_{M_1}}{m_{M_2}} r_\chi^{M_2}\, \Phi_+^{M_1}(u)\, \Phi_\perp^{M_2}(v)\, \frac{2}{u\bar{v}^2} \right\}, \tag{3.38}$$

and $A_1^{f,h} = A_2^{f,h} = A_3^{i,+} = A_3^{f,+} = 0$, where

$$\begin{aligned} &A_1^{i,0}, A_3^{i,0}: && D^{VA} = D^{AV} = -1, \\ &A_2^{i,0}, A_2^{i,\pm}: && C^{VA} = C^{AV} = -1, \\ &A_3^{i,-}, A_3^{f,0}, A_3^{f,-}: && C^{AV} = C^{AA} = -1, \quad D^{VA} = D^{AV} = -1, \end{aligned} \tag{3.39}$$

and the parameters C and D are equal to $+1$ for all other cases. Note that our results for $A_n^{i(f),\pm}$ have opposite signs to that in [13] as Beneke *et al.* adopted the Jacob convention for the transverse polarization vectors. We employ the same convention as in [6] that M_1 contains an antiquark from the weak vertex with longitudinal fraction $\bar{y}$, while M_2 contains a quark from the weak vertex with momentum fraction x.

Since the annihilation contributions $A_{1,2}^{i,\pm}$ are suppressed by a factor of $m_1 m_2/m_B^2$ relative to other terms, in numerical analysis we will consider only the annihilation contributions due to $A_3^{f,0}$, $A_3^{f,-}$, $A_{1,2,3}^{i,0}$ and $A_3^{i,-}$.

Finally, two remarks are in order: (i) Although the parameters $a_i (i \neq 6, 8)$ and $a_{6,8} r_\chi$ are formally renormalization scale and γ_5 scheme independent, in practice there exists some residual scale dependence in $a_i(\mu)$ to finite order. To be specific, we shall evaluate the vertex corrections to the decay amplitude at the scale $\mu = m_b$. (The issue with the renormalization scale μ will be discussed in more detail in Sec. IV). In contrast, as stressed in [5], the hard spectator and annihilation contributions should be evaluated at the hard-collinear scale $\mu_h = \sqrt{\mu \Lambda_h}$ with $\Lambda_h \approx$ 500 MeV. (ii) Power corrections in QCDF always involve troublesome endpoint divergences. For example, the annihilation amplitude has endpoint divergences even at twist-2 level and the hard spectator scattering diagram at twist-3 order is power suppressed and posses soft and collinear divergences arising from the soft spectator quark. Since the treatment of endpoint divergences is model dependent, subleading power corrections generally can be studied only in a phenomenological way. We shall follow [5] to model the endpoint divergence $X \equiv \int_0^1 dx/\bar{x}$ in the annihilation and hard spectator scattering diagrams as

$$X_A = \ln\left(\frac{m_B}{\Lambda_h}\right)(1 + \rho_A e^{i\phi_A}), \qquad X_H = \ln\left(\frac{m_B}{\Lambda_h}\right)(1 + \rho_H e^{i\phi_H}), \tag{3.40}$$

with the unknown real parameters $\rho_{A,H}$ and $\phi_{A,H}$. For simplicity, we shall assume that X_A^h and X_H^h are helicity independent; that is, $X_A^- = X_A^+ = X_A^0$ and $X_H^- = X_H^+ = X_H^0$.

IV. NUMERICAL RESULTS

The decay amplitude of $B \to M_1 M_2$ with $M = V, A$ has the general expression of $\varepsilon_{M_1}^{*\mu}(\lambda_{M_1}) \varepsilon_{M_2}^{*\nu}(\lambda_{M_2}) M_{\mu\nu}$ with λ_{M_1,M_2} being the corresponding helicities. Hence, the decay amplitude can be decomposed into three components, one for each helicity of the final state: $\mathcal{A}_0, \mathcal{A}_+, \mathcal{A}_-$. The transverse amplitudes defined in the transversity basis are related to the helicity ones via

$$\mathcal{A}_\parallel = \frac{\mathcal{A}_+ + \mathcal{A}_-}{\sqrt{2}}, \qquad \mathcal{A}_\perp = \frac{\mathcal{A}_+ - \mathcal{A}_-}{\sqrt{2}}. \tag{4.1}$$

The decay rate can be expressed in terms of these amplitudes as

$$\Gamma = \frac{p_c}{8\pi m_B^2}(|\mathcal{A}_0|^2 + |\mathcal{A}_+|^2 + |\mathcal{A}_-|^2) = \frac{p_c}{8\pi m_B^2}(|\mathcal{A}_L|^2 + |\mathcal{A}_\parallel|^2 + |\mathcal{A}_\perp|^2), \tag{4.2}$$

with p_c being the c.m. momentum of the final-state meson. Polarization fractions are defined as

$$f_\alpha \equiv \frac{\Gamma_\alpha}{\Gamma} = \frac{|\mathcal{A}_\alpha|^2}{|\mathcal{A}_0|^2 + |\mathcal{A}_\parallel|^2 + |\mathcal{A}_\perp|^2}, \tag{4.3}$$

with $\alpha = L, \parallel, \perp$. The relative phases are

$$\phi_\perp = \arg(\mathcal{A}_\perp/\mathcal{A}_0), \qquad \phi_\parallel = \arg(\mathcal{A}_\parallel/\mathcal{A}_0). \tag{4.4}$$

Note that the experimental results of $\phi_\parallel$ and $\phi_\perp$ obtained by BaBar and Belle are for $B \to \phi K^*$ decays [49, 50, 51]. According to the convention given by BaBar and Belle, $|\mathcal{A}_+| > |\mathcal{A}_-|$ and

$\phi_\parallel = \phi_\perp = \pi$ for $B \to \phi K^*$ in the absence of final-state interactions. Since our calculations are for $\overline{B} \to \phi \overline{K}^*$ decays, in Eq. (4.14) below we shall transform BaBar and Belle results from $\phi_\parallel$ to $\pi - \phi_\parallel$ and $\phi_\perp$ to $-\phi_\perp$ so that $|\bar{\mathcal{A}}_+| < |\bar{\mathcal{A}}_-|$ in $\overline{B} \to \phi \overline{K}^*$. When strong phases vanish, $\phi_\parallel = 0$, $\phi_\perp = -\pi$ for $\overline{B} \to \phi \overline{K}^*$.

A. $B \to VV$ decays

The branching ratios and polarization fractions of charmless $\overline{B} \to VV$ decays have been measured for $\rho\rho$, $\rho\omega$, ρK^*, $\phi K^*, \omega K^*$ and $K^* \bar{K}^*$ final states. It is naively expected that the helicity amplitudes $\bar{\mathcal{A}}_h$ (helicities $h = 0, -, +$) for $\overline{B} \to VV$ respect the hierarchy pattern

$$\bar{\mathcal{A}}_0 : \bar{\mathcal{A}}_- : \bar{\mathcal{A}}_+ = 1 : \left(\frac{\Lambda_{\rm QCD}}{m_b}\right) : \left(\frac{\Lambda_{\rm QCD}}{m_b}\right)^2 . \tag{4.5}$$

Hence, they are dominated by the longitudinal polarization states and satisfy the scaling law, namely [11]

$$1 - f_L = \mathcal{O}\left(\frac{m_V^2}{m_B^2}\right), \qquad \frac{f_\perp}{f_\parallel} = 1 + \mathcal{O}\left(\frac{m_V}{m_B}\right), \tag{4.6}$$

with $f_L, f_\perp$ and $f_\parallel$ being the longitudinal, perpendicular, and parallel polarization fractions, respectively. In sharp contrast to the $\rho\rho$ case, the large fraction of transverse polarization observed in $B \to K^*\rho$ and $B \to K^*\phi$ decays at B factories (see Table IV below) is thus a surprise and poses an interesting challenge for any theoretical interpretation. Therefore, in order to obtain a large transverse polarization in $B \to K^*\rho, K^*\phi$, this scaling law must be circumvented in one way or another. Various mechanisms such as sizable penguin-induced annihilation contributions [11], final-state interactions [16, 18], form-factor tuning [43] and new physics [9, 12, 44, 45] (where only the models with large scalar or tensor coupling can explain the observation for $f_\perp \simeq f_\parallel$ [12, 44]) have been proposed for solving the $B \to VV$ polarization puzzle. It has been shown that when the data for ϕK^* and $K\eta^{(\prime)}$ modes are simultaneously taken in into account, the standard model predictions with weak annihilation corrections can explain the observation, while the new physics effect due to scalar-type operators is negligible [46].

Before proceeding, we would like to make a few remarks on the polarization anomaly. First, the hierarchy of helicity amplitudes given by Eq. (4.5) is valid only for factorizable W-emission amplitudes. It may be violated in the presence of nonfactorizable corrections (e.g. vertex, penguin and hard spectator scattering contributions) and annihilation contributions. Indeed, we shall show below that the polarization pattern (4.6) will get modified when nonfactorizable contributions are included in QCD factorization. We shall see later that the polarization anomaly is not so serious as originally believed. Second, it is known that the predicted rates for the penguin dominated $B \to VP, VV$ decays in QCD factorization are generally too small by a factor of $2 \sim 3$ compared to the data. It is obvious that in order to have a reliable calculation for polarization fractions, it is of great importance to first reproduce the decay rates correctly. Otherwise, the estimation of $f_{L,\parallel,\perp}$ will not be trustworthy. Hence, our first priority is to have a mechanism resolving the branching ratio puzzle for the penguin dominated charmless $B \to VV$ decays and hopefully the same mechanism also unravels the polarization anomaly.

1. Tree-dominated decays

Branching ratios and polarization fractions for tree-dominated $B \to \rho\rho$ and $\rho\omega$ are shown in Table IV. The theoretical errors correspond to the uncertainties due to variation of (i) the Gegenbauer moments, the decay constants, (ii) the heavy-to-light form factors and the strange quark mass, and (iii) the wave function of the B meson characterized by the parameter λ_B, the power corrections due to weak annihilation and hard spectator interactions described by the parameters $\rho_{A,H}$, $\phi_{A,H}$, respectively. To obtain the errors shown in Tables VII-XI, we first scan randomly the points in the allowed ranges of the above nine parameters and then add errors in quadrature. More specifically, the second error in the table is referred to the uncertainties caused by the variation of $\rho_{A,H}$ and $\phi_{A,H}$, where all other uncertainties are lumped into the first error. Here we consider the default results for tree-dominated decays by setting the annihilation parameters to be zero, i.e. $\rho_A = \phi_A = 0$, though the predictions are insensitive to the choice of them.

It is obvious from Table IV that the longitudinal amplitude dominates the tree-dominated decays except for the $\rho^0\omega$ mode where the transverse polarization could be equally important. The naive expectation of $f_L \approx 1 - 4m_\rho^2/m_B^2 \approx 0.92$ is experimentally confirmed. The calculated rates are also in agreement with experiment except that the predicted rate for $B^- \to \rho^-\omega$ is slightly high. Its decay amplitude reads

$$\begin{aligned}\sqrt{2}\,\mathcal{A}^h_{B^-\to\rho^-\omega} &\approx \left[\delta_{pu}(\alpha_2^h+\beta_2^h)+2\alpha_3^{p,h}+\alpha_4^{p,h}+\beta_3^{p,h}\right]X_h^{(\overline{B}\rho,\omega)}\\ &+ \left[\delta_{pu}(\alpha_1^h+\beta_2^h)+\alpha_4^{p,h}+\beta_3^{p,h}\right]X_h^{(\overline{B}\omega,\rho)}. \end{aligned} \tag{4.7}$$

It is obvious that this decay is dominantly governed by $B \to \omega$ transition form factors. The data of $B^- \to \rho^-\omega$ and $B \to K^*\omega$ to be discussed below seem to suggest that $B \to \omega$ form factors are slightly smaller than what are expected from the light-cone sum rules [33].

2. Penguin-dominated decays

The decays of interest in this category are $B \to K^*\rho, K^*\phi, K^*\omega$ and $K^*\bar{K}^*$.

$\underline{B \to K^*\rho}$

We first consider $\bar{B} \to K^*\rho$ decays. Retaining the leading contributions, their decay amplitudes are approximated by

$$\begin{aligned}\mathcal{A}_{B^-\to\overline{K}^{*0}\rho^-} &\approx V_c(\alpha_4^{c,h}+\beta_3^h)X^h_{\rho\bar{K}^*},\\ \sqrt{2}\mathcal{A}_{B^-\to K^{*-}\rho^0} &\approx \left[V_u\alpha_1^h+V_c(\alpha_4^{c,h}+\beta_3^h)\right]X^h_{\rho\bar{K}^*}+\left[V_u\alpha_2^h+V_c\frac{3}{2}\alpha^h_{3,\rm EW}\right]X^h_{\bar{K}^*\rho},\\ \mathcal{A}_{\overline{B}^0\to K^{*-}\rho^+} &\approx \left[V_u\alpha_1^h+V_c(\alpha_4^{c,h}+\beta_3^h)\right]X^h_{\rho\bar{K}^*},\\ -\sqrt{2}\mathcal{A}_{\overline{B}^0\to\overline{K}^{*0}\rho^0} &\approx V_c(\alpha_4^{c,h}+\beta_3^h)X^h_{\rho\bar{K}^*}-\left[V_u\alpha_2^h+V_c\frac{3}{2}\alpha^h_{3,\rm EW}\right]X^h_{\bar{K}^*\rho}, \end{aligned} \tag{4.8}$$

where $V_p \equiv V_{pb}V_{ps}^*$ with $|V_c| \gg |V_u|$, β_3 characterizes the penguin-induced weak annihilation (see Eq. (B1) for definition) and $X^h_{\rho\bar{K}^*}$ is a shorthand notation for $X^h_{\bar{B}\to\rho\bar{K}^*}$ with its explicit expression

TABLE IV: CP-averaged branching ratios (in units of 10^{-6}) and polarization fractions for $\bar{B} \to \rho\rho, \rho\omega, K^*\rho, K^*\phi, K^*\omega, K^*\bar{K}^*$ decays. The annihilation parameters are specified to be $\rho_A = 0.78$ and $\phi_A = -43^\circ$ for $K^*\rho, K^*\bar{K}^*$ and $\rho_A = 0.65$ and $\phi_A = -53^\circ$ for $K^*\phi$ and $K^*\omega$ by default. For longitudinal polarization fraction, the theoretical uncertainty is dominated by $\rho_{A,H}$ and $\phi_{A,H}$, and hence only this error is listed in the table for f_L. Experimental results are taken from [3, 4, 47, 48, 49, 50, 51, 52, 53, 54, 55, 56, 57, 58, 59, 60, 61] and the world averages from [62].

Decay	$\mathcal{B}$		f_L		$f_\perp$	
	Theory	Expt	Theory	Expt	Theory	Expt
$B^- \to \rho^-\rho^0$	$20.0^{+4.0+2.0}_{-1.9-0.9}$	18.2 ± 3.0	$0.96^{+0.02}_{-0.02}$	$0.912^{+0.044}_{-0.045}$	0.02 ± 0.01	
$\overline{B}^0 \to \rho^+\rho^-$	$25.5^{+1.5+2.4}_{-2.6-1.5}$	$24.2^{+3.1}_{-3.2}$	$0.92^{+0.01}_{-0.02}$	$0.978^{+0.025}_{-0.022}$	$0.04^{+0.01}_{-0.00}$	
$\overline{B}^0 \to \rho^0\rho^0$	$0.9^{+1.5+1.1}_{-0.4-0.2}$	0.68 ± 0.27	$0.92^{+0.06}_{-0.36}$	0.70 ± 0.15	$0.04^{+0.14}_{-0.03}$	
$B^- \to \rho^-\omega$	$19.2^{+3.3+1.7}_{-1.6-1.0}$	$10.6^{+2.6}_{-2.3}$	$0.96^{+0.02}_{-0.02}$	0.82 ± 0.11	0.02 ± 0.01	
$\overline{B}^0 \to \rho^0\omega$	$0.1^{+0.1+0.4}_{-0.1-0.0}$	< 1.5	$0.55^{+0.47}_{-0.29}$		$0.22^{+0.16}_{-0.23}$	
$B^- \to \bar{K}^{*0}\rho^-$ [a]	$9.2^{+1.2+3.6}_{-1.1-5.4}$	9.2 ± 1.5	$0.48^{+0.52}_{-0.40}$	0.48 ± 0.08	$0.26^{+0.20}_{-0.26}$	
$B^- \to K^{*-}\rho^0$	$5.5^{+0.6+1.3}_{-0.5-2.5}$	< 6.1	$0.67^{+0.31}_{-0.48}$	$0.96^{+0.06}_{-0.16}$ [b]	$0.16^{+0.24}_{-0.15}$	
$\overline{B}^0 \to K^{*-}\rho^+$	$8.9^{+1.1+4.8}_{-1.0-5.5}$	< 12	$0.53^{+0.45}_{-0.32}$		$0.24^{+0.16}_{-0.22}$	
$\overline{B}^0 \to \bar{K}^{*0}\rho^0$	$4.6^{+0.6+3.5}_{-0.5-3.5}$	5.6 ± 1.6	$0.39^{+0.60}_{-0.31}$	0.57 ± 0.12	$0.30^{+0.15}_{-0.30}$	
$B^- \to K^{*-}\phi$ [c]	$10.0^{+1.4+12.3}_{-1.3-\ 6.1}$	10.0 ± 1.1	$0.49^{+0.51}_{-0.42}$	0.50 ± 0.05	$0.25^{+0.21}_{-0.25}$	0.20 ± 0.05
$\overline{B}^0 \to \bar{K}^{*0}\phi$	$9.5^{+1.3+11.9}_{-1.2-\ 5.9}$	9.5 ± 0.8	$0.50^{+0.50}_{-0.42}$	0.484 ± 0.034	$0.25^{+0.21}_{-0.25}$	0.256 ± 0.032
$B^- \to K^{*-}\omega$	$3.5^{+0.4+3.0}_{-0.4-1.7}$	< 3.4	$0.66^{+0.32}_{-0.38}$		$0.17^{+0.20}_{-0.17}$	
$\overline{B}^0 \to \bar{K}^{*0}\omega$	$3.0^{+0.5+2.9}_{-0.4-1.8}$	< 2.7	$0.57^{+0.44}_{-0.46}$		$0.21^{+0.25}_{-0.22}$	
$B^- \to K^{*0}K^{*-}$	$0.6^{+0.1+0.3}_{-0.1-0.3}$	< 71	$0.45^{+0.55}_{-0.38}$		$0.27^{+0.19}_{-0.27}$	
$\overline{B}^0 \to K^{*-}K^{*+}$	$0.1^{+0.0+0.1}_{-0.0-0.1}$	< 141	1		0	
$\overline{B}^0 \to K^{*0}\bar{K}^{*0}$	$0.6^{+0.1+0.2}_{-0.1-0.3}$	$1.28^{+0.37}_{-0.32}$	$0.52^{+0.48}_{-0.48}$	$0.80^{+0.12}_{-0.13}$	$0.24^{+0.24}_{-0.24}$	

[a] This mode is employed as an input for extracting the parameters ρ_A and ϕ_A for $B \to K^*\rho$ decays.
[b] A recent BaBar measurement gives $f_L(K^{*-}\rho^0) = 0.9 \pm 0.2$ [47], but it has only 2.5σ significance.
[c] This mode is employed as an input for extracting the parameters ρ_A and ϕ_A for $B \to K^*\phi$ decays.

shown in Eq. (3.17). The expressions of the flavor parameters $\alpha_i^{h,p}$ in terms of the coefficients $a_i^{h,p}$ can be found in Eq. (A1). To proceed, we shall first neglect annihilation completely by setting $\beta_3 = 0$. In the absence of NLO nonfactorizable corrections, the parameters $\alpha_i^{h,p}$ are helicity independent and hence the hierarchy relation (4.5) for helicity amplitudes is respected as $|X^0_{\bar{K}^*\rho}| : |X^-_{\bar{K}^*\rho}| : |X^+_{\bar{K}^*\rho}| = 1 : 0.26 : 0.03$ and $|X^0_{\rho\bar{K}^*}| : |X^-_{\rho\bar{K}^*}| : |X^+_{\rho\bar{K}^*}| = 1 : 0.30 : 0.005$. When vertex, penguin and hard spectator corrections are taken into account, we see from Table V that $\alpha_2^h, \alpha_4^{p,h}$ and $\alpha^h_{3,\rm EM}$ for negative helicity differ significantly from that the longitudinal ones. For example, the real parts of α_2^h and $\alpha^h_{3,\rm EW}$ have opposite signs for $h = 0$ and $h = -$. Let us consider two extreme cases for the longitudinal polarization fraction. From Eq. (4.8) we have

$$\left.\frac{\mathcal{A}^-}{\mathcal{A}^0}\right|_{\bar{B}^0 \to \bar{K}^{*0}\rho^0} \approx \left(\frac{\alpha_4^{c,-} - \frac{3}{2}\alpha^-_{3,\rm EW}}{\alpha_4^{c,0} - \frac{3}{2}\alpha^0_{3,\rm EW}}\right)\left(\frac{X^-_{\bar{K}^*\rho}}{X^0_{\bar{K}^*\rho}}\right),$$

TABLE V: Longitudinal- and negative-helicity amplitude parameters.

Parameter	$h=0$	$h=-$	Parameter	$h=0$	$h=-$
$\alpha_1(\rho K^*)$	$0.96+0.01i$	$1.11+0.03i$	$\alpha_{3,\rm EW}(K^*\rho)$	$-0.009-0.000i$	$0.010-0.000i$
$\alpha_2(K^*\rho)$	$0.24-0.08i$	$-0.16-0.16i$	$\alpha_{4,\rm EW}(K^*\rho)$	$-0.002+0.001i$	$0.001+0.001i$
$\alpha_4^u(\rho K^*)$	$-0.022-0.014i$	$-0.048-0.016i$	$\beta_3(\rho K^*)$	$0.008-0.018i$	$-0.031+0.060i$
$\alpha_4^c(\rho K^*)$	$-0.030-0.010i$	$-0.047-0.002i$			
$\alpha_3(K^*\phi)$	$0.005-0.001i$	$-0.004-0.001i$	$\alpha_{3,\rm EW}(K^*\phi)$	$-0.009-0.000i$	$0.002-0.000i$
$\alpha_4^u(K^*\phi)$	$-0.022-0.014i$	$-0.048-0.016i$	$\alpha_4^c(K^*\phi)$	$-0.030-0.010i$	$-0.046-0.002i$
$\beta_3(K^*\phi)$	$0.008-0.019i$	$-0.028+0.053i$			

$$\left.\frac{\mathcal{A}^-}{\mathcal{A}^0}\right|_{B^-\to K^{*-}\rho^0} \approx \left(\frac{\alpha_4^{c,-}+\frac{3}{2}\alpha_{3,\rm EW}^-}{\alpha_4^{c,0}+\frac{3}{2}\alpha_{3,\rm EW}^0}\right)\left(\frac{X_{\bar K^*\rho}^-}{X_{\bar K^*\rho}^0}\right). \tag{4.9}$$

From Table V we see that the interference between $\alpha_4^{c,h}$ and $\alpha_{3,\rm EW}^h$ is constructive for $h=-$ and destructive for $h=0$ for the decay $\bar B^0\to\bar K^{*0}\rho^0$ and the other way around for $B^-\to K^{*-}\rho^0$. As a consequence, $\mathcal{A}^-$ is comparable to $\mathcal{A}^0$ for the former but is highly suppressed relative to $\mathcal{A}^0$ for the latter. The longitudinal polarization fraction for the penguin dominated processes can be approximated as

$$\begin{aligned} f_L(\rho K^*) &\simeq 1-\frac{|\alpha_4^{c,-}+c_v\alpha_{3,\rm EW}^{c,-}+\beta_3^-|^2\left|X_{\rho K^*}^-\right|^2}{\sum_{h=0,-}|\alpha_4^{c,h}+c_v\alpha_{3,\rm EW}^{c,-}+\beta_3^h|^2\left|X_{\rho K^*}^h\right|^2},\\ f_L(K^*\phi) &\simeq 1-\frac{|\alpha_3^-+\alpha_4^{c,-}+\frac{1}{2}\alpha_{3,\rm EW}^{c,-}+\beta_3^-|^2\left|X_{K^*\phi}^-\right|^2}{\sum_{h=0,-}|\alpha_3^h+\alpha_4^{c,h}+\frac{1}{2}\alpha_{3,\rm EW}^{c,-}+\beta_3^h|^2\left|X_{K^*\phi}^h\right|^2}, \end{aligned} \tag{4.10}$$

where $|X_{\rho K^*}^-/X_{\rho K^*}^0|^2\simeq(m_{K^*}/m_B)^2A_0^{B\to\rho}/F_-^{B\to\rho}\propto(m_{K^*}/m_B)^2$, $c_v=0$ for $\overline{K}^{*0}\rho^-$ and $K^{*-}\rho^+$ modes, $c_v=1$ for $K^{*-}\rho^0$ and $c_v=-1$ for $\overline{K}^{*0}\rho^0$ (see Ref. [13] for the definitions of the A_0 and F_- form factors). The calculated branching ratios and the longitudinal polarization fractions f_L in QCDF are shown in the case (i) of Table VI. Indeed, we find $f_L(\bar K^{*0}\rho^0)=0.46$ and $f_L(K^{*-}\rho^0)=0.97$. If the coefficients a_i^h are helicity independent, we will have $f_L(\bar K^{*0}\rho^0)=0.91$ rather than 0.46 ! However, the NLO corrections to a_i^- will render the negative helicity amplitude $\mathcal{A}^-(\bar K^{*0}\rho^0)$ comparable to the longitudinal one $\mathcal{A}^0(\bar K^{*0}\rho^0)$ so that even at the short-distance level, f_L for $\overline{B}^0\to\bar K^{*0}\rho^0$ can be as low as 50%. Similar detailed discussions for ϕK^* modes will be given latter.

Comparing with the data, it appears that even though the naive estimate of f_L is too large for $\bar K^{*0}\rho^-$, the experimental observation of a large f_L for $K^{*-}\rho^0$ and a small f_L for $\bar K^{*0}\rho^0$ are well accommodated. However, as stressed before, in order to have a trustworthy estimate of polarization fractions one has to reproduce the rates correctly as the predicted branching fractions for $\bar K^{*0}\rho^-$ and $\bar K^{*0}\rho^0$ are too small compared to experiment (see Table VI). In the present work, we shall follow [11] to ascribe the necessary enhancement to a potentially large penguin annihilation characterized

TABLE VI: CP-averaged branching ratios (in units of 10^{-6}) and the longitudinal polarization fraction f_L for $B \to K^*\rho$ and $K^*\phi$ decays for three cases: (i) no annihilation contribution, (ii) adding annihilation contributions with $\rho_A = 0.78$, $\phi_A = -43^\circ$ for $K^*\rho$ and $\rho_A = 0.65$, $\phi_A = -53^\circ$ for $K^*\phi$. The predictions by Beneke, Rohrer and Yang [13] are shown in the last two columns. For simplicity, only the central values are exhibited. The theoretical uncertainties in case (ii) are shown in Table IV. Experimental results are taken from [3, 47, 48].

Decay	Expt		(i)		(ii)		BRY	
	$\mathcal{B}$	f_L	$\mathcal{B}$	f_L	$\mathcal{B}$	f_L	$\mathcal{B}$	f_L
$B^- \to \bar{K}^{*0}\rho^-$	9.2 ± 1.5	0.48 ± 0.08	4.0	0.82	9.2	0.48	5.9	0.56
$B^- \to K^{*-}\rho^0$	< 6.1	$0.96^{+0.06}_{-0.16}$	3.8	0.97	5.5	0.67	4.5	0.84
$\overline{B}^0 \to K^{*-}\rho^+$	< 12	$-$	3.8	0.86	8.9	0.53	5.5	0.61
$\overline{B}^0 \to \bar{K}^{*0}\rho^0$	5.6 ± 1.6	0.57 ± 0.12	1.1	0.50	4.6	0.39	2.4	0.22
$B^- \to K^{*-}\phi$	10.0 ± 1.1	0.50 ± 0.05	4.1	0.62	10.0	0.49	10.1	0.45
$\overline{B}^0 \to \bar{K}^{*0}\phi$	9.5 ± 0.8	0.484 ± 0.034	3.8	0.62	9.5	0.50	9.3	0.44

by the parameter β_3. We fit the data of $B^- \to \bar{K}^{*0}\rho^-$ by adjusting the parameters ρ_A and ϕ_A that characterize the nonperturbative effects of soft gluon exchanges in annihilation diagrams. From Fig. 1(a) we see that ρ_A is preferred to be around 0.78 in order to fit the rate, while the corresponding f_L is around 0.48 (see Fig. 1(c)). Only the theoretical uncertainty due to the variation of the phase ϕ_A is considered in Fig. 1. It is clear that the total branching ratio and the longitudinal one $\mathcal{B}_L$ increase with ρ_A, whereas f_L decreases slowly with ρ_A. To fit the rate and f_L simultaneously for $B^- \to \bar{K}^{*0}\rho^-$, we find $\rho_A \approx 0.78$ and $\phi_A \approx -43^\circ$. Using this set of parameters, we are able to predict branching ratios and polarization fractions for other $\overline{B} \to K^*\rho$ decays as exhibited in Table IV and in case (ii) of Table VI. In the presence of penguin annihilation, the parameter $\alpha_4^{c,h}$ in Eqs. (4.8) and (4.9) should be replaced by $\alpha_4^{c,h} + \beta_3^h$. From Table V, one can check that both $f_L(\bar{K}^{*0}\rho^0)$ and $f_L(K^{*-}\rho^0)$ will be decreased when penguin annihilation is turned on.

Within the QCDF framework, Beneke, Rohrer and Yang (BRY) have employed the choice $\rho_A = 0.6$ and $\phi_A = -40^\circ$ obtained from a fit to the data of $K^*\phi$ to study $\bar{K}^*\rho$ decays [13]. They have noticed that the calculated $K^*\rho$ branching fractions are systematically below the measurements. This is not a surprise as their ρ_A is smaller than 0.78 [see also Fig. 1(a)], since as emphasized before, the estimation of polarization fractions will not be reliable unless the calculated partial rate agrees with experiment and as shown below that $K^*\phi$ and $K^*\rho$ data cannot be fitted simultaneously by two universal parameters ρ_A and ϕ_A. This may be a potential problem for QCDF.

The large longitudinal polarization fraction of $B^- \to K^{*-}\rho^0$, $f_L = 0.96^{+0.06}_{-0.16}$, measured by BaBar [3] seems to be peculiar as a smaller f_L of order 0.5 is observed in other $K^*\rho$ modes such as $\bar{K}^{*0}\rho^-$ and $\bar{K}^{*0}\rho^0$. At first sight, it appears that the BRY's prediction of $f_L(K^{*-}\rho^0) = 0.84^{+0.02+0.16}_{-0.03-0.25}$ can account for the BaBar measurement. However, as we note in Appendix D, there are sign errors in the expressions of the annihilation terms $A_3^{f,0}$ and $A_3^{i,0}$ (see Eqs. (D2) and (D17), respectively) by BRY: The signs of the $r_\chi^{V_2}$ terms in these two equations are erroneous in [13]. Because of

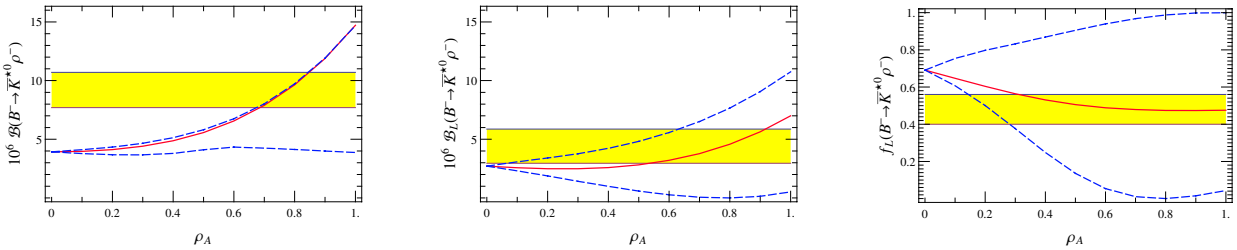

(a) (b) (c)

FIG. 1: Predicted branching ratios [(a) and (b) are for the total and longitudinal branching ratios, respectively] and (c) the longitudinal polarization fraction for $B^- \to \bar{K}^{*0}\rho^-$ as a function of the parameter ρ_A. The solid and dashed curves correspond to the central value and the allowed theoretical uncertainty due to the variation of ϕ_A, respectively. The horizontal band represents experimental values with one sigma errors.

the (incorrect) cancelation between $r_\chi^{V_1}$ and $r_\chi^{V_2}$ terms in $A_3^{f,0}$, BRY claimed (wrongly) that the longitudinal penguin annihilation amplitude β_3^0 is strongly suppressed, while the β_3^- term receives sizable penguin annihilation contribution. If a wrong sign for $r_\chi^{V_2}$ terms is used, both rates and longitudinal polarization fractions will be reduced, especially for the $\bar{K}^{*0}\rho^0$ mode where f_L is reduced by more than a factor of 2 (see the case (iii) of Table VI). For comparison, BRY's predictions are shown in the last two columns of the same table. Using the correct expressions for $A_3^{f,0}$ and $A_3^{i,0}$, we find that $f_L(K^{*-}\rho^0)$ is reduced to the 70% level and $f_L(\bar{K}^{*0}\rho^0)$ is predicted to be $0.39^{+0.60}_{-0.31}$. The latter agrees with the experimental value $f_L(\bar{K}^{*0}\rho^0) = 0.57 \pm 0.12$ [62]. As explained above, the corresponding prediction $0.22^{+0.03+0.53}_{-0.03-0.14}$ by BRY is too small owing to the incorrect signs in their $A_3^{f,0}$ amplitudes.

In short, we have the pattern (see also [13])

$$f_L(K^{*-}\rho^0) > f_L(K^{*-}\rho^+) > f_L(\bar{K}^{*0}\rho^-) > f_L(\bar{K}^{*0}\rho^0) \tag{4.11}$$

for the longitudinal fractions in $B \to K^*\rho$ decays. Note that the quoted experimental value $f_L(K^{*-}\rho^0) = 0.96^{+0.06}_{-0.16}$ in Tables IV and VI was obtained by BaBar in a previous measurement where $K^{*-}\rho^0$ and $K^{*-}f_0(980)$ were not separated [3]. This has been overcome in a recent BaBar measurement, but the resultant value $f_L(K^{*-}\rho^0) = 0.9 \pm 0.2$ has only 2.5σ significance [47]. At any rate, it would be important to have a refined measurement of longitudinal polarization fraction for $K^{*-}\rho^0$ and $\bar{K}^{*0}\rho^0$ and a new measurement of $f_L(K^{*-}\rho^+)$ to test the hierarchy pattern (4.11).

$\underline{B \to K^*\phi}$

Experimentally, $B \to K^*\phi$ decays have been studied with full angular analysis from which information on final-state interactions can be extracted. Historically, it was the observation of large transverse polarization in these decays that had triggered the theoretical and experimental interest in the study of charmless $B \to VV$ decays.

Theoretically, $B \to K^*\phi$ decays can be analyzed in the same manner as the $K^*\rho$ modes. The

decay amplitude of $B^- \to K^{*-}\phi$ can be approximated as

$$\mathcal{A}^h_{B^-\to K^{*-}\phi} \approx V_c(\alpha^h_3 + \alpha^{c,h}_4 + \beta^h_3 - \frac{1}{2}\alpha^h_{3,\rm EW})X^h_{K^*\phi}. \tag{4.12}$$

When the penguin annihilation contribution β_3 is turned off, we have

$$\left.\frac{\mathcal{A}^-}{\mathcal{A}^0}\right|_{B^-\to K^{*-}\phi} \approx \left(\frac{\alpha^-_3 + \alpha^{c,-}_4 - \frac{1}{2}\alpha^-_{3,\rm EW}}{\alpha^0_3 + \alpha^{c,0}_4 - \frac{1}{2}\alpha^0_{3,\rm EW}}\right)\left(\frac{X^-_{K^*\phi}}{X^0_{K^*\phi}}\right). \tag{4.13}$$

From the amplitude parameters given in Table V, it is clear that there exists a constructive (destructive) interference in the $\mathcal{A}^-$ ($\mathcal{A}^0$) amplitude. As a consequence, although the factorizable amplitudes respect the hierarchy $|X^0_{K^*\phi}| : |X^-_{K^*\phi}| : |X^+_{K^*\phi}| = 1 : 0.35 : 0.007$ due to the $(V-A)$ structure of weak interactions and helicity conservation in strong interactions, the negative- and longitudinal-helicity amplitudes are comparable in magnitude. Numerically, we indeed find $f_L = 0.62$ and $f_\parallel \sim f_\perp = 0.19$ (see Table VI). This is very similar to the decay $\overline{B}^0 \to \bar{K}^{*0}\rho^0$ where f_L is also found to be small, of order 0.50 . Experimentally, the naive expectation of $f_L \approx 1 - 4m_V/m^2_B \sim 0.90$ is strongly violated in charmless penguin-dominated VV modes. Nevertheless, a small f_L for $K^*\phi$ is quite natural in QCD factorization because the parameters a^h_i are helicity dependent. The fact that real parts of α_3 and $\alpha_{3,\rm EW}$ flip signs from $h = 0$ to $h = -$ and that α^h_4 is smaller in magnitude for the longitudinal amplitude (see Table V) will render the negative helicity amplitude comparable to the longitudinal one.

Even though the longitudinal polarization fraction is reduced to 60% level in the absence of penguin annihilation, this does not mean that the polarization anomaly is resolved. As stated before, irrespective of the predictions for polarization fractions, the first task we need to focus on is to reproduce the correct rate for $B \to K^*\phi$ because the calculated branching ratio of order 4.1×10^{-6} is too small by a factor of ~ 2.5 compared to the measured one, $\sim 10 \times 10^{-6}$ (cf. Table IV). Assuming weak annihilation to account for the discrepancy between theory and experiment, we can fit the data of branching ratios and f_L simultaneously by adjusting the parameters ρ_A and ϕ_A. However, this also means that QCDF loses its predictive power in this manner. We find that the rate and f_L can be accommodated by having $\rho_A \approx 0.65$ and $\phi_A \approx -53^\circ$. This set of the annihilation parameters differs slightly from that extracted from $B \to K^*\rho$ decays, namely, $\rho_A(K^*\rho) \approx 0.78$ and $\phi_A(K^*\rho) \approx -43^\circ$. Therefore, within the framework of QCDF, one cannot account for all charmless $B \to VV$ data by a universal set of ρ_A and ϕ_A parameters. This could be an indiction that large penguin annihilation cannot be the ultimate story for understanding $B \to VV$ decays.

Since the complete angular analysis of $\overline{B} \to \bar{K}^*\phi$ has been performed by both BaBar and Belle, information on the parallel and perpendicular polarizations and their phases relative to the longitudinal one is available. We see from Table IV that $f_\perp$ and $f_\parallel$ are very similar, of order 0.25. Experimentally, the phases $\phi_\parallel$ and $\phi_\perp$ deviate from either π or zero by more than 4.6σ and 3.3σ for $K^{*-}\phi$ and 5.5σ for $\bar{K}^{*0}\phi$ [62]. This implies the presence of final-state interactions. The relative phases are calculated to be

$$\begin{aligned} \phi_\parallel(K^{*-}\phi) &= (80^{+43}_{-83})^\circ \qquad (\text{expt}: \ (46 \pm 10)^\circ), \\ \phi_\parallel(\bar{K}^{*0}\phi) &= (78^{+43}_{-81})^\circ \qquad (\text{expt}: \ (44^{+8}_{-7})^\circ), \end{aligned} \tag{4.14}$$

and $\phi_\parallel(K^{*-}\phi) - \phi_\perp(K^{*-}\phi) - \pi = \phi_\parallel(\bar{K}^{*0}\phi) - \phi_\perp(\bar{K}^{*0}\phi) - \pi \approx 0.7^\circ$. They are consistent with the data.

Thus far we have chosen the renormalization scale to be $\mu = m_b(m_b)$ in calculations. We now address the issue with μ. In principle, physics should be independent of the choice of μ, but in practice there exists some residual μ dependence in the truncated calculations. We have checked explicitly that the decay rates without annihilation are indeed essentially stable against μ. However, when penguin annihilation is turned on, it is sensitive to the choice of the renormalization scale because the penguin annihilation contribution characterized by the parameter b_3 is dominantly proportional to $\alpha_s(\mu_h)c_6(\mu_h)$ at the hard-collinear scale $\mu_h = \sqrt{\mu\Lambda_h}$. For the hadronic scale $\Lambda_h \approx 500$ MeV, we have $\mu_h \approx 1.45$ GeV and 1 GeV for $\mu = 4.2$ GeV and 2.1 GeV, respectively. At the amplitude level, the enhancement of penguin annihilation at $\mu = 2.1$ GeV is of order $\alpha_s(1)c_6(1)/[\alpha_s(1.45)c_6(1.45)] \sim 1.8$. We find that if the renormalization scale is chosen to be $\mu = m_b(m_b)/2 = 2.1$ GeV, we cannot fit the branching ratios and polarization fractions simultaneously for both $B \to K^*\phi$ and $B \to K^*\rho$ decays. For example, the rate of the former can be accommodated with $\rho_A \sim 0.25$, but the corresponding $f_L \sim 0.28$ is too small. Likewise, although $\mathcal{B}(B^- \to \bar{K}^{*0}\rho^-)$ can be fitted well with $\rho_A \sim 0.55$, the resultant $f_L \lesssim 0.12$ is highly suppressed. This is ascribed to the fact that at the scale $\mu = 2.1$ GeV, the negative-helicity amplitude receives much more enhancement than the longitudinal one and hence the longitudinal polarization is suppressed at the small μ scale. In order to ensure the validity of the penguin-annihilation mechanism for describing $B \to VV$ decays, we will confine ourselves to the renormalization scale $\mu = m_b(m_b)$ in the ensuing study.

$\underline{B \to K^*\omega}$

The decay amplitudes for $B \to K^*\omega$ read

$$\begin{aligned}
\sqrt{2}\mathcal{A}_{B^-\to K^{*-}\omega} &\approx \left[V_u\alpha_1^h + V_c(\alpha_4^{c,h} + \beta_3^h)\right] X^h_{\omega\bar{K}^*} + \left[V_u\alpha_2^h + V_c(2\alpha_3^h + \frac{1}{2}\alpha^h_{3,\rm EW})\right] X^h_{\bar{K}^*\omega}, \\
\sqrt{2}\mathcal{A}_{\bar{B}^0\to \bar{K}^{*0}\omega} &\approx \left[V_c(\alpha_4^{c,h} + \beta_3^h)\right] X^h_{\omega\bar{K}^*} + \left[V_u\alpha_2^h + V_c(2\alpha_3^h + \frac{1}{2}\alpha^h_{3,\rm EW})\right] X^h_{\bar{K}^*\omega}. \qquad (4.15)
\end{aligned}$$

From the previous analysis of $K^*\rho$ and $K^*\phi$ decays, we found two distinct sets of the penguin annihilation parameters ρ_A and ϕ_A. If the set of parameters inferred from $B \to K^*\rho$ decays, namely, $\rho_A = 0.78$ and $\phi_A = -43^\circ$, is employed, we obtain $\mathcal{B}(B^- \to K^{*-}\omega) \approx 4.5 \times 10^{-6}$ and $\mathcal{B}(\overline{B}^0 \to \bar{K}^{*0}\omega) \approx 3.9 \times 10^{-6}$, which are slightly higher than the respective experimental upper limits, 3.4×10^{-6} and 2.7×10^{-6} [58, 61]. By contrast, if the parameters $\rho_A = 0.65$ and $\phi_A = -53^\circ$ extracted from $K^*\phi$ modes are used, the resultant predictions $\mathcal{B}(B^- \to K^{*-}\omega) \approx 3.5 \times 10^{-6}$ and $\mathcal{B}(\overline{B}^0 \to \bar{K}^{*0}\omega) \approx 3.0 \times 10^{-6}$ are consistent with experiment (see Table IV). Of course, if the $B \to \omega$ form factors are smaller than what we expected as implied by the measurement of $B^- \to \rho^-\omega$, then $\mathcal{B}(B \to K^*\omega)$ will be safely below the current bounds.

$\underline{B \to K^*\bar{K}^*}$

The expressions of $B \to K^* \bar{K}^*$ decay amplitudes read

$$\begin{aligned}
\mathcal{A}_{B^- \to K^{*0} K^{*-}} &= \frac{G_F}{\sqrt{2}} \sum_{p=u,c} \lambda_p^{(d)} \Big[\delta_{pu} \beta_2 + \alpha_4^p - \frac{1}{2} \alpha_{4,\rm EW}^p + \beta_3^p + \beta_{3,\rm EW}^p \Big] X^{(\overline{B} \bar{K}^*, K^*)}, \\
\mathcal{A}_{\overline{B}^0 \to K^{*-} K^{*+}} &= \frac{G_F}{\sqrt{2}} \sum_{p=u,c} \lambda_p^{(d)} \Bigg\{ \Big[\delta_{pu} \beta_1 + \beta_4^p + \beta_{4,\rm EW}^p \Big] X^{(\overline{B} \bar{K}^*, K^*)} + f_B f_{K^*}^2 \left[b_4^p - \frac{1}{2} b_{4,\rm EW}^p \right]_{K^* \bar{K}^*} \Bigg\}, \\
\mathcal{A}_{\overline{B}^0 \to \bar{K}^{*0} K^{*0}} &= \frac{G_F}{\sqrt{2}} \sum_{p=u,c} \lambda_p^{(d)} \Bigg\{ \Big[\alpha_4^p - \frac{1}{2} \alpha_{4,\rm EW}^p + \beta_3^p + \beta_4^p - \frac{1}{2} \beta_{3,\rm EW}^p - \frac{1}{2} \beta_{4,\rm EW}^p \Big] X^{(\overline{B} \bar{K}^*, K^*)} \\
&+ f_B f_{K^*}^2 \left[b_4^p - \frac{1}{2} b_{4,\rm EW}^p \right]_{K^* \bar{K}^*} \Bigg\}. \qquad (4.16)
\end{aligned}$$

Both $\overline{B}^0 \to \bar{K}^{*0} K^{*0}$ and $B^- \to K^{*0} K^{*-}$ are $b \to d$ penguin-dominated decays, while $\overline{B}^0 \to K^{*-} K^{*+}$ proceeds only through weak annihilation. Hence, their branching ratios are expected to be small, of order $\lesssim 10^{-6}$. Recently, the $\bar{K}^{*0} K^{*0}$ mode was first measured by BaBar with the branching ratio $(1.28^{+0.37}_{-0.32}) \times 10^{-6}$ [59]. Our prediction is slightly smaller, about 1σ away from the BaBar measurement (Table IV). The absence of transverse polarization in the $K^{*-} K^{*+}$ mode is due to the approximation we have adapted; that is, we have neglected the transverse annihilation contributions $A_{1,2}^{\pm}$ relative to other terms. Hence, transverse polarization does not receive contributions from the annihilation terms $b_1^{\pm}, b_2^{\pm}, b_4^{\pm}, b_{4,\rm EW}^{\pm}$ within our approximation [see Eq. (3.28)].

Comparison with other works

Within the framework of QCD factorization, we have studied charmless $B \to VV$ decays closely to the works of Kagan [11] and Beneke, Rohrer and Yang (BRY) [13]. Nevertheless, there are some differences between our work and theirs as we are going to discuss below.

Without penguin annihilation, Kagan found $f_L \approx 0.90$ for the $\bar{K}^{*0} \phi$ mode, while BRY got $f_L \approx 0.67$ and we obtained $f_L \approx 0.62$. Kagan did not consider vertex corrections and hard spectator interactions in his realistic calculations of $a_i^{p,h}$, though he has discussed the latter briefly. It seems to us that a_i^h are essentially helicity independent in the Kagan's calculation and this accounts for the difference in the estimation of f_L. Moreover, what is the initial value of f_L in the absence of penguin annihilation is immaterial because we will use the unknown annihilation parameters to *accommodate* the data of branching ratios and f_L rather than to *predict* them.

We differ from BRY mainly for using different ρ_A and ϕ_A parameters for describing $B \to K^* \rho$ decays. If we follow BRY to use the set of ρ_A and ϕ_A parameters extracted from $B \to K^* \phi$ decays to describe $K^* \rho$ modes, the rates for the latter will be systematically below the measurements. Since it is necessary to reproduce the measured rates first in order to have a reliable estimate of polarization fractions, we need to fit the $K^* \rho$ data separately. The resultant ρ_A and ϕ_A parameters differ from the ones determined from $K^* \phi$ modes. This can be viewed as a potential problem of QCDF.

In the pQCD approach, the calculated branching ratio of $\overline{B} \to \bar{K}^* \phi$ is too large, of order 15×10^{-6} and $f_L \sim 0.75$ [14]. It has been proposed in [43] that a smaller form factor $A_0^{BK^*}(0) \approx 0.30$ will bring down both the rates and f_L and bring up $f_\parallel$ and $f_\perp$. While this sounds plausible, the NLO

corrections to helicity-dependent coefficients a_i^h should be taken into account in this approach as we have demonstrated that NLO corrections to a_i^- and a_i^0 will bring down f_L significantly. It is also important to compute the rates and polarization fractions for $\overline{B} \to \bar{K}^* \rho$ decays in this framework and compare with experiment.

Another plausible solution is to consider the long-distance rescattering contributions from some charm intermediate states such as $D^{(*)} D_s^{(*)}$ [16, 17, 18]. The idea is simple: First, $B \to D^* D_s^*$ decays are CKM favored and hence final-state interactions via charm intermediate states will bring up the $K^*\phi$ rates. This is welcome since the short-distance predictions of the branching fractions for penguin-dominated $B \to VV$ modes in most of the models under consideration are too small compared to experiment. Second, large transverse polarization induced from $B \to D^* D_s^*$ will be propagated to ϕK^* via final-state rescattering. The unknown parameter in the model for final-state rescattering is fixed by the measured rate [18]. However, this approach has one drawback. That is, while the longitudinal polarization fraction can be reduced significantly from short-distance predictions due to final-state interaction effects, no sizable perpendicular polarization $f_\perp$ is found owing mainly to the large cancelations occurring in the processes $B \to D_s^* D \to \phi K^*$ and $B \to D_s D^* \to \phi K^*$ and this can be understood as a consequence of CP and SU(3) symmetry [18]. That is, final-state rescattering leads to the suppression of $f_T (= f_\perp + f_\parallel)$ at the expense of $f_\parallel \gg f_\perp$. As pointed out in [18], one possibility to circumvent the aforementioned cancelation is to consider the contributions from the even-parity charmed meson intermediate states. In view of the fact that even at the short-distance level, f_L can be as small as 40% to 70% after NLO corrections to effective Wilson coefficients are taken into account, it is worth re-examining this type of solution again.

In soft-collinear effective theory (SCET) [15], large transverse polarization in penguin-dominated VV modes may arise from the long-distance charming penguin contribution. Indeed, the aforementioned mechanism of final-state rescattering of charm intermediate states mimics the charming penguin in SCET, while both QCDF and pQCD approaches rely on penguin annihilation to resolve the polarization anomaly.[2]

B. $B \to VA$ decays

The calculated branching ratios and longitudinal polarization fractions for the decays $B \to A\rho$, AK^*, $A\omega$, $A\phi$ with $A = a_1(1260), b_1(1235), K_1(1270), K_1(1400), f_1(1285), f_1(1420), h_1(1170), h_1(1380)$ are collected in Tables VII-IX.

1. $\overline{B} \to a_1 V,\ b_1 V$ *decays*

The decays $\overline{B}^0 \to (a_1^+, b_1^+)(\rho^-, \pi^-)$ are governed by the decay constants of the ρ and π, respectively. Since $f_\rho \gg f_\pi$, we thus expect to have $\mathcal{B}(\overline{B}^0 \to a_1^+ \rho^-) \gg \mathcal{B}(\overline{B}^0 \to a_1^+ \pi^-)$ and

[2] Ways of distinguishing penguin annihilation from rescattering have been recently proposed in [63].

$\mathcal{B}(\overline{B}^0 \to b_1^+\rho^-) \gg \mathcal{B}(\overline{B}^0 \to b_1^+\pi^-) \sim 10\times 10^{-6}$. These features are borne out in our realistic calculations (see Table VII). Calderón, Muñoz and Vera (CMV) [21] found the other way around: $(a_1^+, b_1^+)\rho^-$ modes have rates smaller than $(a_1^+, b_1^+)\pi^-$ ones, which we strongly disagree. Since the modes $(a_1^-, b_1^-)(\rho^+, \pi^+)$ are governed by f_{a_1} and f_{b_1}, respectively, and since $f_{a_1} \sim f_\rho$ and f_{b_1} is very small (vanishing for the neutral b_1), we anticipate that $a_1^-\rho^+$ and $a_1^-\pi^+$ have comparable rates and the $b_1^-\rho^+$ mode is highly suppressed relative to the $b_1^+\rho^-$ one. [3] The decays $(a_1^-, b_1^-)\rho^0$ receive both color-allowed and color-suppressed contributions:

$$\begin{aligned}
\mathcal{A}_{B^-\to a_1^-\rho^0} &\propto (a_1^h + \cdots)X_h^{(\bar{B}\rho,a_1)} + (a_2^h + \cdots)X_h^{(\bar{B}a_1,\rho)},\\
\mathcal{A}_{B^-\to b_1^-\rho^0} &\propto (a_1^h + \cdots)X_h^{(\bar{B}\rho,b_1)} + (a_2^h + \cdots)X_h^{(\bar{B}b_1,\rho)},
\end{aligned} \tag{4.17}$$

where $X^{(\bar{B}M_1,M_2)}$ is the factorizable amplitude defined by Eq. (3.16). Since the color-allowed amplitude of the $b_1^-\rho^0$ mode is highly suppressed by the smallness of the b_1 decay constant and the color-suppressed amplitude is suppressed by the small ratio of a_2/a_1, it is clear that $\mathcal{B}(B^- \to a_1^-\rho^0) \gg \mathcal{B}(B^- \to b_1^-\rho^0)$. The decays $(a_1^-, b_1^-)\omega$ should have rates similar to $(a_1^-, b_1^-)\rho^0$. So far there is only one experimental measurement of $B \to VA$ decays, namely, $B^0 \to a_1^\pm\rho^\mp$ with the result [64]

$$\mathcal{B}(B^0 \to a_1^\pm\rho^\mp)\mathcal{B}(a_1^\pm \to (3\pi)^\pm) < 61\times 10^{-6}. \tag{4.18}$$

Assuming that $a_1^\pm$ decays exclusively to $\rho^0\pi^\pm$, we then have the upper limit of 61×10^{-6} for the branching ratio of $B^0 \to a_1^\pm\rho^\mp$. Our prediction $\mathcal{B}(B^0 \to a_1^\pm\rho^\mp) \approx 59\times 10^{-6}$ is thus consistent with experiment.

To discuss the effect of the annihilation contribution, let us take the penguin-dominated decays $\overline{B}^0 \to (a_1^+, b_1^+)K^{*-}$ as an example. From Eq. (A3) of [1] we have

$$\begin{aligned}
\mathcal{A}_{\bar{B}^0\to a_1^+K^{*-}} &\propto (\alpha_4^c + \alpha_{4,\rm EW}^c)X^{(\bar{B}a_1,K^*)} + if_Bf_{a_1}f_{K^*}(b_3^c - \frac{1}{2}b_{3,\rm EW}^c)_{a_1K^*},\\
\mathcal{A}_{\bar{B}^0\to b_1^+K^{*-}} &\propto (\alpha_4^c + \alpha_{4,\rm EW}^c)X^{(\bar{B}b_1,K^*)} + if_Bf_{b_1}^\perp f_{K^*}(b_3^c - \frac{1}{2}b_{3,\rm EW}^c)_{b_1K^*},
\end{aligned} \tag{4.19}$$

where we have replaced the decay constant f_{b_1} by $f_{b_1}^\perp$ as explained before (see the paragraph after Eq. (2.52)). From penguin-dominated $B \to VV$ decays we learn that the predicted rates in default are typically too small by a factor of $2 \sim 3$. In the absence of the experimental information for penguin-dominated $B \to VA$ decays, we shall use the penguin-annihilation parameters $\rho_A = 0.65$ and $\phi_A = -53^\circ$ inferred from $B \to K^*\phi$ decays as a guidance for annihilation enhancement. Since the magnitude of b_3 is large for the b_1K^* modes (specifically, $b_3^0(b_1K^*) = -1.78 + 9.92i$ and $b_3^0(a_1K^*) = -0.19 + 4.11i$), $B \to b_1K^*$ decays receive more enhancement from penguin annihilation than $B \to a_1K^*$ ones. When penguin annihilation is turned off, we have, for example,

$$\begin{aligned}
&\mathcal{B}(\overline{B}^0 \to a_1^+K^{*-}) = (3.6^{+1.6+0.5}_{-1.3-0.1})\times 10^{-6}, \qquad \mathcal{B}(\overline{B}^0 \to b_1^+K^{*-}) = (4.1^{+2.3+0.3}_{-2.0-0.3})\times 10^{-6},\\
&\mathcal{B}(B^- \to a_1^-\bar{K}^{*0}) = (4.1^{+2.0+1.7}_{-1.6-0.1})\times 10^{-6}, \qquad \mathcal{B}(B^- \to b_1^-\bar{K}^{*0}) = (4.0^{+2.0+0.7}_{-2.5-0.6})\times 10^{-6}.
\end{aligned} \tag{4.20}$$

[3] As explained in [1], within the QCD factorization approach, the suppression of $b_1^-(\pi^+, \rho^+)$ modes is not directly related to the smallness of the b_1 decay constant, but is ascribed to the tiny coefficient a_1. However, the smallness of a_1 has to do with the decay constant suppression. For more details, see [1].

TABLE VII: Branching ratios (in units of 10^{-6}) and the longitudinal polarization fraction (in parentheses) for the decays $B \to (a_1,\ b_1)(\rho,\ \omega,\ \phi,\ K^*)$ with $a_1 = a_1(1260)$ and $b_1 = b_1(1235)$. The theoretical errors correspond to the uncertainties due to variation of (i) Gegenbauer moments, decay constants, quark masses, form factors, the λ_B parameter for the B meson wave function, and (ii) $\rho_{A,H}$, $\phi_{A,H}$, respectively. For longitudinal polarization fractions, we add all errors in quadrature as the theoretical uncertainty is usually dominated by (ii). Default results are for $\rho_A = 0.65$ and $\phi_A = -53^\circ$. We use the light-cone sum rule results for the $B \to a_1$ and $B \to b_1$ transition form factors (see Table II). The model predictions by Calderón, Muñoz and Vera (CMV) [21] are also displayed here for comparison.

Mode	This work	CMV	Mode	This work	CMV
$\overline{B}^0 \to a_1^+\rho^-$	$23.9^{+10.5+3.2}_{-\ 9.2-0.4}(0.82^{+0.05}_{-0.13})$	4.3	$\overline{B}^0 \to b_1^+\rho^-$	$32.1^{+16.5+12.0}_{-14.7-\ 4.6}(0.96^{+0.01}_{-0.02})$	1.6
$\overline{B}^0 \to a_1^-\rho^+$	$36.0^{+3.5+3.5}_{-4.0-0.7}\ (0.84^{+0.02}_{-0.06})$	4.7	$\overline{B}^0 \to b_1^-\rho^+$	$0.6^{+0.6+1.9}_{-0.3-0.2}\ (0.98^{+0.00}_{-0.33})$	0.55
$\overline{B}^0 \to a_1^0\rho^0$	$1.2^{+2.0+5.1}_{-0.7-0.3}\ (0.82^{+0.06}_{-0.68})$	0.01	$\overline{B}^0 \to b_1^0\rho^0$	$3.2^{+5.2+1.7}_{-2.0-0.4}\ (0.99^{+0.00}_{-0.18})$	0.002
$B^- \to a_1^0\rho^-$	$17.8^{+10.1+3.1}_{-\ 6.4-0.2}(0.91^{+0.03}_{-0.10})$	2.4	$B^- \to b_1^0\rho^-$	$29.1^{+16.2+5.4}_{-10.6-5.9}\ (0.96^{+0.01}_{-0.06})$	0.86
$B^- \to a_1^-\rho^0$	$23.2^{+3.6+4.8}_{-2.9-0.1}\ (0.89^{+0.11}_{-0.18})$	3.0	$B^- \to b_1^-\rho^0$	$0.9^{+1.7+2.6}_{-0.6-0.5}\ (0.90^{+0.05}_{-0.38})$	0.36
$\overline{B}^0 \to a_1^0\omega$	$0.2^{+0.1+0.4}_{-0.1-0.0}\ (0.75^{+0.11}_{-0.65})$	0.003	$\overline{B}^0 \to b_1^0\omega$	$0.1^{+0.2+1.6}_{-0.0-0.0}\ (0.04^{+0.96}_{-0.00})$	0.004
$B^- \to a_1^-\omega$	$22.5^{+3.4+3.0}_{-2.7-0.7}\ (0.88^{+0.10}_{-0.14})$	2.2	$B^- \to b_1^-\omega$	$0.8^{+1.4+3.1}_{-0.5-0.3}\ (0.91^{+0.07}_{-0.33})$	0.38
$\overline{B}^0 \to a_1^0\phi$	$0.002^{+0.002+0.009}_{-0.001-0.000}\ (0.94^{+0.00}_{-0.69})$	0.0005	$\overline{B}^0 \to b_1^0\phi$	$0.01^{+0.01+0.01}_{-0.00-0.00}\ (0.98^{+0.01}_{-0.33})$	0.0002
$B^- \to a_1^-\phi$	$0.01^{+0.01+0.04}_{-0.00-0.00}\ (0.94^{+0.01}_{-0.69})$	0.001	$B^- \to b_1^-\phi$	$0.02^{+0.02+0.03}_{-0.01-0.00}\ (0.98^{+0.01}_{-0.33})$	0.0004
$\overline{B}^0 \to a_1^+K^{*-}$	$10.6^{+5.7+31.7}_{-4.0-\ 8.1}(0.37^{+0.39}_{-0.29})$	0.92	$\overline{B}^0 \to b_1^+K^{*-}$	$12.5^{+4.7+20.1}_{-3.7-\ 9.0}\ (0.82^{+0.18}_{-0.41})$	0.32
$\overline{B}^0 \to a_1^0\overline{K}^{*0}$	$4.2^{+2.8+15.5}_{-1.9-4.2}(0.23^{+0.45}_{-0.19})$	0.64	$\overline{B}^0 \to b_1^0\overline{K}^{*0}$	$6.4^{+2.4+8.8}_{-1.7-4.8}\ (0.79^{+0.21}_{-0.73})$	0.15
$B^- \to a_1^-\overline{K}^{*0}$	$11.2^{+6.1+31.9}_{-4.4-\ 9.0}(0.37^{+0.48}_{-0.37})$	0.51	$B^- \to b_1^-\overline{K}^{*0}$	$12.8^{+5.0+20.1}_{-3.8-\ 9.6}\ (0.79^{+0.21}_{-0.74})$	0.18
$B^- \to a_1^0K^{*-}$	$7.8^{+3.2+16.3}_{-2.5-\ 4.3}(0.52^{+0.41}_{-0.42})$	0.86	$B^- \to b_1^0K^{*-}$	$7.0^{+2.6+12.0}_{-2.0-\ 4.8}\ (0.82^{+0.16}_{-0.26})$	0.12

We see from Table VII that a_1K^* and b_1K^* modes are substantially enhanced by penguin annihilation. Experimentally, it is thus very important to measure them to test the importance of the penguin annihilation mechanism.

We have checked explicitly that, in the absence of penguin annihilation, the longitudinal polarization fractions are close to one half in a_1K^* modes and 90% in b_1K^* ones. This can be seen from the ratio of the negative- and longitudinal-helicity amplitudes

$$\left.\frac{\mathcal{A}^-}{\mathcal{A}^0}\right|_{\bar{B}\to a_1^+K^{*-}} \approx \left(\frac{\alpha_4^{c,-}+\alpha_{4,\rm EW}^-}{\alpha_4^{c,0}+\alpha_{4,\rm EW}^0}\right)\left(\frac{X^-_{\bar{B}a_1,K^*}}{X^0_{\bar{B}a_1,K^*}}\right). \tag{4.21}$$

As discussed in the section of $B \to VV$ decays, the interference between $\alpha_4^{c,h}$ and $\alpha_{4,\rm EW}^h$ is generally constructive for $h = -$ and destructive for $h = 0$. Since $|X^0_{\bar{B}a_1,K^*}| : |X^-_{\bar{B}a_1,K^*}| : |X^+_{\bar{B}a_1,K^*}| = 1 : 0.50 : 0.06$, and $|X^0_{\bar{B}b_1,K^*}| : |X^-_{\bar{B}b_1,K^*}| : |X^+_{\bar{B}b_1,K^*}| = 1 : 0.21 : 0.03$, it is obvious that the $\mathcal{A}^-$ amplitude of a_1K^* channels has more chance to be comparable to $\mathcal{A}^0$ than the b_1K^* ones. When penguin annihilation is turned on, it is evident from Table VII that a_1K^* modes are dominated by transverse polarization amplitudes, whereas b_1K^* are governed by longitudinal polarization states.

The decays $B \to (a_1, b_1)\phi$ are highly suppressed relative to the tree-dominated $(a_1, b_1)\rho$ modes

as they proceed through $b \to d$ penguin process and are thus suppressed by the small coefficients for penguin operators. Moreover, they do not receive any annihilation contribution!

On the experimental ground, our calculations suggest that the tree-dominated channels $a_1^+\rho^-$, $a_1^-\rho^-$, $a_1^0\rho^-$, $a_1^-\rho^0$, $a_1^-\omega$, $b_1^+\rho^-$ and $b_1^0\rho^-$ should be readily accessible to B factories. Measurements of the penguin-dominated modes a_1K^* and b_1K^* are crucial for testing the mechanism of penguin annihilation.

2. $B \to K_1(1270)V,\ K_1(1400)V$ *decays*

To obtain the branching ratios and f_L listed in Table VIII for $B \to K_1V$ decays, we have used the light-cone sum rule results for the $B \to K_{1A}$ and $B \to K_{1B}$ form factors given in Table II. The decays $B \to K_1\phi$ have been considered in [20] based on the generalized factorization framework where nonfactorizable effects are lumped into $N_c^{\rm eff}$, the effective number of colors. It is interesting to note that the results of [20] for $B \to K_1(1270)\phi$ are similar to ours when $N_c^{\rm eff}$ is close to 5, but the predicted rates for $K_1(1400)\phi$ are smaller than ours irrespective of the value of $N_c^{\rm eff}$. From Eqs. (B10) and (B11) we have the decay amplitudes given by

$$\begin{aligned}
\mathcal{A}^h_{B^-\to K_1^-(1270)\phi} &\propto [\alpha_3^c+\alpha_4^c+\beta_3^c]X_h^{(\bar B K_1(1270),\phi)} \\
&\propto [\alpha_3^c+\alpha_4^c+\beta_3^c]_{K_{1A}\phi}F^{BK_{1A}}\sin\theta_{K_1} + [\alpha_3^c+\alpha_4^c+\beta_3^c]_{K_{1B}\phi}F^{BK_{1B}}\cos\theta_{K_1}, \\
\mathcal{A}^h_{B^-\to K_1^-(1400)\phi} &\propto [\alpha_3^c+\alpha_4^c+\beta_3^c]X_h^{(\bar B K_1(1400),\phi)} \\
&\propto [\alpha_3^c+\alpha_4^c+\beta_3^c]_{K_{1A}\phi}F^{BK_{1A}}\cos\theta_{K_1} - [\alpha_3^c+\alpha_4^c+\beta_3^c]_{K_{1B}\phi}F^{BK_{1B}}\sin\theta_{K_1},
\end{aligned} \tag{4.22}$$

where $F^{BK_{1A}}$ denotes generic form factors for the $B \to K_{1A}$ transition and likewise for $F^{BK_{1B}}$. In our convention, form factors $F^{BK_{1A}}$ and $F^{BK_{1B}}$ have opposite signs (see Table II). Since the mixing angle θ_{K_1} is negative, it follows that the two amplitudes in Eq. (4.22) contribute constructively to $B^- \to K_1(1270)^-\phi$ and destructively to $B^- \to K_1(1400)^-\phi$. Hence, it is naively expected that the former has a rate larger than the latter. Indeed, when the penguin annihilation (β_3) is turned off, we find $\mathcal{B}(B^- \to K_1(1270)^-\phi) \approx 3.2\times10^{-6} \gg \mathcal{B}(B^- \to K_1(1400)^-\phi) \approx 3.1\times10^{-7}$. However, this feature is dramatically changed in the presence of weak annihilation with $\rho_A = 0.65$ and $\phi_A = -53^\circ$. Since $\beta_3(K_{1A}\phi)$ and $\beta_3(K_{1B}\phi)$ are opposite in sign, the interference becomes destructive in $B^- \to K_1(1270)^-\phi$ and constructive in $B^- \to K_1(1400)^-\phi$. This explains why we have $\mathcal{B}(B^- \to K_1(1270)^-\phi) < \mathcal{B}(B^- \to K_1(1400)^-\phi)$ in Table VIII. If this relation is not borne out by experiment, this will indicate that the parameter ρ_A and hence weak annihilation are small.

The decays $B \to K_1(1270)\rho$ have rates larger than that of $B \to K_1(1400)\rho$ and this can be understood as follows. Their decay amplitudes have the expressions, for example,

$$\begin{aligned}
\mathcal{A}^h_{\overline{B}^0\to K_1^-(1270)\rho^+} &\propto [\alpha_4^c+\beta_3^c]X_h^{(\bar B\rho,K_1(1270))} \\
&\propto [\alpha_4^c+\beta_3^c]_{\rho K_{1A}}f_{K_{1A}}\sin\theta_{K_1} + [\alpha_4^c+\beta_3^c]_{\rho K_{1B}}f^\perp_{K_{1B}}\cos\theta_{K_1}, \\
\mathcal{A}^h_{\overline{B}^0\to K_1^-(1400)\rho^+} &\propto [\alpha_4^c+\beta_3^c]X_h^{(\bar B\rho,K_1(1400))} \\
&\propto [\alpha_4^c+\beta_3^c]_{\rho K_{1A}}f_{K_{1A}}\cos\theta_{K_1} - [\alpha_4^c+\beta_3^c]_{\rho K_{1B}}f_{K^\perp_{1B}}\sin\theta_{K_1}.
\end{aligned} \tag{4.23}$$

TABLE VIII: Same as Table VII except for $b \to s$ penguin-dominated decays (top) $B \to K_1(\rho, K^*, \omega)$ and $b \to d$ penguin-dominated ones (bottom) $B \to K_1\bar{K}^*$ for two different mixing angles $\theta_{K_1} = -37^\circ$ and -58°. Default results are for $\rho_A = 0.65$ and $\phi_A = -53^\circ$.

Decay	$\theta_{K_1} = -37^\circ$		$\theta_{K_1} = -58^\circ$	
	$\mathcal{B}$	f_L	$\mathcal{B}$	f_L
$\overline{B}^0 \to K_1^-(1270)\rho^+$	$16.8^{+9.8+54.7}_{-6.8-13.8}$	$0.57^{+0.39}_{-0.30}$	$19.4^{+12.1+47.6}_{-\ 8.5-14.8}$	$0.49^{+0.48}_{-0.36}$
$\overline{B}^0 \to \overline{K}_1^0(1270)\rho^0$	$9.1^{+5.3+34.2}_{-3.5-\ 8.6}$	$0.50^{+0.39}_{-0.37}$	$9.8^{+6.0+30.4}_{-4.1-\ 8.0}$	$0.40^{+0.49}_{-0.30}$
$B^- \to \overline{K}_1^0(1270)\rho^-$	$17.0^{+10.7+53.0}_{-\ 7.3-15.3}$	$0.52^{+0.47}_{-0.36}$	$20.1^{+12.5+48.5}_{-\ 8.9-15.2}$	$0.47^{+0.51}_{-0.46}$
$B^- \to K_1^-(1270)\rho^0$	$8.2^{+5.0+20.4}_{-3.7-\ 6.1}$	$0.56^{+0.39}_{-0.34}$	$10.3^{+5.9+19.1}_{-4.5-\ 6.7}$	$0.56^{+0.41}_{-0.37}$
$\overline{B}^0 \to \overline{K}_1^0(1270)\omega$	$7.3^{+4.7+24.0}_{-3.1-\ 7.5}$	$0.59^{+0.39}_{-0.32}$	$8.2^{+5.3+21.5}_{-3.7-\ 7.4}$	$0.48^{+0.50}_{-0.47}$
$B^- \to K_1^-(1270)\omega$	$7.4^{+4.7+22.6}_{-3.2-\ 6.9}$	$0.56^{+0.41}_{-0.22}$	$8.7^{+5.4+20.6}_{-3.7-\ 7.1}$	$0.52^{+0.46}_{-0.34}$
$\overline{B}^0 \to \overline{K}_1^0(1270)\phi$	$3.6^{+1.7+4.8}_{-1.3-2.9}$	$0.67^{+0.33}_{-0.64}$	$3.2^{+2.1+5.2}_{-1.4-2.7}$	$0.31^{+0.69}_{-0.31}$
$B^- \to K_1^-(1270)\phi$	$3.8^{+1.9+5.1}_{-1.5-3.1}$	$0.67^{+0.33}_{-0.64}$	$3.4^{+2.2+5.5}_{-1.5-2.8}$	$0.31^{+0.69}_{-0.37}$
$\overline{B}^0 \to K_1^-(1400)\rho^+$	$8.6^{+2.8+13.0}_{-2.3-\ 4.3}$	$0.64^{+0.30}_{-0.23}$	$5.7^{+1.2+17.5}_{-1.0-\ 4.7}$	$0.87^{+0.09}_{-0.43}$
$\overline{B}^0 \to \overline{K}_1^0(1400)\rho^0$	$11.4^{+3.2+15.5}_{-2.8-\ 5.8}$	$0.65^{+0.32}_{-0.21}$	$9.8^{+2.1+22.4}_{-2.0-\ 8.0}$	$0.90^{+0.07}_{-0.28}$
$B^- \to \overline{K}_1^0(1400)\rho^-$	$10.9^{+2.6+15.2}_{-3.1-\ 5.4}$	$0.65^{+0.33}_{-0.26}$	$7.5^{+2.06+19.4}_{-1.6-\ 6.0}$	$0.85^{+0.11}_{-0.44}$
$B^- \to K_1^-(1400)\rho^0$	$3.8^{+1.3+6.4}_{-1.1-1.9}$	$0.61^{+0.32}_{-0.22}$	$1.5^{+0.7+7.7}_{-0.3-1.0}$	$0.70^{+0.24}_{-0.48}$
$\overline{B}^0 \to \overline{K}_1^0(1400)\omega$	$5.6^{+2.8+6.8}_{-2.2-2.5}$	$0.72^{+0.31}_{-0.36}$	$4.6^{+2.8+9.5}_{-1.7-3.5}$	$0.90^{+0.07}_{-0.28}$
$B^- \to K_1^-(1400)\omega$	$4.5^{+1.8+6.0}_{-1.4-2.1}$	$0.68^{+0.32}_{-0.32}$	$3.1^{+1.3+8.1}_{-0.8-2.4}$	$0.87^{+0.09}_{-0.40}$
$\overline{B}^0 \to \overline{K}_1^0(1400)\phi$	$10.4^{+7.9+38.3}_{-5.1-10.4}$	$0.46^{+0.26}_{-0.02}$	$10.7^{+7.1+37.69}_{-4.6-10.4}$	$0.57^{+0.31}_{-0.22}$
$B^- \to K_1^-(1400)\phi$	$11.1^{+8.5+41.1}_{-5.4-11.4}$	$0.45^{+0.13}_{-0.09}$	$11.3^{+7.5+40.2}_{-4.9-11.1}$	$0.57^{+0.32}_{-0.22}$
$\overline{B}^0 \to K_1^-(1270)K^{*+}$	$0.01^{+0.01+0.03}_{-0.01-0.00}$	1.0	$0.00^{+0.00+0.01}_{-0.00-0.00}$	1.0
$\overline{B}^0 \to K_1^+(1270)K^{*-}$	$0.06^{+0.03+1.43}_{-0.02-0.02}$	1.0	$0.06^{+0.02+0.91}_{-0.02-0.00}$	1.0
$\overline{B}^0 \to K_1^-(1400)K^{*+}$	$0.08^{+0.04+0.28}_{-0.03-0.00}$	1.0	$0.09^{+0.05+0.30}_{-0.03-0.00}$	1.0
$\overline{B}^0 \to K_1^+(1400)K^{*-}$	$0.00^{+0.00+0.20}_{-0.00-0.00}$	1.0	$0.00^{+0.01+0.69}_{-0.00-0.00}$	1.0
$\overline{B}^0 \to \overline{K}_1^0(1270)K^{*0}$	$0.40^{+0.25+0.65}_{-0.26-0.35}$	$0.86^{+0.08}_{-0.25}$	$0.29^{+0.19+0.41}_{-0.20-0.07}$	$0.84^{+0.16}_{-0.59}$
$\overline{B}^0 \to K_1^0(1270)\overline{K}^{*0}$	$0.09^{+0.04+3.52}_{-0.03-0.00}$	$0.34^{+0.62}_{-0.24}$	$0.25^{+0.09+3.53}_{-0.08-0.00}$	$0.52^{+0.44}_{-0.52}$
$B^- \to K_1^0(1270)K^{*-}$	$0.05^{+0.04+2.21}_{-0.02-0.00}$	$0.33^{+0.58}_{-0.06}$	$0.13^{+0.04+2.00}_{-0.05-0.00}$	$0.54^{+0.38}_{-0.49}$
$B^- \to K_1^-(1270)K^{*0}$	$0.19^{+0.13+0.28}_{-0.13-0.15}$	$0.84^{+0.07}_{-0.30}$	$0.15^{+0.10+0.20}_{-0.10-0.03}$	$0.80^{+0.08}_{-0.62}$
$\overline{B}^0 \to \overline{K}_1^0(1400)K^{*0}$	$0.01^{+0.01+3.41}_{-0.01-0.00}$	$0.97^{+0.00}_{-0.97}$	$0.08^{+0.05+3.01}_{-0.06-0.01}$	$0.89^{+0.06}_{-0.79}$
$\overline{B}^0 \to K_1^0(1400)\overline{K}^{*0}$	$0.51^{+0.08+1.30}_{-0.11-0.29}$	$0.71^{+0.28}_{-0.29}$	$0.36^{+0.08+1.60}_{-0.01-0.30}$	$0.85^{+0.11}_{-0.54}$
$B^- \to K_1^0(1400)K^{*-}$	$0.28^{+0.04+0.53}_{-0.06-0.14}$	$0.77^{+0.20}_{-0.34}$	$0.19^{+0.04+0.73}_{-0.04-0.10}$	$0.85^{+0.12}_{-0.18}$
$B^- \to K_1^-(1400)K^{*0}$	$0.01^{+0.00+2.00}_{-0.01-0.00}$	$0.93^{+0.00}_{-0.72}$	$0.05^{+0.03+1.77}_{-0.04-0.01}$	$0.92^{+0.05}_{-0.67}$

Just as the case for $B \to K_1\phi$ decays, the interference is constructive (destructive) in $K_1^-(1270)\rho^+$ and destructive (constructive) in $K_1^-(1400)\rho^+$ in the presence (absence) of weak annihilation with $\rho_A = 0.65$ and $\phi_A = -53^\circ$. This explains why the rates of the former are larger than the latter, especially for $\theta_{K_1} = -58^\circ$, in Table VIII. Hence, measurements of the relative rates of $K_1(1270)\rho$ and $K_1(1400)\rho$ will enable us to see the role played by the weak annihilation effect.

If $\mathcal{B}(B \to K_1(1270)\rho) < \mathcal{B}(B \to K_1(1400)\rho)$ is observed, this will hint at the smallness of weak annihilation. The reader may notice that the decay modes involving $K_1(1270)$ and $K_1(1400)$ always have opposite dependence on the mixing angle θ_{K_1}. For example, $K_1^-(1270)\rho^+$ gets enhanced whereas $K_1^-(1400)\rho^+$ is suppressed when θ_{K_1} is changed from -37° to -58°.

Decay rates of $B \to K_1(1270)K^*$ and $K_1(1400)K^*$ are generally small because they proceed through $b \to d$ penguin diagrams and are suppressed by the smallness of the penguin Wilson coefficients. Their branching ratios are of order $10^{-7} - 10^{-8}$. The decay modes $K_1^- K^{*+}$ and $K_1^+ K^{*-}$ are of particular interest as they are the only AV modes which receive contributions solely from weak annihilation. Just as the decay $\overline{B}^0 \to K^{*+}K^{*-}$ discussed before, the absence of transverse polarization in the $K_1^- K^{*+}$ and $K_1^+ K^{*-}$ modes is due to the fact that the annihilation terms $b_1^\pm, b_2^\pm, b_4^\pm, b_{4,\rm EW}^\pm$ vanish under our approximation.

From Table VIII, it is clear that the channels $K_1^-\rho^+$, $\bar{K}_1^0\rho^-$ for $K_1 = K_1(1270)$ and $K_1(1400)$ have sizable rates and the experimental search of them would be encouraging.

3. $B \to f_1 V,\ h_1 V$ decays

Results for the decays $B \to (f_1, h_1)(\rho, \omega, K^*, \phi)$ with $f_1 = f_1(1285), f_1(1420)$ and $h_1 = h_1(1170), h_1(1380)$ for two distinct sets of the mixing angles $\theta_{^3P_1}$ and $\theta_{^1P_1}$ are summarized in Table IX. Among tree-dominated decays, the channels $h_1(1380)\rho^-$ for $\theta_{^1P_1} = 0^\circ$, $f_1(1285)\rho^-$ and $h_1(1170)\rho^-$ have branching ratios of order 10^{-5} as they receive color-allowed tree contributions. Many of the penguin-dominated modes e.g. $f_1(1420)K^*$ have branching ratios in the range of $(5 \sim 15) \times 10^{-6}$. It is of interest to notice that the decays involving $h_1(1380)$ in the final state have a sharp dependence of the rates on the mixing angle $\theta_{^1P_1}$.

C. $B \to AA$ decays

For the axial vector mesons $a_1(1260), b_1(1235), f_1(1285), f_1(1420), h_1(1170), h_1(1380)$ and $K_1(1270), K_1(1400)$, there exist many possible $B \to AA$ two-body decay channels. We will classify them into tree- and penguin-dominated decays. The latter involves the strange axial-vector meson K_1.

1. Tree-dominated decays

The decay amplitudes for some of tree-dominated $B \to AA$ decays are shown in Appendix B. Since the decay constant of the b_1 is either vanishing or very small, it is anticipated that $b_1 b_1$ channels are highly suppressed relative to $a_1 a_1$. Some of $a_1 b_1$ decays are comparable to $a_1 a_1$. We find that $a_1^+ a_1^-$ and $a_1^- a_1^0$ modes have rates larger than the corresponding $\rho^+\rho^-$ and $\rho^-\rho^0$ ones, but $a_1^0 a_1^0$ is very similar to $\rho^0\rho^0$. While $a_1^+ a_1^-$, $a_1^- a_1^0$, $a_1^- b_1^+$ and $a_1^- b_1^0$ modes have branching ratios of order $(20 \sim 40) \times 10^{-6}$, the other channels are suppressed by the smallness of either f_{b_1} or the coefficient a_2.

TABLE IX: Same as Table VII except for the decays $B \to (f_1, h_1)(\rho, \omega, K^*, \phi)$ with $f_1 = f_1(1285), f_1(1420)$ and $h_1 = h_1(1170), h_1(1380)$. We use two different sets of mixing angles: (i) $\theta_{^3P_1} = 27.9^\circ$ and $\theta_{^1P_1} = 25.2^\circ$ (in first entry), corresponding to $\theta_{K_1} = -37^\circ$, and (ii) $\theta_{^3P_1} = 53.2^\circ$, $\theta_{^1P_1} = 0^\circ$ (in second entry), corresponding to $\theta_{K_1} = -58^\circ$.

Mode	$\mathcal{B}$	f_L	Mode	$\mathcal{B}$	f_L
$B^- \to f_1(1285)\rho^-$	$10.2^{+5.5+0.5}_{-3.5-0.4}$	$0.91^{+0.02}_{-0.02}$	$B^- \to f_1(1420)\rho^-$	$0.1^{+0.2+0.1}_{-0.1-0.0}$	$0.70^{+0.19}_{-0.07}$
	$8.9^{+5.1+0.4}_{-3.2-0.3}$	$0.90^{+0.04}_{-0.03}$		$1.3^{+0.6+0.2}_{-0.3-0.0}$	$0.93^{+0.04}_{-0.03}$
$\overline{B}^0 \to f_1(1285)\rho^0$	$0.2^{+0.2+0.3}_{-0.1-0.0}$	$0.77^{+0.09}_{-0.40}$	$\overline{B}^0 \to f_1(1420)\rho^0$	$0.01^{+0.03+0.02}_{-0.00-0.00}$	$0.38^{+0.57}_{-0.22}$
	$0.2^{+0.1+0.3}_{-0.1-0.0}$	$0.71^{+0.09}_{-0.36}$		$0.04^{+0.12+0.08}_{-0.03-0.00}$	$0.87^{+0.08}_{-0.40}$
$\overline{B}^0 \to f_1(1285)\omega$	$1.0^{+1.1+2.5}_{-0.4-0.2}$	$0.87^{+0.07}_{-0.62}$	$\overline{B}^0 \to f_1(1420)\omega$	$0.02^{+0.03+0.05}_{-0.01-0.00}$	$0.53^{+0.31}_{-0.39}$
	$0.9^{+1.0+2.2}_{-0.4-0.1}$	$0.86^{+0.07}_{-0.62}$		$0.1^{+0.2+0.3}_{-0.1-0.0}$	$0.86^{+0.04}_{-0.76}$
$B^- \to f_1(1285)K^{*-}$	$5.8^{+8.3+10.8}_{-2.8-\ 2.3}$	$0.90^{+0.11}_{-0.74}$	$B^- \to f_1(1420)K^{*-}$	$15.9^{+8.4+18.0}_{-5.3-\ 7.0}$	$0.50^{+0.48}_{-0.52}$
	$5.7^{+3.8+21.4}_{-2.2-\ 4.8}$	$0.47^{+0.49}_{-0.45}$		$15.6^{+10.9+10.4}_{-\ 5.2-\ 4.7}$	$0.64^{+0.37}_{-0.61}$
$\overline{B}^0 \to f_1(1285)\overline{K}^{*0}$	$5.5^{+7.9+10.1}_{-2.7-\ 1.7}$	$0.89^{+0.14}_{-0.79}$	$\overline{B}^0 \to f_1(1420)\overline{K}^{*0}$	$14.8^{+8.0+17.4}_{-5.0-\ 6.7}$	$0.49^{+0.49}_{-0.50}$
	$5.1^{+3.6+20.0}_{-2.1-\ 4.7}$	$0.45^{+0.55}_{-0.50}$		$14.9^{+10.2+10.1}_{-\ 5.0-\ 4.6}$	$0.64^{+0.38}_{-0.61}$
$\overline{B}^0 \to f_1(1285)\phi$	$0.002^{+0.002+0.010}_{-0.001-0.000}$	$0.93^{+0.02}_{-0.68}$	$\overline{B}^0 \to f_1(1420)\phi$	$0.0001^{+0.0001+0.0006}_{-0.0000-0.0000}$	$0.97^{+0.03}_{-0.75}$
	$0.002^{+0.002+0.009}_{-0.001-0.000}$	$0.90^{+0.03}_{-0.71}$		$0.0008^{+0.0009+0.0009}_{-0.0001-0.0001}$	$0.98^{+0.02}_{-0.44}$
$B^- \to h_1(1170)\rho^-$	$17.4^{+10.1+2.8}_{-\ 6.6-3.3}$	$0.96^{+0.01}_{-0.06}$	$B^- \to h_1(1380)\rho^-$	$0.9^{+0.5+0.2}_{-0.3-0.2}$	$0.95^{+0.00}_{-0.08}$
	$10.9^{+6.5+1.8}_{-4.2-2.1}$	$0.96^{+0.01}_{-0.06}$		$5.9^{+3.2+1.0}_{-2.1-1.1}$	$0.95^{+0.01}_{-0.07}$
$\overline{B}^0 \to h_1(1170)\rho^0$	$0.05^{+0.11+1.16}_{-0.03-0.00}$	$0.22^{+0.75}_{-0.11}$	$\overline{B}^0 \to h_1(1380)\rho^0$	$0.01^{+0.01+0.04}_{-0.00-0.00}$	$0.30^{+0.59}_{-0.13}$
	$0.04^{+0.09+0.78}_{-0.02-0.00}$	$0.30^{+0.61}_{-0.16}$		$0.02^{+0.03+0.40}_{-0.01-0.00}$	$0.01^{+0.99}_{-0.00}$
$\overline{B}^0 \to h_1(1170)\omega$	$1.5^{+2.4+1.2}_{-0.9-0.2}$	$0.99^{+0.01}_{-0.10}$	$\overline{B}^0 \to h_1(1380)\omega$	$0.1^{+0.1+0.1}_{-0.1-0.0}$	$0.97^{+0.02}_{-0.14}$
	$0.9^{+1.4+0.8}_{-0.6-0.1}$	$0.99^{+0.01}_{-0.10}$		$0.5^{+0.7+0.4}_{-0.3-0.1}$	$0.98^{+0.01}_{-0.12}$
$B^- \to h_1(1170)K^{*-}$	$5.3^{+2.5+12.8}_{-1.6-\ 4.3}$	$0.84^{+0.13}_{-0.16}$	$B^- \to h_1(1380)K^{*-}$	$8.1^{+4.0+21.3}_{-2.8-\ 6.6}$	$0.87^{+0.13}_{-0.75}$
	$7.7^{+5.1+31.6}_{-3.0-\ 7.1}$	$0.81^{+0.17}_{-0.21}$		$3.7^{+2.0+7.8}_{-1.3-2.2}$	$0.88^{+0.12}_{-0.53}$
$\overline{B}^0 \to h_1(1170)\overline{K}^{*0}$	$4.5^{+2.2+11.5}_{-1.4-\ 4.2}$	$0.82^{+0.18}_{-0.40}$	$\overline{B}^0 \to h_1(1380)\overline{K}^{*0}$	$8.3^{+4.4+21.8}_{-2.9-\ 6.9}$	$0.88^{+0.12}_{-0.80}$
	$7.1^{+5.1+30.1}_{-2.9-\ 6.9}$	$0.81^{+0.19}_{-0.42}$		$3.9^{+1.9+8.3}_{-1.3-2.6}$	$0.88^{+0.12}_{-0.64}$
$\overline{B}^0 \to h_1(1170)\phi$	$0.006^{+0.007+0.010}_{-0.002-0.005}$	$0.97^{+0.02}_{-0.90}$	$\overline{B}^0 \to h_1(1380)\phi$	$0.004^{+0.003+0.230}_{-0.002-0.000}$	$1.00^{+0.00}_{-0.04}$
	$0.001^{+0.005+0.074}_{-0.003-0.000}$	$0.93^{+0.07}_{-0.55}$		$0.007^{+0.005+0.170}_{-0.003-0.001}$	$0.99^{+0.01}_{-0.14}$

Among various $B \to (a_1, b_1)(f_1, h_1)$ decays, we see from Table X that only $a_1^- f_1(1285)$ and $a_1^- h_1(1170)$ modes and $a_1^- h_1(1380)$ with $\theta_{^1P_1} = 0^\circ$ can have sizable rates and all other charged and neutral channels are suppressed.

2. Penguin-dominated decays

The penguin-dominated $B \to AA$ decays involve at least one K_1 meson. Results for the decay modes $K_1(a_1, b_1, f_1, h_1, K_1)$ are summarized in Table XI. Some salient features are (i) $\Gamma(B \to K_1(1270)a_1) > \Gamma(B \to K_1(1400)b_1) > \Gamma(B \to K_1(1270)b_1) > \Gamma(B \to K_1(1400)a_1)$, (ii) $B \to$

TABLE X: Branching ratios (in units of 10^{-6}) and the longitudinal polarization fraction for tree-dominated $B \to AA$ decays. For decays involving f_1 and h_1 states, we use two different sets of mixing angles: (i) $\theta_{^3P_1} = 27.9^\circ$ and $\theta_{^1P_1} = 25.2^\circ$ (in first entry) and (ii) $\theta_{^3P_1} = 53.2^\circ$, $\theta_{^1P_1} = 0^\circ$ (in second entry).

Mode	$\mathcal{B}$	f_L	Mode	$\mathcal{B}$	f_L
$B^- \to a_1^- a_1^0$	$22.4^{+10.7+6.6}_{-\ 8.2-1.5}$	$0.74^{+0.24}_{-0.32}$	$\overline{B}^0 \to a_1^+ a_1^-$	$37.4^{+16.1+9.7}_{-13.7-1.4}$	$0.64^{+0.07}_{-0.17}$
$B^- \to a_1^- b_1^0$	$37.8^{+23.9+11.4}_{-15.3-\ 5.3}$	$0.92^{+0.02}_{-0.24}$	$\overline{B}^0 \to a_1^0 a_1^0$	$0.5^{+0.8+9.3}_{-0.2-0.0}$	$0.60^{+0.00}_{-0.70}$
$B^- \to a_1^0 b_1^-$	$1.0^{+1.6+6.2}_{-0.5-0.1}$	$0.73^{+0.12}_{-0.82}$	$\overline{B}^0 \to a_1^- b_1^+$	$41.3^{+20.7+16.6}_{-18.2-\ 3.4}$	$0.90^{+0.02}_{-0.05}$
$B^- \to b_1^- b_1^0$	$1.4^{+2.5+2.8}_{-1.0-0.0}$	$0.95^{+0.00}_{-0.82}$	$\overline{B}^0 \to a_1^+ b_1^-$	$0.8^{+1.09+3.6}_{-0.4-0.1}$	$0.98^{+0.00}_{-0.80}$
$\overline{B}^0 \to b_1^0 b_1^0$	$3.2^{+5.6+11.0}_{-2.3-\ 0.8}$	$0.95^{+0.02}_{-0.80}$	$\overline{B}^0 \to a_1^0 b_1^0$	$3.8^{+6.2+2.6}_{-2.3-0.5}$	$0.98^{+0.01}_{-0.31}$
$\overline{B}^0 \to b_1^+ b_1^-$	$1.0^{+1.6+15.7}_{-0.7-\ 0.3}$	$0.96^{+0.03}_{-0.65}$			
$B^- \to a_1^- f_1(1285)$	$12.4^{+5.6+6.9}_{-4.3-\ 0.7}$	$0.73^{+0.22}_{-0.32}$	$\overline{B}^0 \to a_1^0 f_1(1285)$	$0.1^{+0.1+3.1}_{-0.1-0.0}$	$0.53^{+0.13}_{-0.59}$
	$11.0^{+5.4+6.0}_{-4.1-0.8}$	$0.71^{+0.23}_{-0.31}$		$0.1^{+0.1+2.7}_{-0.0-0.0}$	$0.49^{+0.06}_{-0.52}$
$B^- \to a_1^- f_1(1420)$	$0.2^{+0.2+0.3}_{-0.1-0.0}$	$0.42^{+0.42}_{-0.19}$	$\overline{B}^0 \to a_1^0 f_1(1420)$	$0.02^{+0.02+0.12}_{-0.01-0.01}$	$0.14^{+0.75}_{-0.10}$
	$1.5^{+0.4+0.9}_{-0.3-0.0}$	$0.77^{+0.16}_{-0.33}$		$0.02^{+0.02+0.12}_{-0.01-0.01}$	$0.18^{+0.80}_{-0.15}$
$B^- \to a_1^- h_1(1170)$	$22.4^{+14.5+5.3}_{-\ 9.3-3.1}$	$0.91^{+0.02}_{-0.22}$	$\overline{B}^0 \to a_1^0 h_1(1170)$	$0.1^{+0.3+2.1}_{-0.1-0.0}$	$0.24^{+0.76}_{-0.26}$
	$14.1^{+9.5+3.4}_{-6.0-1.9}$	$0.91^{+0.02}_{-0.22}$		$0.08^{+0.17+1.36}_{-0.06-0.02}$	$0.30^{+0.70}_{-0.34}$
$B^- \to a_1^- h_1(1380)$	$1.2^{+0.7+0.3}_{-0.5-0.1}$	$0.90^{+0.02}_{-0.24}$	$\overline{B}^0 \to a_1^0 h_1(1380)$	$0.01^{+0.01+0.12}_{-0.01-0.00}$	$0.32^{+0.67}_{-0.21}$
	$7.6^{+4.7+1.6}_{-3.0-0.7}$	$0.89^{+0.03}_{-0.24}$		$0.05^{+0.07+0.79}_{-0.03-0.00}$	$0.08^{+0.92}_{-0.03}$
$B^- \to b_1^- f_1(1285)$	$0.8^{+1.3+4.3}_{-0.5-0.3}$	$0.82^{+0.16}_{-0.56}$	$\overline{B}^0 \to b_1^0 f_1(1285)$	$0.2^{+0.4+2.7}_{-0.1-0.1}$	$0.48^{+0.53}_{-0.38}$
	$0.7^{+1.0+3.5}_{-0.4-0.1}$	$0.79^{+0.19}_{-0.57}$		$0.2^{+0.3+2.5}_{-0.1-0.0}$	$0.36^{+0.63}_{-0.22}$
$B^- \to b_1^- f_1(1420)$	$0.03^{+0.17+0.16}_{-0.02-0.01}$	$0.73^{+0.23}_{-0.33}$	$\overline{B}^0 \to b_1^0 f_1(1420)$	$0.01^{+0.08+0.10}_{-0.01-0.01}$	$0.66^{+0.29}_{-0.49}$
	$0.2^{+0.6+0.8}_{-0.1-0.1}$	$0.89^{+0.08}_{-0.51}$		$0.1^{+0.3+0.5}_{-0.1-0.0}$	$0.81^{+0.14}_{-0.49}$
$B^- \to b_1^- h_1(1170)$	$1.2^{+2.0+9.2}_{-0.9-\ 0.5}$	$0.95^{+0.03}_{-0.76}$	$\overline{B}^0 \to b_1^0 h_1(1170)$	$0.2^{+0.2+5.1}_{-0.1-0.0}$	$0.86^{+0.12}_{-0.79}$
	$0.8^{+1.3+3.0}_{-0.3-0.1}$	$0.94^{+0.03}_{-0.79}$		$0.1^{+0.2+3.4}_{-0.1-0.0}$	$0.86^{+0.12}_{-0.79}$
$B^- \to b_1^- h_1(1380)$	$0.05^{+0.10+0.34}_{-0.04-0.00}$	$0.85^{+0.06}_{-0.80}$	$\overline{B}^0 \to b_1^0 h_1(1380)$	$0.01^{+0.01+0.20}_{-0.01-0.00}$	$0.47^{+0.45}_{-0.46}$
	$0.3^{+0.5+3.0}_{-0.2-0.2}$	$0.94^{+0.03}_{-0.77}$		$0.04^{+0.04+1.73}_{-0.02-0.00}$	$0.81^{+0.17}_{-0.70}$
$\overline{B}^0 \to f_1(1285) f_1(1285)$	$0.3^{+0.3+3.1}_{-0.1-0.0}$	$0.67^{+0.06}_{-0.84}$	$\overline{B}^0 \to h_1(1170) h_1(1170)$	$0.8^{+1.6+1.6}_{-0.6-0.3}$	$0.97^{+0.01}_{-0.55}$
	$0.2^{+0.2+2.5}_{-0.1-0.0}$	$0.66^{+0.07}_{-0.84}$		$0.4^{+0.7+1.2}_{-0.3-0.1}$	$0.97^{+0.02}_{-0.60}$
$\overline{B}^0 \to f_1(1285) f_1(1420)$	$0.01^{+0.01+0.10}_{-0.01-0.00}$	$0.26^{+0.31}_{-0.28}$	$\overline{B}^0 \to h_1(1170) h_1(1380)$	$0.1^{+0.1+0.1}_{-0.0-0.0}$	$0.97^{+0.01}_{-0.74}$
	$0.05^{+0.05+0.63}_{-0.02-0.00}$	$0.57^{+0.10}_{-0.66}$		$0.3^{+0.6+0.7}_{-0.3-0.1}$	$0.96^{+0.01}_{-0.70}$
$\overline{B}^0 \to f_1(1420) f_1(1420)$	$0.01^{+0.00+0.03}_{-0.01-0.00}$	$0.94^{+0.05}_{-0.34}$	$\overline{B}^0 \to h_1(1380) h_1(1380)$	$0.01^{+0.01+0.42}_{-0.01-0.00}$	$0.97^{+0.03}_{-0.39}$
	$0.01^{+0.01+0.06}_{-0.00-0.00}$	$0.68^{+0.23}_{-0.58}$		$0.08^{+0.14+0.79}_{-0.05-0.02}$	$0.96^{+0.03}_{-0.62}$
$\overline{B}^0 \to f_1(1285) h_1(1170)$	$1.1^{+1.9+1.1}_{-0.7-0.2}$	$0.98^{+0.02}_{-0.07}$	$\overline{B}^0 \to f_1(1285) h_1(1380)$	$0.05^{+0.09+0.07}_{-0.03-0.01}$	$0.97^{+0.02}_{-0.22}$
	$0.6^{+1.1+0.6}_{-0.4-0.1}$	$0.97^{+0.02}_{-0.09}$		$0.3^{+0.6+0.3}_{-0.2-0.0}$	$0.97^{+0.03}_{-0.11}$
$\overline{B}^0 \to f_1(1420) h_1(1170)$	$0.02^{+0.06+0.03}_{-0.01-0.00}$	$0.87^{+0.11}_{-0.23}$	$\overline{B}^0 \to f_1(1420) h_1(1380)$	$0.001^{+0.001+0.003}_{-0.000-0.000}$	$0.74^{+0.22}_{-0.25}$
	$0.08^{+0.17+0.10}_{-0.04-0.01}$	$0.96^{+0.03}_{-0.12}$		$0.04^{+0.10+0.08}_{-0.03-0.01}$	$0.95^{+0.04}_{-0.12}$

TABLE XI: Branching ratios (in units of 10^{-6}) and the longitudinal polarization fraction for penguin-dominated $B \to K_1 A$ decays for the mixing angles: (i) $\theta_{K_1} = -37^\circ$, $\theta_{^3P_1} = 27.9^\circ$ and $\theta_{^1P_1} = 25.2^\circ$, and (ii) $\theta_{K_1} = -58^\circ$, $\theta_{^3P_1} = 53.2^\circ$ and $\theta_{^1P_1} = 0^\circ$. Default results are for $\rho_A = 0.65$ and $\phi_A = -53^\circ$.

Decay	$\theta_{K_1} = -37^\circ$		$\theta_{K_1} = -58^\circ$	
	$\mathcal{B}$	f_L	$\mathcal{B}$	f_L
$\overline{B}^0 \to K_1^-(1270)a_1^+$	$42.3^{+58.2+165.6}_{-27.3-\ 41.1}$	$0.24^{+0.16}_{-0.07}$	$46.1^{+60.9+176.8}_{-29.8-\ 43.7}$	$0.16^{+0.28}_{-0.06}$
$\overline{B}^0 \to \bar{K}_1^0(1270)a_1^0$	$21.6^{+29.7+81.2}_{-13.9-20.9}$	$0.27^{+0.69}_{-0.21}$	$22.4^{+30.8+88.7}_{-15.0-22.2}$	$0.15^{+0.28}_{-0.03}$
$B^- \to \bar{K}_1^0(1270)a_1^-$	$44.3^{+60.9+165.9}_{-28.6-\ 43.5}$	$0.23^{+0.09}_{-0.19}$	$48.3^{+63.4+175.7}_{-31.1-\ 47.0}$	$0.15^{+0.25}_{-0.14}$
$B^- \to K_1^-(1270)a_1^0$	$23.8^{+30.1+84.7}_{-14.3-21.4}$	$0.26^{+0.35}_{-0.15}$	$26.3^{+31.6+87.6}_{-15.6-23.2}$	$0.20^{+0.41}_{-0.11}$
$\overline{B}^0 \to K_1^-(1400)a_1^+$	$12.0^{+10.6+12.0}_{-\ 6.1-\ 7.9}$	$0.36^{+0.38}_{-0.32}$	$7.5^{+7.3+21.7}_{-3.3-\ 6.1}$	$0.96^{+0.04}_{-0.43}$
$\overline{B}^0 \to \bar{K}_1^0(1400)a_1^0$	$6.7^{+5.5+7.4}_{-3.3-4.5}$	$0.45^{+0.48}_{-0.41}$	$5.5^{+4.2+12.4}_{-2.3-\ 4.1}$	$0.98^{+0.13}_{-0.36}$
$B^- \to \bar{K}_1^0(1400)a_1^-$	$13.8^{+11.4+17.1}_{-\ 6.8-10.1}$	$0.42^{+0.58}_{-0.40}$	$9.0^{+8.4+23.8}_{-3.9-\ 7.4}$	$0.98^{+0.15}_{-0.43}$
$B^- \to K_1^-(1400)a_1^0$	$6.0^{+5.4+7.0}_{-3.0-4.3}$	$0.33^{+0.35}_{-0.30}$	$3.1^{+3.6+10.2}_{-1.5-\ 2.6}$	$0.94^{+0.01}_{-0.59}$
$\overline{B}^0 \to K_1^-(1270)b_1^+$	$14.8^{+12.9+65.8}_{-\ 7.2-13.7}$	$0.28^{+0.52}_{-0.12}$	$14.1^{+15.7+63.1}_{-\ 6.7-11.1}$	$0.13^{+0.71}_{-0.14}$
$\overline{B}^0 \to \bar{K}_1^0(1270)b_1^0$	$7.3^{+6.3+33.0}_{-3.5-\ 6.7}$	$0.29^{+0.48}_{-0.18}$	$6.9^{+7.4+34.1}_{-3.1-\ 5.2}$	$0.12^{+0.69}_{-0.16}$
$B^- \to \bar{K}_1^0(1270)b_1^-$	$15.3^{+13.8+72.6}_{-\ 7.5-14.9}$	$0.31^{+0.31}_{-0.13}$	$13.0^{+15.1+69.5}_{-\ 6.0-10.8}$	$0.06^{+0.67}_{-0.09}$
$B^- \to K_1^-(1270)b_1^0$	$9.0^{+8.3+36.3}_{-4.5-\ 7.7}$	$0.39^{+0.49}_{-0.20}$	$8.1^{+9.2+32.2}_{-3.9-\ 5.9}$	$0.22^{+0.65}_{-0.22}$
$\overline{B}^0 \to K_1^-(1400)b_1^+$	$25.0^{+27.3+205.5}_{-11.1-\ 22.9}$	$0.91^{+0.03}_{-0.34}$	$26.2^{+24.2+209.2}_{-12.0-\ 24.7}$	$0.99^{+0.01}_{-0.56}$
$\overline{B}^0 \to \bar{K}_1^0(1400)b_1^0$	$13.0^{+13.4+110.1}_{-\ 5.6-\ 12.3}$	$0.91^{+0.05}_{-0.66}$	$13.7^{+12.3+109.4}_{-\ 6.2-\ 13.1}$	$0.98^{+0.02}_{-0.92}$
$B^- \to \bar{K}_1^0(1400)b_1^-$	$27.7^{+28.6+231.4}_{-12.0-\ 26.1}$	$0.91^{+0.05}_{-0.66}$	$30.4^{+27.2+235.5}_{-13.9-\ 29.3}$	$0.98^{+0.02}_{-0.97}$
$B^- \to K_1^-(1400)b_1^0$	$13.3^{+14.4+107.9}_{-\ 5.9-\ 12.2}$	$0.92^{+0.01}_{-0.35}$	$14.4^{+13.4+112.7}_{-\ 6.7-\ 13.8}$	$0.99^{+0.01}_{-0.74}$
$\overline{B}^0 \to \bar{K}_1^0(1270)f_1(1285)$	$14.5^{+20.1+68.4}_{-\ 8.2-11.1}$	$0.56^{+0.52}_{-0.70}$	$5.7^{+8.8+31.0}_{-3.7-\ 5.2}$	$0.22^{+0.72}_{-0.29}$
$\overline{B}^0 \to \bar{K}_1^0(1270)f_1(1420)$	$10.4^{+9.3+51.7}_{-3.5-\ 6.3}$	$0.93^{+0.08}_{-0.55}$	$18.9^{+20.9+82.1}_{-\ 8.0-10.7}$	$0.64^{+0.48}_{-0.67}$
$\overline{B}^0 \to \bar{K}_1^0(1270)h_1(1170)$	$5.3^{+8.7+25.7}_{-3.4-\ 4.4}$	$0.52^{+0.46}_{-0.60}$	$4.1^{+11.3+7.8}_{-\ 3.4-2.3}$	$0.83^{+0.17}_{-0.83}$
$\overline{B}^0 \to \bar{K}_1^0(1270)h_1(1380)$	$8.5^{+13.3+38.4}_{-\ 5.6-\ 5.2}$	$0.93^{+0.05}_{-0.76}$	$8.5^{+11.5+33.5}_{-\ 4.9-\ 4.3}$	$0.50^{+0.45}_{-0.45}$
$B^- \to K_1^-(1270)f_1(1285)$	$15.7^{+21.5+73.4}_{-\ 8.7-11.7}$	$0.60^{+0.46}_{-0.75}$	$6.2^{+9.0+34.2}_{-3.8-\ 5.2}$	$0.29^{+0.60}_{-0.35}$
$B^- \to K_1^-(1270)f_1(1420)$	$10.9^{+9.7+53.7}_{-3.7-\ 6.4}$	$0.93^{+0.09}_{-0.55}$	$19.7^{+21.8+85.6}_{-\ 8.2-11.0}$	$0.65^{+0.46}_{-0.69}$
$B^- \to K_1^-(1270)h_1(1170)$	$6.5^{+9.3+27.4}_{-3.9-\ 4.9}$	$0.56^{+0.38}_{-0.62}$	$5.6^{+12.2+9.2}_{-\ 4.0-0.8}$	$0.85^{+0.13}_{-0.76}$
$B^- \to K_1^-(1270)h_1(1380)$	$9.2^{+14.7+40.4}_{-\ 6.1-\ 5.8}$	$0.93^{+0.05}_{-0.73}$	$8.9^{+12.3+33.5}_{-\ 5.2-\ 4.4}$	$0.50^{+0.25}_{-0.73}$
$\overline{B}^0 \to \bar{K}_1^0(1400)f_1(1285)$	$4.0^{+5.3+12.2}_{-2.1-\ 4.5}$	$0.12^{+0.48}_{-0.13}$	$2.2^{+2.2+10.7}_{-0.5-\ 1.7}$	$0.52^{+0.39}_{-0.56}$
$\overline{B}^0 \to \bar{K}_1^0(1400)f_1(1420)$	$18.9^{+25.4+87.6}_{-16.7-19.0}$	$0.04^{+0.95}_{-0.03}$	$21.5^{+26.2+95.4}_{-13.5-17.6}$	$0.26^{+0.74}_{-0.16}$
$\overline{B}^0 \to \bar{K}_1^0(1400)h_1(1170)$	$8.9^{+10.4+75.4}_{-\ 4.5-\ 8.3}$	$0.96^{+0.02}_{-0.76}$	$21.0^{+21.6+148.3}_{-11.4-\ 19.7}$	$0.90^{+0.09}_{-0.81}$
$\overline{B}^0 \to \bar{K}_1^0(1400)h_1(1380)$	$16.6^{+22.0+81.9}_{-10.1-16.9}$	$0.55^{+0.10}_{-0.11}$	$6.5^{+8.4+33.2}_{-3.9-\ 6.5}$	$0.39^{+0.16}_{-0.08}$
$B^- \to K_1^-(1400)f_1(1285)$	$4.3^{+5.9+13.2}_{-2.4-\ 4.4}$	$0.15^{+0.57}_{-0.10}$	$2.2^{+2.5+10.4}_{-0.5-\ 1.7}$	$0.50^{+0.25}_{-0.73}$
$B^- \to K_1^-(1400)f_1(1420)$	$19.4^{+26.2+89.7}_{-13.0-19.8}$	$0.03^{+0.95}_{-0.03}$	$22.5^{+27.3+99.9}_{-14.1-18.1}$	$0.27^{+0.73}_{-0.15}$
$B^- \to K_1^-(1400)h_1(1170)$	$9.1^{+11.1+74.5}_{-\ 4.6-\ 8.3}$	$0.96^{+0.02}_{-0.44}$	$22.0^{+23.2+154.5}_{-12.1-\ 20.8}$	$0.91^{+0.08}_{-0.83}$
$B^- \to K_1^-(1400)h_1(1380)$	$17.7^{+23.4+87.8}_{-10.8-18.0}$	$0.56^{+0.12}_{-0.09}$	$7.0^{+9.1+35.9}_{-4.2-\ 6.9}$	$0.42^{+0.45}_{-0.18}$

Table XI. (Continued)

Decay	$\theta_{K_1}=-37^\circ$		$\theta_{K_1}=-58^\circ$	
	$\mathcal{B}$	f_L	$\mathcal{B}$	f_L
$\overline{B}^0\to K_1^-(1270)K_1^+(1270)$	$0.07^{+0.12+1.07}_{-0.05-0.00}$	1	$0.10^{+0.10+1.23}_{-0.06-0.00}$	1
$\overline{B}^0\to K_1^-(1270)K_1^+(1400)$	$0.01^{+0.02+0.35}_{-0.01-0.00}$	1	$0.01^{+0.02+0.34}_{-0.01-0.00}$	1
$\overline{B}^0\to K_1^-(1400)K_1^+(1270)$	$0.20^{+0.20+3.72}_{-0.11-0.00}$	1	$0.23^{+0.24+3.03}_{-0.17-0.00}$	1
$\overline{B}^0\to K_1^-(1400)K_1^+(1400)$	$0.04^{+0.05+0.42}_{-0.02-0.00}$	1	$0.04^{+0.08+0.63}_{-0.03-0.00}$	1
$\overline{B}^0\to \bar{K}_1^0(1270)K_1^0(1270)$	$0.16^{+0.17+1.03}_{-0.12-0.01}$	$0.67^{+0.31}_{-0.62}$	$0.44^{+0.33+8.35}_{-0.31-0.00}$	$0.75^{+0.21}_{-0.73}$
$\overline{B}^0\to \bar{K}_1^0(1400)K_1^0(1400)$	$0.29^{+0.23+4.99}_{-0.21-0.01}$	$0.64^{+0.32}_{-0.72}$	$0.06^{+0.06+0.13}_{-0.01-0.0}$	$0.46^{+0.57}_{-0.29}$
$\overline{B}^0\to \bar{K}_1^0(1270)K_1^0(1400)$	$0.85^{+0.44+10.95}_{-0.41-\ 0.38}$	$0.77^{+0.25}_{-0.59}$	$0.54^{+0.37+4.17}_{-0.27-0.23}$	$0.83^{+0.18}_{-0.88}$
$\overline{B}^0\to K_1^0(1270)\bar{K}_1^0(1400)$	$0.00^{+0.01+19.0}_{-0.00-\ 0.0}$	$0.66^{+0.26}_{-0.70}$	$0.02^{+0.02+14.12}_{-0.01-\ 0.0}$	$0.40^{+0.39}_{-0.38}$
$B^-\to K_1^0(1270)K_1^-(1400)$	$0.03^{+0.02+17.1}_{-0.01-\ 0.0}$	$0.94^{+0.03}_{-0.86}$	$0.10^{+0.05+13.07}_{-0.07-\ 0.00}$	$0.91^{+0.04}_{-0.91}$
$B^-\to K_1^-(1270)K_1^0(1270)$	$0.13^{+0.11+0.43}_{-0.07-0.02}$	$0.51^{+0.23}_{-0.40}$	$0.23^{+0.17+4.28}_{-0.13-0.02}$	$0.42^{+0.26}_{-0.51}$
$B^-\to K_1^-(1270)K_1^0(1400)$	$0.79^{+0.42+8.01}_{-0.39-0.29}$	$0.74^{+0.28}_{-0.53}$	$0.46^{+0.30+2.29}_{-0.21-0.13}$	$0.79^{+0.20}_{-0.84}$
$B^-\to K_1^-(1400)K_1^0(1400)$	$0.21^{+0.16+3.16}_{-0.12-0.02}$	$0.41^{+0.28}_{-0.47}$	$0.11^{+0.10+0.36}_{-0.05-0.04}$	$0.61^{+0.34}_{-0.49}$

$K_1(a_1,b_1)$ decays are dominated by transverse polarization amplitudes except for $K_1(1400)b_1$ and $K_1(1400)a_1$ with $\theta_{K_1}=-58^\circ$, and (iii) the charged and neutral B decays have similar rates and longitudinal polarization fractions. For example, $\mathcal{B}(B^-\to K_1^-(f_1,h_1))\approx\mathcal{B}(\overline{B}^0\to\bar{K}_1(f_1,h_1))$, $\mathcal{B}(B^-\to K_1^-(a_1^0,b_1^0))\approx\mathcal{B}(\overline{B}^0\to\bar{K}_1^0(a_1^0,b_1^0))$ and $\mathcal{B}(B^-\to\bar{K}_1^0(a_1^-,b_1^-))\approx\mathcal{B}(\overline{B}^0\to K_1^-(a_1^+,b_1^+))$.

The first feature can be understood as follows. Consider the decays $\overline{B}^0\to K_1^-(a_1^+,b_1^+)$ as an illustration. Their decay amplitudes are given by

$$\begin{aligned}
\mathcal{A}^h_{\overline{B}^0\to K_1^-(1270)a_1^+} &\propto \left[\alpha_4^{c,h}+\alpha_{4,\rm EW}^{c,h}+\beta_3^{c,h}-\frac{1}{2}\beta_{3,\rm EW}^{c,h}\right]_{a_1K_1}X_h^{(\overline{B}a_1,\overline{K}_1)}\\
&\propto [\cdots]_{a_1K_{1A}}f_{K_{1A}}\sin\theta_{K_1}+[\cdots]_{a_1K_{1B}}f^\perp_{K_{1B}}\cos\theta_{K_1},\\
\mathcal{A}^h_{\overline{B}^0\to K_1^-(1400)a_1^+} &\propto [\cdots]_{a_1K_{1A}}f_{K_{1A}}\cos\theta_{K_1}-[\cdots]_{a_1K_{1B}}f^\perp_{K_{1B}}\sin\theta_{K_1},\\
\mathcal{A}^h_{\overline{B}^0\to K_1^-(1270)b_1^+} &\propto [\cdots]_{b_1K_{1A}}f_{K_{1A}}\sin\theta_{K_1}+[\cdots]_{b_1K_{1B}}f^\perp_{K_{1B}}\cos\theta_{K_1},\\
\mathcal{A}^h_{\overline{B}^0\to K_1^-(1400)b_1^+} &\propto [\cdots]_{b_1K_{1A}}f_{K_{1A}}\cos\theta_{K_1}-[\cdots]_{b_1K_{1B}}f^\perp_{K_{1B}}\sin\theta_{K_1}.
\end{aligned}\tag{4.24}$$

Since K_1a_1 modes are dominated by transverse amplitudes and since the negative-helicity parameters such as $\alpha_4^-(a_1K_{1A})$ and $\alpha_4^-(a_1K_{1B})$ have opposite signs, it is clear that the interference is constructive in $B\to K_1(1270)a_1$ and destructive in $B\to K_1(1400)a_1$ for a negative mixing angle θ_{K_1}. This also explains why the former increases and the latter decreases when the mixing angle is changed from -37° to -58°. For the $K_1(1400)b_1$ modes dominated by the longitudinal amplitudes, they have large rates as $\alpha_4^0(b_1K_{1A})$ and $\alpha_4^0(b_1K_{1B})$ are of the same sign. In general, K_1a_1 and K_1b_1 rates are insensitive to the value of θ_{K_1}, -37° or -58°, except for $K_1(1400)a_1$ modes. It is interesting to notice that $K_1(1400)a_1$ channels are dominated by transverse amplitudes for $\theta_{K_1}=-37^\circ$ and by longitudinal ones for $\theta_{K_1}=-58^\circ$. Therefore, measurement of polarization fractions in $B\to K_1(1400)a_1$ will yield a clear discrimination between the two different $K_{1A}-K_{1B}$ mixing angles. Branching ratios of $B\to K_1(f_1,h_1)$ fall into the range of $10^{-6}\sim10^{-5}$. At first

sight, it appears that they depend on the mixing angles θ_{K_1} and $\theta_{^1P_1}$ or $\theta_{^3P_1}$. However, the latter two angles are correlated to the first one [see Eq. (2.4)]. Consequently, the decays $B \to K_1(f_1, h_1)$ depend on only one mixing angle θ_{K_1}. From Table XI it is clear that the mode $\bar{K}_1(1400)h_1(1380)$ has a strong dependence on θ_{K_1}.

Just as $B \to K_1\bar{K}^*$ decays, branching ratios of the $b \to d$ penguin-dominated $K_1\bar{K}_1$ modes are small, of order $10^{-7} - 10^{-8}$ owing to the smallness of the penguin coefficients.

In short, there are many penguin-dominated $B \to AA$ decays within the reach of B factories: $K_1(1270)a_1$, $K_1(1400)b_1$, $K_1(1270)b_1^{\pm}$, $K_1(1400)a_1^{\pm}$, $K_1(1270)(f_1(1285), f_1(1420))$ and $K_1(1400)(f_1(1420), h_1(1170))$. In most cases, transverse polarization is large except for $K_1(1400)(b_1, h_1(1170))$, $K_1(1270)(f_1(1420), h_1(1380))$ with $\theta_{K_1} = -37^\circ$ and $K_1(1400)a_1$ with $\theta_{K_1} = -58^\circ$ where longitudinal polarization dominates.

V. CONCLUSIONS

In this work we have presented a detailed study of charmless two-body B decays into final states involving two vector mesons (VV) or two axial-vector mesons (AA) or one vector and one axial-vector meson (VA), within the framework of QCD factorization, where A is either a $^3P_1$ or $^1P_1$ axial-vector meson. Owing to the G-parity, the chiral-even two-parton light-cone distribution amplitudes of the $^3P_1$ ($^1P_1$) mesons are symmetric (antisymmetric) under the exchange of quark and anti-quark momentum fractions in the SU(3) limit. For chiral-odd light-cone distribution amplitudes, it is other way around. The main results are as follows.

- We have worked out the hard spectator scattering and annihilation contributions to $B \to VA$ and $B \to AA$ decays.

- NLO nonfactorizable corrections to longitudinal- and negative-helicity effective Wilson coefficients a_i^h generally differ in magnitude and even in sign. For some VV modes, the constructive (destructive) interference in the negative-helicity (longitudinal-helicity) amplitude of the $\overline{B} \to VV$ decay will render the former comparable to the latter and bring up the transverse polarization. Any serious solution to the polarization puzzle should take into account NLO effects on a_i^h.

- The measured rates and f_L of penguin-dominated charmless VV modes can be *accommodated* (but cannot be *predicted* at first place) in QCD factorization by allowing for sizable penguin annihilation contributions. However, the parameters ρ_A and ϕ_A fit to the data of $K^*\phi$ and $K^*\rho$ are not the same. Hence, we do not have a good hint at the values of ρ_A and ϕ_A for $B \to AV$ and $B \to AA$ decays.

- While NLO contributions due to vertex, penguin and hard scattering corrections are insensitive to the choice of the renormalization scale μ, the penguin annihilation contribution at the hard-collinear scale is sensitive to μ. In the present work, we choose $\mu = m_b(m_b)$ for the reason that if $\mu = m_b(m_b)/2$ is selected, the decay rates and polarization fractions of

$B \to K^*\phi$ or $B \to K^*\rho$ cannot be simultaneously fitted by the annihilation parameters ρ_A and ϕ_A.

- The predicted rates and longitudinal polarization fractions by QCD factorization for tree-dominated $\rho\rho$ modes are in good agreement with experiment, but the calculated $\mathcal{B}(B^- \to \rho^-\omega)$ is slightly high. The latter may imply that the $B \to \omega$ transition form factors are slightly smaller than what are expected from the light-cone sum rules. Only in the decay $B^0 \to \rho^0\omega$ where a large deviation from the naive expectation of $f_L \sim 1$ is possible. We found $f_L(\rho^0\omega) \sim 0.55$.

- Using the measured $\bar{K}^{*0}\rho^-$ channel as an input, we predict the branching ratios and polarization fractions for other $B \to K^*\rho$ decays and find the relation $f_L(K^{*-}\rho^0) > f_L(K^{*-}\rho^+) > f_L(\bar{K}^{*0}\rho^-) > f_L(\bar{K}^{*0}\rho^0)$. Experimentally, it is quite important to measure them to test theory. Our result of $f_L(\bar{K}^{*0}\rho^0) \sim 0.39$ is consistent with experiment and is higher than the prediction ~ 0.22 made by Beneke, Rohrer and Yang.

- The calculations suggest that the tree-dominated channels $a_1^+\rho^-$, $a_1^-\rho^-$, $a_1^0\rho^-$, $a_1^-\rho^0$, $a_1^-\omega$, $b_1^+\rho^-$ and $b_1^0\rho^-$ should be readily accessible to B factories. One of the salient features of the $^1P_1$ axial vector meson is that its axial-vector decay constant is small, vanishing in the SU(3) limit. This can be tested by measuring various $b_1\rho$ modes to see if $\Gamma(\overline{B}^0 \to b_1^-\rho^+) \ll \Gamma(\overline{B}^0 \to b_1^+\rho^-)$ and $\Gamma(B^- \to b_1^-\rho^0) \ll \Gamma(B^- \to b_1^0\rho^-)$.

- In the absence of the experimental guideline, we employed the penguin annihilation parameters $\rho_A = 0.65$ and $\phi_A = -53^\circ$ inferred from the channel $B \to K^*\phi$ to describe penguin-dominated $B \to VA, AA$ decays. It is very crucial to measure the penguin-dominated modes a_1K^* and b_1K^* to test the importance of penguin annihilation. We found that a_1K^* modes are dominated by transverse polarization amplitudes, whereas b_1K^* are governed by longitudinal polarization states.

- For $B \to K_1V$ decays involving the $K_1(1270)$ or $K_1(1400)$ meson, the channels $K_1^-\rho^+$, $\bar{K}_1^0\rho^-$ have sizable rates and the experimental search of them would be encouraging. Measurements of the relative strengths of $K_1(1270)\phi(\rho)$ and $K_1(1400)\phi(\rho)$ will enable us to test the importance of weak annihilation. The rates of $B \to K_1(1270)K^*$ and $K_1(1400)K^*$ are generally very small. The decay modes $K_1^-K^{*+}$ and $K_1^+K^{*-}$ are of particular interest as they are the only VA modes which receive contributions solely from weak annihilation.

- Among the decays $B \to (f_1, h_1)(\rho, \omega, K^*, \phi)$ with $f_1 = f_1(1285), f_1(1420)$ and $h_1 = h_1(1170), h_1(1380)$, the tree-dominated modes $h_1(1380)\rho^-$, $f_1(1285)\rho^-$, $h_1(1170)\rho^-$ and several of the penguin-dominated channels e.g. $f_1(1420)K^*$ have appreciable rates.

- For tree-dominated $B \to AA$ decays, the $a_1^+a_1^-$, $a_1^-a_1^0$, $a_1^-b_1^+$ and $a_1^-b_1^0$ modes have sizable branching ratios, of order $(20 \sim 40) \times 10^{-6}$. Among various $B \to (a_1, b_1)(f_1, h_1)$ decays, only $a_1^-f_1(1285)$ and $a_1^-h_1(1170)$ modes and $a_1^-h_1(1380)$ with $\theta_{^1P_1} = 0^\circ$ can have large rates and all other charged and neutral channels are suppressed.

- There are two salient features for penguin-dominated $B \to AA$ decays: (i) $\Gamma(B \to K_1(1270)a_1) > \Gamma(B \to K_1(1400)b_1) > \Gamma(B \to K_1(1270)b_1) > \Gamma(B \to K_1(1400)a_1)$ and (ii) most of them are dominated by transverse polarization amplitudes except for $K_1(1400)b_1$ and $K_1(1400)a_1$ with $\theta_{K_1} = -58^\circ$. Since the $K_1(1400)a_1$ channels are dominated by transverse amplitudes for $\theta_{K_1} = -37^\circ$ and by longitudinal ones for $\theta_{K_1} = -58^\circ$, measurement of polarization fractions in $B \to K_1(1400)a_1$ will yield a clear discrimination between the two different $K_{1A} - K_{1B}$ mixing angles. Many penguin-dominated $B \to AA$ decays are are readily detectable at B factories: $K_1(1270)a_1$, $K_1(1400)b_1$, $K_1(1270)b_1^\pm$, $K_1(1400)a_1^\pm$, $K_1(1270)(f_1(1285), f_1(1420))$ and $K_1(1400)(f_1(1420), h_1(1170))$.

Acknowledgments

We are grateful to Hsiang-nan Li, James Smith and Deshan Yang for valuable discussions and to Wei Wang for providing us Table III. This research was supported in part by the National Science Council of R.O.C. under Grant Nos. NSC96-2112-M-001-003 and NSC96-2112-M-033-004-MY3.

APPENDIX A: FLAVOR OPERATORS

The coefficients of the flavor operators $\alpha_i^{h,p}$ can be expressed in terms of $a_i^{h,p}$ [5, 6] as follows:[4]

$$\begin{aligned}
\alpha_1^h(M_1M_2) &= a_1^h(M_1M_2)\,,\\
\alpha_2^h(M_1M_2) &= a_2^h(M_1M_2)\,,\\
\alpha_3^{h,p}(M_1M_2) &= \begin{cases} a_3^{h,p}(M_1M_2) - a_5^{h,p}(M_1M_2) & \text{for } M_1M_2 = VA,\, AA,\\ a_3^{h,p}(M_1M_2) + a_5^{h,p}(M_1M_2) & \text{for } M_1M_2 = VV,\, AV, \end{cases}\\
\alpha_4^{h,p}(M_1M_2) &= \begin{cases} a_4^{h,p}(M_1M_2) + r_\chi^{M_2}\, a_6^{h,p}(M_1M_2) & \text{for } M_1M_2 = AV,\, VA,\\ a_4^{h,p}(M_1M_2) - r_\chi^{M_2}\, a_6^{h,p}(M_1M_2) & \text{for } M_1M_2 = AA\,, VV, \end{cases}\\
\alpha_{3,\rm EW}^{h,p}(M_1M_2) &= \begin{cases} a_9^{h,p}(M_1M_2) - a_7^{h,p}(M_1M_2) & \text{for } M_1M_2 = VA,\, AA,\\ a_9^{h,p}(M_1M_2) + a_7^{h,p}(M_1M_2) & \text{for } M_1M_2 = VV,\, AV, \end{cases}\\
\alpha_{4,\rm EW}^{h,p}(M_1M_2) &= \begin{cases} a_{10}^{h,p}(M_1M_2) + r_\chi^{M_2}\, a_8^{h,p}(M_1M_2) & \text{for } M_1M_2 = AV,\, VA,\\ a_{10}^{h,p}(M_1M_2) - r_\chi^{M_2}\, a_8^{h,p}(M_1M_2) & \text{for } M_1M_2 = AA\,, VV. \end{cases}
\end{aligned} \tag{A1}$$

Note that the order of the arguments of $\alpha_i^p(M_1M_2)$ and $a_i^p(M_1M_2)$ is relevant. For vector mesons we have

$$r_\chi^V(\mu) = \frac{2m_V}{m_b(\mu)}\,\frac{f_V^\perp(\mu)}{f_V}\,, \tag{A2}$$

while for axial-vector mesons we have

$$r_\chi^A(\mu) = \frac{2m_A}{m_b(\mu)}\,\frac{f_A^\perp(\mu)}{f_A}\,. \tag{A3}$$

APPENDIX B: DECAY AMPLITUDES

For simplicity, here we do not explicitly show the arguments, M_1 and M_2, of $\alpha_i^{p,h}$ and $\beta_i^{p,h}$ coefficients. The order of the arguments of $\alpha_i^p(M_1M_2)$ and $\beta_i^p(M_1M_2)$ is consistent with the order of the arguments of $X^{(\overline{B}M_1,M_2)}$, where

$$\beta_i^p(M_1M_2) = \frac{if_Bf_{M_1}f_{M_2}}{X^{(\overline{B}M_1,M_2)}}b_i^p. \tag{B1}$$

The decay amplitudes for $(a_1,b_1)\rho, (a_1,b_1)K^*, (f_1,h_1)\rho, (f_1,h_1)K^*, K_1\rho$ and K_1K^* can be obtained from Appendix A of [1] by the replacement of P by V with the same quark content.

For VA modes, we only list those channels involving ω and ϕ vector mesons. For other $B\to VA$ decay amplitudes, the reader is referred to Appendix A of [1] with a simple replacement of the pseudoscalar meson by the vector meson.

$$\sqrt{2}\,\mathcal{A}^h_{B^-\to a_1^-\omega} = \frac{G_F}{\sqrt{2}}\sum_{p=u,c}\lambda_p^{(d)}\Bigg\{\Bigg[\delta_{pu}\,(\alpha_2^h+\beta_2^h) + 2\alpha_3^{p,h} + \alpha_4^{p,h} + \frac{1}{2}\alpha_{3,\rm EW}^{p,h}$$

[4] The numerical values of the coefficients $\alpha_i(M_1M_2)$ also depend on the nature of the initial-state B meson. This dependence is not indicated explicitly in our notation. The same remark applies to the annihilation coefficients b_i^p defined below.

$$
\begin{aligned}
&-\frac{1}{2}\alpha_{4,\rm EW}^{p,h}+\beta_3^{p,h}+\beta_{3,\rm EW}^{p,h}\Big]X_h^{(\overline{B}a_1,\omega)}\\
&+\Big[\delta_{pu}\left(\alpha_1^h+\beta_2^h\right)+\alpha_4^{p,h}+\alpha_{4,\rm EW}^{p,h}+\beta_3^{p,h}+\beta_{3,\rm EW}^{p,h}\Big]X_h^{(\overline{B}\omega,a_1)}\Bigg\},
\end{aligned}
\tag{B2}
$$

$$
\begin{aligned}
-2\,\mathcal{A}^h_{\bar{B}^0\to a_1^0\omega} &= \frac{G_F}{\sqrt{2}}\sum_{p=u,c}\lambda_p^{(d)}\Bigg\{\Big[\delta_{pu}\left(\alpha_2^h-\beta_1^h\right)+2\alpha_3^{p,h}+\alpha_4^{p,h}+\frac{1}{2}\alpha_{3,\rm EW}^{p,h}-\frac{1}{2}\alpha_{4,\rm EW}^{p,h}\\
&\quad+\beta_3^{p,h}-\frac{1}{2}\beta_{3,\rm EW}^{p,h}-\frac{3}{2}\beta_{4,\rm EW}^{p,h}\Big]X_h^{(\overline{B}a_1,\omega)}\\
&\quad+\Big[\delta_{pu}\left(-\alpha_2^h-\beta_1^h\right)+\alpha_4^{p,h}-\frac{3}{2}\alpha_{3,\rm EW}^{p,h}-\frac{1}{2}\alpha_{4,\rm EW}^{p,h}\\
&\quad+\beta_3^{p,h}-\frac{1}{2}\beta_{3,\rm EW}^{p,h}-\frac{3}{2}\beta_{4,\rm EW}^{p,h}\Big]X_h^{(\overline{B}\omega,a_1)}\Bigg\},
\end{aligned}
\tag{B3}
$$

$$
\mathcal{A}^h_{B^-\to a_1^-\phi} = \frac{G_F}{\sqrt{2}}\sum_{p=u,c}\lambda_p^{(d)}\Bigg\{\left[\alpha_3^{p,h}-\frac{1}{2}\alpha_{3,\rm EW}^{p,h}\right]X_h^{(\overline{B}a_1,\phi)}\Bigg\},
\tag{B4}
$$

$$
-\sqrt{2}\,\mathcal{A}^h_{\bar{B}^0\to a_1^0\phi} = \frac{G_F}{\sqrt{2}}\sum_{p=u,c}\lambda_p^{(d)}\Bigg\{\left[\alpha_3^{p,h}-\frac{1}{2}\alpha_{3,\rm EW}^{p,h}\right]X_h^{(\overline{B}a_1,\phi)}\Bigg\},
\tag{B5}
$$

for $\overline{B}\to a_1(\omega,\phi)$,

$$
\begin{aligned}
2\mathcal{A}^h_{\overline{B}^0\to f_1\omega} &= \frac{G_F}{\sqrt{2}}\sum_{p=u,c}\lambda_p^{(d)}\Bigg\{\Big[\delta_{pu}(\alpha_2^h+\beta_1^h)+2\alpha_3^{p,h}+\alpha_4^{p,h}+\frac{1}{2}\alpha_{3,\rm EW}^{p,h}\\
&\quad-\frac{1}{2}\alpha_{4,\rm EW}^{p,h}+\beta_3^{p,h}+2\beta_4^{p,h}-\frac{1}{2}\beta_{3,\rm EW}^{p,h}+\frac{1}{2}\beta_{4,\rm EW}^{p,h}\Big]X_h^{(\overline{B}f_1^q,\omega)}\\
&\quad+\Big[\delta_{pu}(\alpha_2^h+\beta_1^h)+2\alpha_3^{p,h}+\alpha_4^{p,h}+\frac{1}{2}\alpha_{3,\rm EW}^{p,h}-\frac{1}{2}\alpha_{4,\rm EW}^{p,h}+\beta_3^{p,h}+2\beta_4^{p,h}\\
&\quad-\frac{1}{2}\beta_{3,\rm EW}^{p,h}+\frac{1}{2}\beta_{4,\rm EW}^{p,h}\Big]X_h^{(\overline{B}\omega,f_1^q)}+\sqrt{2}\Big[\alpha_3^{p,h}-\frac{1}{2}\alpha_{3,\rm EW}^{p,h}\Big]X_h^{(\overline{B}\omega,f_1^s)}\Bigg\}
\end{aligned}
\tag{B6}
$$

$$
\begin{aligned}
2\mathcal{A}^h_{\overline{B}^0\to f_1\phi} &= \frac{G_F}{\sqrt{2}}\sum_{p=u,c}\lambda_p^{(d)}\Bigg\{\sqrt{2}\Big[\alpha_3^{p,h}-\frac{1}{2}\alpha_{3,\rm EW}^{p,h}\Big]X_h^{(\overline{B}f_1^q,\phi)}\\
&\quad+2f_Bf_{f_1^s}f_\phi\Big[\beta_4^{p,h}-\frac{1}{2}\beta_{4,\rm EW}^{p,h}\Big]_{f_1^s\phi}+2f_Bf_{f_1^s}f_\phi\Big[\beta_4^{p,h}-\frac{1}{2}\beta_{4,\rm EW}^{p,h}\Big]_{\phi f_1^s}\Bigg\},
\end{aligned}
\tag{B7}
$$

for $\overline{B}\to f_1(\omega,\phi)$,

$$
\begin{aligned}
\sqrt{2}\mathcal{A}^h_{B^-\to K_1^-\omega} &= \frac{G_F}{\sqrt{2}}\sum_{p=u,c}\lambda_p^{(s)}\Bigg\{\Big[\delta_{pu}(\alpha_1^h+\beta_2^h)+\alpha_4^{p,h}+\alpha_{4,\rm EW}^{p,h}+\beta_3^{p,h}+\beta_{3,\rm EW}^{p,h}\Big]X_h^{(\overline{B}\omega,\overline{K}_1)}\\
&\quad+\Big[\delta_{pu}\alpha_2^h+2\alpha_3^{p,h}+\frac{1}{2}\alpha_{3,\rm EW}^{p,h}\Big]X_h^{(\overline{BK}_1,\omega)}\Bigg\},
\end{aligned}
\tag{B8}
$$

$$
\begin{aligned}
\sqrt{2}\mathcal{A}^h_{\overline{B}^0\to\overline{K}_1^0\omega} &= \frac{G_F}{\sqrt{2}}\sum_{p=u,c}\lambda_p^{(s)}\Bigg\{\Big[\alpha_4^{p,h}-\frac{1}{2}\alpha_{4,\rm EW}^{p,h}+\beta_3^{p,h}-\frac{1}{2}\beta_{3,\rm EW}^{p,h}\Big]X_h^{(\overline{B}\omega,\overline{K}_1)}\\
&\quad+\Big[\delta_{pu}\alpha_2^h+2\alpha_3^{p,h}+\frac{1}{2}\alpha_{3,\rm EW}^{p,h}\Big]X_h^{(\overline{BK}_1,\omega)}\Bigg\},
\end{aligned}
\tag{B9}
$$

$$
\mathcal{A}^h_{B^-\to K_1^-\phi} = \frac{G_F}{\sqrt{2}}\sum_{p=u,c}\lambda_p^{(s)}\Bigg\{\Big[\delta_{pu}\beta_2^h+\alpha_3^{p,h}+\alpha_4^{p,h}-\frac{1}{2}\alpha_{3,\rm EW}^{p,h}
$$

$$-\frac{1}{2}\alpha_{4,\rm EW}^{p,h}+\beta_3^{p,h}+\beta_{3,\rm EW}^{p,h}\Big]X_h^{(\overline{BK}_1,\phi)}\Bigg\}, \tag{B10}$$

$$\mathcal{A}^h_{\overline{B}^0\to\overline{K}_1^0\phi} = \frac{G_F}{\sqrt{2}}\sum_{p=u,c}\lambda_p^{(s)}\Bigg\{\Big[\alpha_3^{p,h}+\alpha_4^{p,h}-\frac{1}{2}\alpha_{3,\rm EW}^{p,h}-\frac{1}{2}\alpha_{4,\rm EW}^{p,h} +\beta_3^{p,h}-\frac{1}{2}\beta_{3,\rm EW}^{p,h}\Big]X_h^{(\overline{BK}_1,\phi)}\Bigg\}, \tag{B11}$$

for $\overline{B}\to\overline{K}_1(\omega,\phi)$.

The relevant decay amplitudes for $B\to AA$ decays are

$$\sqrt{2}\,\mathcal{A}^h_{B^-\to a_1^-a_1^0} = \frac{G_F}{\sqrt{2}}\sum_{p=u,c}\lambda_p^{(d)}\left[\delta_{pu}\,(\alpha_1^h+\alpha_2^h)+\frac{3}{2}\alpha_{3,\rm EW}^{p,h}+\frac{3}{2}\alpha_{4,\rm EW}^{p,h}\right]X_h^{(\overline{B}a_1,a_1)}, \tag{B12}$$

$$\mathcal{A}^h_{\bar{B}^0\to a_1^-a_1^+} = \frac{G_F}{\sqrt{2}}\sum_{p=u,c}\lambda_p^{(d)}\Bigg[\delta_{pu}\,(\alpha_1^h+\beta_1^h)+\alpha_4^{p,h}+\alpha_{4,\rm EW}^{p,h}+\beta_3^{p,h} +2\beta_4^{p,h}-\frac{1}{2}\beta_{3,\rm EW}^{p,h}+\frac{1}{2}\beta_{4,\rm EW}^{p,h}\Bigg]X_h^{(\overline{B}a_1,a_1)}, \tag{B13}$$

$$-\mathcal{A}^h_{\bar{B}^0\to a_1^0a_1^0} = \frac{G_F}{\sqrt{2}}\sum_{p=u,c}\lambda_p^{(d)}\Bigg[\delta_{pu}\,(\alpha_2^h-\beta_1^h)-\alpha_4^{p,h}+\frac{3}{2}\alpha_{3,\rm EW}^{p,h}+\frac{1}{2}\alpha_{4,\rm EW}^{p,h}-\beta_3^{p,h}-2\beta_4^{p,h} +\frac{1}{2}\beta_{3,\rm EW}^{p,h}-\frac{1}{2}\beta_{4,\rm EW}^{p,h}\Bigg]X_h^{(\overline{B}a_1,a_1)}, \tag{B14}$$

$$\sqrt{2}\,\mathcal{A}^h_{B^-\to a_1^-f_1} = \frac{G_F}{\sqrt{2}}\sum_{p=u,c}\lambda_p^{(d)}\Bigg\{\Big[\delta_{pu}\,(\alpha_2^h+\beta_2^h)+2\alpha_3^{p,h}+\alpha_4^{p,h}+\frac{1}{2}\alpha_{3,\rm EW}^{p,h} -\frac{1}{2}\alpha_{4,\rm EW}^{p,h}+\beta_3^{p,h}+\beta_{3,\rm EW}^{p,h}\Big]X_h^{(\overline{B}a_1,f_1^q)}+\sqrt{2}\left[\alpha_3^{p,h}-\frac{1}{2}\alpha_{4,\rm EW}^{p,h}\right]X_h^{(\overline{B}a_1,f_1^s)} +\Big[\delta_{pu}\,(\alpha_1^h+\beta_2^h)+\alpha_4^{p,h}+\alpha_{4,\rm EW}^{p,h}+\beta_3^{p,h}+\beta_{3,\rm EW}^{p,h}\Big]X_h^{(\overline{B}f_1^q,a_1)}\Bigg\}, \tag{B15}$$

$$-2\,\mathcal{A}^h_{\bar{B}^0\to a_1^0f_1} = \frac{G_F}{\sqrt{2}}\sum_{p=u,c}\lambda_p^{(d)}\Bigg\{\Big[\delta_{pu}\,(\alpha_2^h-\beta_1^h)+2\alpha_3^{p,h}+\alpha_4^{p,h}+\frac{1}{2}\alpha_{3,\rm EW}^{p,h}-\frac{1}{2}\alpha_{4,\rm EW}^{p,h} +\beta_3^{p,h}-\frac{1}{2}\beta_{3,\rm EW}^{p,h}-\frac{3}{2}\beta_{4,\rm EW}^{p,h}\Big]X_h^{(\overline{B}f_1^q,a_1)}+\sqrt{2}\left[\alpha_3^{p,h}-\frac{1}{2}\alpha_{4,\rm EW}^{p,h}\right]X_h^{(\overline{B}a_1,f_1^s)} +\Big[\delta_{pu}\,(-\alpha_2^h-\beta_1^h)+\alpha_4^{p,h}-\frac{3}{2}\alpha_{3,\rm EW}^{p,h}-\frac{1}{2}\alpha_{4,\rm EW}^{p,h} +\beta_3^{p,h}-\frac{1}{2}\beta_{3,\rm EW}^{p,h}-\frac{3}{2}\beta_{4,\rm EW}^{p,h}\Big]X_h^{(\overline{B}a_1,f_1^q)}\Bigg\}, \tag{B16}$$

for $\overline{B}\to a_1(a_1,f_1)$, and

$$\sqrt{2}\mathcal{A}^h_{B^-\to K_1^-a_1^0} = \frac{G_F}{\sqrt{2}}\sum_{p=u,c}\lambda_p^{(s)}\Bigg\{\Big[\delta_{pu}(\alpha_1^h+\beta_2^h)+\alpha_4^{p,h}+\alpha_{4,\rm EW}^{p,h}+\beta_3^{p,h}+\beta_{3,\rm EW}^{p,h}\Big]X_h^{(\overline{B}a_1,\overline{K}_1)} +\Big[\delta_{pu}\alpha_2^h+\frac{3}{2}\alpha_{3,\rm EW}^{p,h}\Big]X_h^{(\overline{BK}_1,a_1)}\Bigg\}, \tag{B17}$$

$$\mathcal{A}^h_{B^-\to\overline{K}_1^0a_1^-} = \frac{G_F}{\sqrt{2}}\sum_{p=u,c}\lambda_p^{(s)}\Big[\delta_{pu}\beta_2^h+\alpha_4^{p,h}-\frac{1}{2}\alpha_{4,\rm EW}^{p,h}+\beta_3^{p,h}+\beta_{3,\rm EW}^{p,h}\Big]X_h^{(\overline{B}a_1,\overline{K}_1)}, \tag{B18}$$

$$\mathcal{A}^h_{\overline{B}^0\to K_1^- a_1^+} = \frac{G_F}{\sqrt{2}}\sum_{p=u,c}\lambda_p^{(s)}\Big[\delta_{pu}\alpha_1^h+\alpha_4^{p,h}+\alpha_{4,\rm EW}^{p,h}+\beta_3^{p,h}-\frac{1}{2}\beta_{3,\rm EW}^{p,h}\Big]X_h^{(\overline{B}a_1,\overline{K}_1)}, \tag{B19}$$

$$\begin{aligned}\sqrt{2}\mathcal{A}^h_{\overline{B}^0\to\overline{K}_1^0 a_1^0} &= \frac{G_F}{\sqrt{2}}\sum_{p=u,c}\lambda_p^{(s)}\Big\{\Big[-\alpha_4^{p,h}+\frac{1}{2}\alpha_{4,\rm EW}^{p,h}-\beta_3^{p,h}+\frac{1}{2}\beta_{3,\rm EW}^{p,h}\Big]X_h^{(\overline{B}a_1,\overline{K}_1)}\\ &+\Big[\delta_{pu}\alpha_2^h+\frac{3}{2}\alpha_{3,\rm EW}^{p,h}\Big]X_h^{(\overline{B}\overline{K}_1,a_1)}\Big\},\end{aligned} \tag{B20}$$

$$\begin{aligned}\sqrt{2}\mathcal{A}^h_{B^-\to K_1^- f_1} &= \frac{G_F}{\sqrt{2}}\sum_{p=u,c}\lambda_p^{(s)}\Big\{\Big[\delta_{pu}(\alpha_1^h+\beta_2^h)+\alpha_4^{p,h}+\alpha_{4,\rm EW}^{p,h}+\beta_3^{p,h}+\beta_{3,\rm EW}^{p,h}\Big]X_h^{(\overline{B}f_1^q,\overline{K}_1)}\\ &+\Big[\delta_{pu}\alpha_2^h+2\alpha_3^{p,h}+\frac{1}{2}\alpha_{3,\rm EW}^{p,h}\Big]X_h^{(\overline{B}\overline{K}_1,f_1^q)}+\sqrt{2}\Big[\delta_{pu}\beta_2^h+\alpha_3^{p,h}+\alpha_4^{p,h}-\frac{1}{2}\alpha_{3,\rm EW}^{p,h}\\ &-\frac{1}{2}\alpha_{4,\rm EW}^{p,h}+\beta_3^{p,h}+\beta_{3,\rm EW}^{p,h}\Big]X_h^{(\overline{B}\overline{K}_1,f_1^s)}\Big\},\end{aligned} \tag{B21}$$

$$\begin{aligned}\sqrt{2}\mathcal{A}^h_{\overline{B}^0\to\overline{K}_1^0 f_1} &= \frac{G_F}{\sqrt{2}}\sum_{p=u,c}\lambda_p^{(s)}\Big\{\Big[\alpha_4^{p,h}-\frac{1}{2}\alpha_{4,\rm EW}^{p,h}+\beta_3^{p,h}-\frac{1}{2}\beta_{3,\rm EW}^{p,h}\Big]X_h^{(\overline{B}f_1^q,\overline{K}_1)}\\ &+\Big[\delta_{pu}\alpha_2^h+2\alpha_3^{p,h}+\frac{1}{2}\alpha_{3,\rm EW}^{p,h}\Big]X_h^{(\overline{B}\overline{K}_1,f_1^q)}+\sqrt{2}\Big[\alpha_3^{p,h}+\alpha_4^{p,h}-\frac{1}{2}\alpha_{3,\rm EW}^{p,h}\\ &-\frac{1}{2}\alpha_{4,\rm EW}^{p,h}+\beta_3^{p,h}-\frac{1}{2}\beta_{3,\rm EW}^{p,h}\Big]X_h^{(\overline{B}\overline{K}_1,f_1^s)}\Big\},\end{aligned} \tag{B22}$$

for $\overline{B}\to\overline{K}_1(a_1,f_1)$, where $\lambda_p^{(d)}\equiv V_{pb}V_{pd}^*$, $\lambda_p^{(s)}\equiv V_{pb}V_{ps}^*$, and the helicity-dependent factorizable amplitudes $X_h^{(\bar{B}M_1,M_2)}$ are defined in Eq. (3.16). The decay amplitudes for $\overline{B}\to b_1(\omega,\phi)$ are obtained from $\overline{B}\to a_1(\omega,\phi)$ by replacing $a_1\to b_1$. Likewise, the expressions for $\overline{B}\to h_1(\omega,\phi)$ decay amplitudes are obtained by setting $(f_1\omega\to h_1\omega)$ and $(f_1\phi\to h_1\phi)$.

APPENDIX C: AN EXAMPLE OF THE ANNIHILATION AMPLITUDES IN $B\to AV$ DECAYS

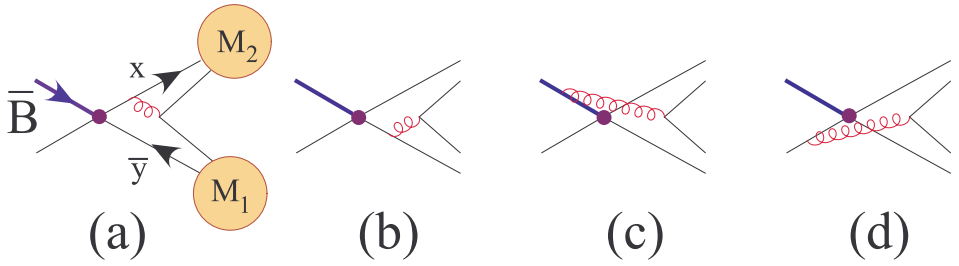

FIG. 2: Annihilation contributions to the decay amplitude of $\bar{B}\to AV$, where (a) and (b) correspond to A_n^f, (c) and (d) give rise to A_n^i.

In this appendix we show an explicit evaluation of the annihilation diagrams in Fig. 2 with $(M_1,M_2)=(A,V)$ and the conventions $p_V^\mu\simeq En_-^\mu$ and $p_A^\mu\simeq En_+^\mu$. The longitudinal annihilation amplitudes of Figs. 2(a) and 2(b) read

$$A_{\rm Fig.2(a)} = -2\langle 0|\bar{d}(1-\gamma_5)b|\bar{B}\rangle (ig_s)^2 \frac{{\rm Tr}(t^a t^a)}{N_c^2}$$
$$\times \int_0^1 \int_0^1 dxdy(-1){\rm Tr}\Big[M_\parallel^A(y)\gamma_\delta M_\parallel^V(x)\gamma^\delta\gamma_\alpha(1+\gamma_5)\Big]\frac{i(-i)(k+p_V)^\alpha}{(k+p_V)^2(\bar{x}p_V+k)^2}\Big|_{k=yp_A}, \quad \text{(C1)}$$

and

$$A_{\rm Fig.2(b)} = -2\langle 0|\bar{d}(1-\gamma_5)b|\bar{B}\rangle (ig_s)^2 \frac{{\rm Tr}(t^a t^a)}{N_c^2}$$
$$\times \int_0^1 \int_0^1 dxdy(-1){\rm Tr}\Big[-\gamma_\alpha\gamma_\delta M_\parallel^A(y)\gamma^\delta M_\parallel^V(x)(1+\gamma_5)\Big]\frac{i(-i)(p_A+\bar{k})^\alpha}{(\bar{k}+yp_A)^2(\bar{k}+p_A)^2}\Big|_{\bar{k}=\bar{x}p_V}. \quad \text{(C2)}$$

The longitudinal projectors $M_\parallel^A$ and $M_\parallel^V$ are given in Eqs. (2.28) and (2.30), respectively.

Case 1: Taking

$$M_\parallel^V(x) \to -i\frac{f_V}{4}\frac{m_V(\epsilon_V^*\cdot n_+)}{2}\not{n}_-\,\Phi_\parallel^V(x),$$
$$M_\parallel^A(y) \to -i\frac{f_A^\perp m_A}{4}\frac{m_A(\epsilon_A^*\cdot n_-)}{2E}\left\{\frac{i}{2}\,\sigma_{\mu\nu}\gamma_5\, n_+^\mu n_-^\nu\, h_\parallel^{(t)}(y) - \gamma_5\frac{h_\parallel^{\prime(p)}(y)}{2}\right\}, \quad \text{(C3)}$$

and using

$$\langle 0|\bar{d}(1-\gamma_5)b|\bar{B}\rangle = i\frac{f_B m_B^2}{m_b+m_d}, \quad \text{(C4)}$$

we have

$$A^{(1)}_{\rm Figs.2(a)+2(b)} = -i\pi\alpha_s\frac{C_F}{N_c}\, f_B f_V f_A\, r_\chi^A \int_0^1\int_0^1 dxdy\,\Phi_\parallel^V(x)\left(\frac{h_\parallel^{(t)}(y)+\frac{1}{2}h_\parallel^{\prime(p)}(y)}{\bar{x}y} - \frac{h_\parallel^{\prime(p)}(y)}{\bar{x}^2 y}\right)$$
$$= -2i\pi\alpha_s\frac{C_F}{N_c}\, f_B f_V f_A\, r_\chi^A \int_0^1\int_0^1 dxdy\,\Phi_\parallel^V(x)\Phi_a(y)\left(\frac{1}{\bar{x}^2 y}\right), \quad \text{(C5)}$$

where use of $\int_0^1 dy\,\Phi_a(y) = 0$ has been made.

Case 2: Taking

$$M_\parallel^V(x) \to -i\frac{f_V^\perp m_V}{4}\frac{m_V(\epsilon^*\cdot n_+)}{2E}\left\{-\frac{i}{2}\,\sigma_{\mu\nu}\, n_-^\mu n_+^\nu\, h_\parallel^{(t)}(x) + \frac{h_\parallel^{\prime(s)}(x)}{2}\right\}, \quad \text{(C6)}$$

and

$$M_\parallel^A(y) \to -i\frac{f_A}{4}\frac{m_V(\epsilon^*\cdot n_-)}{2}\not{n}_+\gamma_5\,\Phi_\parallel^A(y), \quad \text{(C7)}$$

we obtain

$$A^{(2)}_{\rm Figs.2(a)+2(b)} = -i\pi\alpha_s\frac{C_F}{N_c}\, f_B f_V f_A\, r_\chi^V \int_0^1\int_0^1 dxdy\,\Phi_\parallel^A(y)\left(\frac{h_\parallel^{(t)}(x)+\frac{1}{2}h_\parallel^{\prime(s)}(x)}{\bar{x}^2 y} + \frac{h_\parallel^{\prime(s)}(x)}{\bar{x}y^2}\right)$$
$$= 2i\pi\alpha_s\frac{C_F}{N_c}\, f_B f_V f_A\, r_\chi^V \int_0^1\int_0^1 dxdy\,\Phi_\parallel^A(y)\Phi_v(x)\left(\frac{1}{\bar{x}y^2}\right). \quad \text{(C8)}$$

Case 3: If

$$M_\parallel^V(x) \to -i\frac{f_V}{4}\frac{m_V(\epsilon^*\cdot n_+)}{2}\not{n}_-\,\Phi_\parallel^V(x), \quad \text{(C9)}$$

and

$$M_\parallel^A(y) \;\to\; -i\frac{f_A^\perp m_A}{4}\,\frac{m_A(\epsilon^*\cdot n_-)}{2E}\left\{iE\,y\bar{y}\Phi_a(y)\sigma_{\mu\nu}\gamma_5 n_+^\mu\,\frac{\partial}{\partial k_{\perp\nu}}\right\}, \tag{C10}$$

then we have

$$A^{(3)}_{\rm Figs.2(a)+2(b)} \;=\; -2i\pi\alpha_s\frac{C_F}{N_c}\,f_B f_V f_A\,r_\chi^A\int_0^1\int_0^1 dxdy\,\Phi_\parallel^V(x)\Phi_a(y)\left(\frac{1}{\bar{x}y}\right). \tag{C11}$$

Case 4: For

$$M_\parallel^V(x) \;\to\; i\frac{f_V^\perp m_V}{4}\,\frac{m_V(\epsilon^*\cdot n_+)}{2E}\left\{iE\,x\bar{x}\Phi_v(x)\;\sigma_{\mu\nu}n_-^\mu\,\frac{\partial}{\partial k_{\perp\nu}}\right\}, \tag{C12}$$

and

$$M_\parallel^A(x) \;\to\; -i\frac{f_A}{4}\,\frac{m_A(\epsilon^*\cdot n_+)}{2}\;\not{n}_-\gamma_5\,\Phi_\parallel^A(x), \tag{C13}$$

we have

$$A^{(4)}_{\rm Fig.2(b)} \;=\; 2i\pi\alpha_s\frac{C_F}{N_c}\,f_B f_V f_A\,r_\chi^V\int_0^1\int_0^1 dxdy\,\Phi_\parallel^A(y)\Phi_v(x)\left(\frac{1}{\bar{x}y}\right). \tag{C14}$$

Finally, we obtain

$$A^{(1)+(3)}_{\rm Eqs.\ 2(a)+2(b)} \;=\; -2i\pi\alpha_s\frac{C_F}{N_c}\,f_B f_V f_A\,r_\chi^A\int_0^1\int_0^1 dxdy\,\Phi_a(y)\Phi_\parallel^V(x)\left(\frac{1+\bar{x}}{\bar{x}^2y}\right), \tag{C15}$$

and

$$A^{(2)+(4)}_{\rm Eqs.\ 2(a)+2(b)} \;=\; 2i\pi\alpha_s\frac{C_F}{N_c}\,f_B f_V f_A\,r_\chi^V\int_0^1\int_0^1 dxdy\,\Phi_\parallel^A(y)\Phi_v(x)\left(\frac{1+y}{\bar{x}y^2}\right). \tag{C16}$$

We are led to

$$\begin{aligned} A_3^{f,\,0}(A\;V) \;=\; \pi\alpha_s\int_0^1 dx\,dy\,\Bigg\{ & -r_\chi^A\,\Phi_a(x)\Phi_\parallel^V(y)\,\frac{2(1+\bar{y})}{x\bar{y}^2} \\ & +r_\chi^V\,\Phi_\parallel^A(x)\,\Phi_v(y)\frac{2(1+x)}{x^2\bar{y}}\Bigg\}. \end{aligned} \tag{C17}$$

Likewise,

$$\begin{aligned} A_3^{f,\,0}(V_1V_2) \;=\; \pi\alpha_s\int_0^1 dx\,dy\,\Bigg\{ & r_\chi^{V_1}\,\Phi_{v1}(x)\Phi_\parallel^{V_2}(y)\,\frac{2(1+\bar{y})}{x\bar{y}^2} \\ & -r_\chi^{V_2}\,\Phi_\parallel^{V_1}(x)\,\Phi_{v2}(y)\frac{2(1+x)}{x^2\bar{y}}\Bigg\}, \\ A_3^{f,\,0}(A_1A_2) \;=\; \pi\alpha_s\int_0^1 dx\,dy\,\Bigg\{ & -r_\chi^{A_1}\,\Phi_{a1}(x)\Phi_\parallel^{A_2}(y)\,\frac{2(1+\bar{y})}{x\bar{y}^2} \qquad\qquad (C18) \\ & -r_\chi^{A_2}\,\Phi_\parallel^{A_1}(x)\,\Phi_{a2}(y)\frac{2(1+x)}{x^2\bar{y}}\Bigg\}, \qquad\qquad (C19) \\ A_3^{f,\,0}(V\;A) \;=\; \pi\alpha_s\int_0^1 dx\,dy\,\Bigg\{ & r_\chi^V\,\Phi_v(x)\Phi_\parallel^A(y)\,\frac{2(1+\bar{y})}{x\bar{y}^2} \\ & +r_\chi^A\,\Phi_\parallel^V(x)\,\Phi_a(y)\frac{2(1+x)}{x^2\bar{y}}\Bigg\}. \qquad\qquad (C20) \end{aligned}$$

This implies

$$\begin{aligned} C^{VV} = C^{VA} = -C^{AV} = -C^{AA} = 1, \\ D^{VV} = D^{AA} = -D^{AV} = -D^{VA} = 1, \end{aligned} \tag{C21}$$

which lead to the third line of Eq. (3.39).

APPENDIX D: EXPLICIT EXPRESSIONS OF ANNIHILATION AMPLITUDES

The general expressions of the helicity-dependent annihilation amplitudes are given in Eqs. (3.29)-(3.38). They can be further simplified by considering the asymptotic distribution amplitudes for $\Phi_V, \Phi_v, \Phi_\parallel^{^3P_1}, \Phi_a^{^1P_1}$ and the leading contributions to $\Phi_\parallel^{^1P_1}, \Phi_a^{^3P_1}$:

$$\begin{aligned}
&\Phi_\parallel^V(u) = 6u\bar{u}, \qquad \Phi_\parallel^{^3P_1}(u) = 6u\bar{u}, \qquad \Phi_\parallel^{^1P_1}(u) = 18\, a_1^{\parallel,\,^1P_1} u\bar{u}(2u-1),\\
&\Phi_v(u) = 3(2u-1), \quad \Phi_a^{^3P_1}(u) = 3\, a_1^{\perp,\,^3P_1}(6u^2-6u+1), \qquad \Phi_a^{^1P_1}(u) = 3(2u-1),\\
&\Phi_\perp^V(u) = 6u\bar{u}, \qquad \Phi_\perp^{^3P_1}(u) = 18\, a_1^{\perp,\,^3P_1} u\bar{u}(2u-1), \qquad \Phi_\perp^{^1P_1}(u) = 6u\bar{u},\\
&\Phi_+^M = \int_u^1 dv \frac{\Phi_\parallel^M(v)}{v}, \qquad \Phi_-^M = \int_0^u dv \frac{\Phi_\parallel^M(v)}{\bar{v}}.
\end{aligned} \tag{D1}$$

We find

$$A_3^{f,\,0}(V_1\, V_2) \approx -18\pi\alpha_s\left(r_\chi^{V_1} + r_\chi^{V_2}\right)(X_A^0 - 2)(2X_A^0 - 1), \tag{D2}$$

$$A_3^{f,\,-}(V_1\, V_2) \approx -18\pi\alpha_s\left(\frac{m_{V_2}}{m_{V_1}} r_\chi^{V_1} + \frac{m_{V_1}}{m_{V_2}} r_\chi^{V_2}\right)(2X_A^- - 3)(X_A^- - 1), \tag{D3}$$

$$A_3^{f,\,0}(V\,^3P_1) \;\approx\; 18\pi\alpha_s(2X_A^0 - 1)\left[a_1^{\perp,\,^3P_1} r_\chi^{^3P_1}(X_A^0 - 3) - r_\chi^V(X_A^0 - 2)\right], \tag{D4}$$

$$\begin{aligned}
A_3^{f,\,-}(V\,^3P_1) \;\approx\; & -18\pi\alpha_s(2X_A^- - 3)\\
& \times\left[\frac{m_{^3P_1}}{m_V} r_\chi^V(X_A^- - 1) - 3a_1^{\perp,\,^3P_1}\frac{m_V}{m_{^3P_1}}\, r_\chi^{^3P_1}(X_A^- - 2)\right],
\end{aligned} \tag{D5}$$

$$A_3^{f,\,0}(V\,^1P_1) \;\approx\; 18\pi\alpha_s(X_A^0 - 2)\left[r_\chi^{^1P_1}(2X_A^0 - 1) - a_1^{\parallel,\,^1P_1}\, r_\chi^V(6X_A^0 - 11)\right], \tag{D6}$$

$$\begin{aligned}
A_3^{f,\,-}(V\,^1P_1) \;\approx\; & -18\pi\alpha_s(X_A^- - 1)\\
& \times\left[-\frac{m_V}{m_{^1P_1}} r_\chi^{^1P_1}(2X_A^- - 3) + a_1^{\parallel,\,^1P_1}\frac{m_{^1P_1}}{m_V} r_\chi^V\left(2X_A^- - \frac{17}{3}\right)\right],
\end{aligned} \tag{D7}$$

$$A_3^{f,\,0}(^3P_1\, V) \;=\; -A_3^{f,\,0}(V\,^3P_1), \qquad A_3^{f,\,-}(^3P_1\, V) = -A_3^{f,\,-}(V\,^3P_1), \tag{D8}$$

$$A_3^{f,\,0}(^1P_1\, V) \;=\; A_3^{f,\,0}(V\,^1P_1), \qquad A_3^{f,\,-}(^1P_1\, V) = A_3^{f,\,-}(V\,^1P_1), \tag{D9}$$

$$\begin{aligned}
A_3^{f,\,0}([^3P_1]_1\;[^3P_1]_2) \;\approx\; & -18\pi\alpha_s(2X_A^0 - 1)(X_A^0 - 3)\\
& \times\left[a_1^{\perp,\,[^3P_1]_1} r_\chi^{[^3P_1]_1} + a_1^{\perp,\,[^3P_1]_2} r_\chi^{[^3P_1]_2}\right],
\end{aligned} \tag{D10}$$

$$\begin{aligned}
A_3^{f,\,-}([^3P_1]_1\;[^3P_1]_2) \;\approx\; & -54\pi\alpha_s(2X_A^- - 3)(X_A^- - 2)\\
& \times\left[a_1^{\perp,[^3P_1]_1}\frac{m_{[^3P_1]_2}}{m_{[^3P_1]_1}}\; r_\chi^{[^3P_1]_1} + a_1^{\perp,[^3P_1]_2}\frac{m_{[^3P_1]_1}}{m_{[^3P_1]_2}}\; r_\chi^{[^3P_1]_2}\right],
\end{aligned} \tag{D11}$$

$$A_3^{f,\,0}([^1P_1]_1\ [^1P_1]_2) \approx 18\pi\alpha_s(X_A^0-2)(6X_A^0-11) \times\Big[a_1^{\parallel,\,[^1P_1]_2} r_\chi^{[^1P_1]_1} + a_1^{\parallel,\,[^1P_1]_1} r_\chi^{[^1P_1]_2}\Big], \tag{D12}$$

$$A_3^{f,\,-}([^1P_1]_1\ [^1P_1]_2) \approx 18\pi\alpha_s(X_A^- -1)\Big(2X_A^- -\frac{17}{3}\Big) \times\Big[a_1^{\parallel,[^1P_1]_2}\frac{m_{[^1P_1]_2}}{m_{[^1P_1]_1}}\ r_\chi^{[^1P_1]_1} + a_1^{\parallel,[^1P_1]_1}\frac{m_{[^1P_1]_1}}{m_{[^1P_1]_2}}\ r_\chi^{[^1P_1]_2}\Big], \tag{D13}$$

$$A_3^{f,\,0}(^3P_1\ ^1P_1) \approx -18\pi\alpha_s\Big[r_\chi^{^1P_1}(X_A^0-2)(2X_A^0-1) +a_1^{\parallel,\,^1P_1}\ a_1^{\perp,\,^3P_1} r_\chi^{^3P_1}(X_A^0-3)(6X_A^0-11)\Big], \tag{D14}$$

$$A_3^{f,\,-}(^3P_1\ ^1P_1) \approx -18\pi\alpha_s\Big[\frac{m_{^3P_1}}{m_{^1P_1}} r_\chi^{^1P_1}(X_A^- -1)(2X_A^- -3) +3a_1^{\parallel,\,^1P_1} a_1^{\perp,\,^3P_1}\frac{m_{^1P_1}}{m_{^3P_1}} r_\chi^{^3P_1}(X_A^- -2)\Big(2X_A^- -\frac{17}{3}\Big)\Big], \tag{D15}$$

$$A_3^{f,\,0}(^1P_1\ ^3P_1) \ =\ A_3^{f,\,0}(^3P_1\ ^1P_1), \qquad A_3^{f,\,-}(^1P_1\ ^3P_1) = -A_3^{f,\,-}(^3P_1\ ^1P_1), \tag{D16}$$

$$A_3^{i,\,0}(V_1\,V_2) \approx 18\pi\alpha_s\Big(-r_\chi^{V_1}+r_\chi^{V_2}\Big)\Big({X_A^0}^2 - 2X_A^0 + 4 - \frac{\pi^2}{3}\Big), \tag{D17}$$

$$A_3^{i,\,-}(V_1\,V_2) \approx -18\pi\alpha_s\Big(-\frac{m_{V_2}}{m_{V_1}} r_\chi^{V_1} + \frac{m_{V_1}}{m_{V_2}} r_\chi^{V_2}\Big)({X_A^-}^2 - 2X_A^- + 2), \tag{D18}$$

$$A_3^{i,\,0}(V\,^3P_1) \approx -18\pi\alpha_s\Big[a_1^{\perp,\,^3P_1} r_\chi^{^3P_1}\Big({X_A^0}^2 - 2X_A^0 - 6 + \frac{\pi^2}{3}\Big) +r_\chi^V\Big({X_A^0}^2 - 2X_A^0 + 4 - \frac{\pi^2}{3}\Big)\Big], \tag{D19}$$

$$A_3^{i,\,-}(V\,^3P_1) \approx 18\pi\alpha_s\Big[\frac{m_{^3P_1}}{m_V} r_\chi^V({X_A^-}^2 - 2X_A^- + 2) +3a_1^{\perp,\,^3P_1}\frac{m_V}{m_{^3P_1}}\ r_\chi^{^3P_1}({X_A^-}^2 - 4X_A^- + \frac{2\pi^2}{3})\Big], \tag{D20}$$

$$A_3^{i,\,0}(V\,^1P_1) \approx -18\pi\alpha_s\Big[r_\chi^{^1P_1}\Big({X_A^0}^2 - 2X_A^0 + 4 - \frac{\pi^2}{3}\Big) +3a_1^{\parallel,\,^1P_1}\ r_\chi^V({X_A^0}^2 - 4X_A^0 - 4 + \pi^2)\Big], \tag{D21}$$

$$A_3^{i,\,-}(V\,^1P_1) \approx 18\pi\alpha_s \times\Big[\frac{m_V}{m_{^1P_1}} r_\chi^{^1P_1}({X_A^-}^2 - 2X_A^- + 2) + a_1^{\parallel,\,^1P_1}\frac{m_{^1P_1}}{m_V} r_\chi^V({X_A^-}^2 - 2X_A^- - 2)\Big], \tag{D22}$$

$$A_3^{i,0}({}^3P_1\,V) \;\approx\; 18\pi\alpha_s\Big[a_1^{\perp,\,{}^3P_1} r_\chi^{{}^3P_1}\Big({X_A^0}^2 - 2X_A^0 - 6 + \frac{\pi^2}{3}\Big) - r_\chi^V\Big({X_A^0}^2 - 2X_A^0 + 4 - \frac{\pi^2}{3}\Big)\Big], \tag{D23}$$

$$A_3^{i,0}({}^1P_1\,V) \;\approx\; 18\pi\alpha_s\Big[-r_\chi^{{}^1P_1}\Big({X_A^0}^2 - 2X_A^0 + 4 - \frac{\pi^2}{3}\Big) + 3a_1^{\parallel,\,{}^1P_1}\, r_\chi^V({X_A^0}^2 - 4X_A^0 - 4 + \pi^2)\Big], \tag{D24}$$

$$A_3^{i,-}({}^3P_1\,V) = A_3^{i,-}(V\,{}^3P_1), \qquad A_3^{i,-}({}^1P_1\,V) = -A_3^{i,-}(V\,{}^1P_1), \tag{D25}$$

$$A_3^{i,0}([{}^3P_1]_1\;[{}^3P_1]_2) \;\approx\; 18\pi\alpha_s\Big({X_A^0}^2 - 2X_A^0 - 6 + \frac{\pi^2}{3}\Big) \times\Big[a_1^{\perp,\,[{}^3P_1]_1} r_\chi^{[{}^3P_1]_1} - a_1^{\perp,\,[{}^3P_1]_2} r_\chi^{[{}^3P_1]_2}\Big], \tag{D26}$$

$$A_3^{i,-}([{}^3P_1]_1\;[{}^3P_1]_2) \;\approx\; -54\pi\alpha_s\Big({X_A^-}^2 - 4X_A^- + \frac{2\pi^2}{3}\Big) \times\Big[-a_1^{\perp,[{}^3P_1]_1}\frac{m_{[{}^3P_1]_2}}{m_{[{}^3P_1]_1}}\; r_\chi^{[{}^3P_1]_1} + a_1^{\perp,[{}^3P_1]_2}\frac{m_{[{}^3P_1]_1}}{m_{[{}^3P_1]_2}}\; r_\chi^{[{}^3P_1]_2}\Big], \tag{D27}$$

$$A_3^{i,0}([{}^1P_1]_1\;[{}^1P_1]_2) \;\approx\; -54\pi\alpha_s({X_A^0}^2 - 4X_A^0 - 4 + \pi^2) \times\Big[a_1^{\parallel,\,[{}^1P_1]_2} r_\chi^{[{}^1P_1]_1} + a_1^{\parallel,\,[{}^1P_1]_1} r_\chi^{[{}^1P_1]_2}\Big], \tag{D28}$$

$$A_3^{i,-}([{}^1P_1]_1\;[{}^1P_1]_2) \;\approx\; -18\pi\alpha_s({X_A^-}^2 - 2X_A^- - 2) \times\Big[a_1^{\parallel,[{}^1P_1]_2}\frac{m_{[{}^1P_1]_2}}{m_{[{}^1P_1]_1}}\; r_\chi^{[{}^1P_1]_1} - a_1^{\parallel,[{}^1P_1]_1}\frac{m_{[{}^1P_1]_1}}{m_{[{}^1P_1]_2}}\; r_\chi^{[{}^1P_1]_2}\Big], \tag{D29}$$

$$A_3^{i,0}({}^3P_1\;{}^1P_1) \;\approx\; 18\pi\alpha_s\Big[r_\chi^{{}^1P_1}\Big({X_A^0}^2 - 2X_A^0 + 4 - \frac{\pi^2}{3}\Big) + 3a_1^{\parallel,\,{}^1P_1}\, a_1^{\perp,\,{}^3P_1} r_\chi^{{}^3P_1}\Big({X_A^0}^2 - 4X_A^0 + 40 - \frac{11\pi^2}{3}\Big)\Big], \tag{D30}$$

$$A_3^{i,-}({}^3P_1\;{}^1P_1) \;\approx\; -18\pi\alpha_s\Big[\frac{m_{{}^3P_1}}{m_{{}^1P_1}} r_\chi^{{}^1P_1}({X_A^-}^2 - 2X_A^- + 2) - 3a_1^{\parallel,\,{}^1P_1}\, a_1^{\perp,\,{}^3P_1}\frac{m_{{}^1P_1}}{m_{{}^3P_1}} r_\chi^{{}^3P_1}\Big({X_A^-}^2 - 4X_A^- + 24 - 2\pi^2\Big)\Big], \tag{D31}$$

$$A_3^{i,0}({}^1P_1\;{}^3P_1) \;\approx\; -18\pi\alpha_s\Big[r_\chi^{{}^1P_1}\Big({X_A^0}^2 - 2X_A^0 + 4 - \frac{\pi^2}{3}\Big) + 3a_1^{\parallel,\,{}^1P_1}\, a_1^{\perp,\,{}^3P_1} r_\chi^{{}^3P_1}\Big({X_A^0}^2 - 4X_A^0 + 40 - \frac{11\pi^2}{3}\Big)\Big], \tag{D32}$$

$$A_3^{i,-}({}^1P_1\ {}^3P_1) = A_3^{i,-}({}^3P_1\ {}^1P_1), \tag{D33}$$

$$A_{1,2}^{i,0}(V_1\,V_2) \approx 18\pi\alpha_s\left[\left(X_A^0 - 4 + \frac{\pi^2}{3}\right) + r_\chi^{V_1} r_\chi^{V_2}(X_A^0-2)^2\right] \tag{D34}$$

$$\begin{aligned} A_1^{i,0}(V\,{}^3P_1) \approx -A_2^{i,0}(V\,{}^3P_1) \;\approx\; 18\pi\alpha_s\Bigg[&\left(X_A^0 - 4 + \frac{\pi^2}{3}\right) \\ &- a_1^{\perp,\,{}^3P_1} r_\chi^V r_\chi^{{}^3P_1}({X_A^0}^2 - 5X_A^0 + 6)\Bigg], \end{aligned} \tag{D35}$$

$$A_1^{i,0}(V\,{}^1P_1) \;\approx\; 18\pi\alpha_s\left[a_1^{\parallel,\,{}^1P_1}(3X_A^0 + 4 - \pi^2) - r_\chi^V r_\chi^{{}^1P_1}(X_A^0-2)^2\right], \tag{D36}$$

$$A_2^{i,0}(V\,{}^1P_1) \;\approx\; 18\pi\alpha_s\left[-a_1^{\parallel,\,{}^1P_1}(X_A^0 + 29 - 3\pi^2) + r_\chi^V r_\chi^{{}^1P_1}(X_A^0-2)^2\right], \tag{D37}$$

$$A_1^{i,0}({}^1P_1\,V) \;\approx\; -18\pi\alpha_s\left[a_1^{\parallel,\,{}^1P_1}(X_A^0 + 29 - 3\pi^2) + r_\chi^V r_\chi^{{}^1P_1}(X_A^0-2)^2\right], \tag{D38}$$

$$A_2^{i,0}({}^1P_1\,V) \;\approx\; 18\pi\alpha_s\left[a_1^{\parallel,\,{}^1P_1}(3X_A^0 + 4 - \pi^2) + r_\chi^V r_\chi^{{}^1P_1}(X_A^0-2)^2\right], \tag{D39}$$

$$\begin{aligned} A_1^{i,0}({}^3P_1\,V) \approx -A_2^{i,0}({}^3P_1\,V) \;\approx\; 18\pi\alpha_s\Bigg[&\left(X_A^0 - 4 + \frac{\pi^2}{3}\right) \\ &+ a_1^{\perp,\,{}^3P_1} r_\chi^V r_\chi^{{}^3P_1}({X_A^0}^2 - 5X_A^0 + 6)\Bigg], \end{aligned} \tag{D40}$$

$$A_{1,2}^{i,0}({}^1P_1\,V) \;=\; A_{2,1}^{i,0}(V\,{}^1P_1), \tag{D41}$$

$$\begin{aligned} A_{1,2}^{i,0}([{}^3P_1]_1\ [{}^3P_1]_2) \;\approx\; 18\pi\alpha_s\Bigg[&\left(X_A^0 - 4 + \frac{\pi^2}{3}\right) \\ &- \;a_1^{\perp,\,[{}^3P_1]_1}\, a_1^{\perp,\,[{}^3P_1]_2}\, r_\chi^{[{}^3P_1]_1}\, r_\chi^{[{}^3P_1]_2}(X_A - 3)^2\Bigg], \end{aligned} \tag{D42}$$

$$\begin{aligned} A_{1,2}^{i,0}([{}^1P_1]_1\ [{}^1P_1]_2) \;\approx\; 18\pi\alpha_s\Big[&-3\, a_1^{\parallel,\,[{}^1P_1]_1}\, a_1^{\parallel,\,[{}^1P_1]_2}(X_A^0 - 71 + 7\pi^2) \\ &+ \;r_\chi^{[{}^1P_1]_1}\, r_\chi^{[{}^1P_1]_2}(X_A^0 - 2)^2\Big], \end{aligned} \tag{D43}$$

$$A_1^{i,0}({}^3P_1\ {}^1P_1) \approx 18\pi\alpha_s\left[a_1^{\parallel,{}^1P_1}\left(3X_A^0+4-\pi^2\right)\right.$$
$$\left.-a_1^{\perp,{}^3P_1}\, r_\chi^{{}^3P_1}\, r_\chi^{{}^1P_1}({X_A^0}^2-5X_A^0+6)\right], \tag{D44}$$
$$A_2^{i,0}({}^3P_1\ {}^1P_1) \approx 18\pi\alpha_s\left[a_1^{\parallel,{}^1P_1}\left(X_A^0+29-3\pi^2\right)\right.$$
$$\left.-a_1^{\perp,{}^3P_1}\, r_\chi^{{}^3P_1}\, r_\chi^{{}^1P_1}({X_A^0}^2-5X_A^0+6)\right], \tag{D45}$$

$$A_{1,2}^{i,0}({}^1P_1\ {}^3P_1) = -A_{2,1}^{i,0}({}^3P_1\ {}^1P_1), \tag{D46}$$

where the logarithmic divergences occurred in weak annihilation are described by the variable X_A

$$\int_0^1 \frac{du}{u} \to X_A, \qquad \int_0^1 \frac{\ln u}{u} \to -\frac{1}{2}X_A. \tag{D47}$$

Following [5], these variables are parameterized as

$$X_A = \ln\left(\frac{m_B}{\Lambda_h}\right)(1+\rho_A e^{i\phi_A}), \tag{D48}$$

with the unknown real parameters ρ_A and ϕ_A. For simplicity, we shall assume in practical calculations that X_A^h are helicity independent, $X_A^- = X_A^+ = X_A^0$.

Note that while our result for $A_3^{f-}(VV)$ is in agreement with Kagan [11] and Beneke et al. [13] (up to a sign), the relative sign between $r_\chi^{V_1}$ and $r_\chi^{V_2}$ in $A_3^{f,0}(VV)$ ($A_3^{i,0}(VV)$) is positive (negative) in our case [see Eqs. (D2) and (D17)] and in [11], but negative (positive) in [13].

APPENDIX E: EXPLICIT EXPRESSIONS FOR HARD SPECTATOR TERMS

Using the asymptotic distribution amplitudes, the explicit expressions of the integrals $\int_0^1 dudv$ appearing in the transverse hard spectator interaction amplitudes $H_i^-(M_1M_2)$ and $H_i^+(M_1M_2)$ [see Eqs. (3.9)-(3.13)] are summarized in Table XII.

TABLE XII: The explicit expressions for the integrals $\int_0^1 dudv\cdots$ appearing in the transverse hard spectator interaction amplitudes $H_i^-(M_1M_2)$ and $H_i^+(M_1M_2)$ described by Eqs. (3.9)-(3.13), where $\alpha \equiv a_1^{\perp,\,^3P_1}$, $\beta \equiv a_1^{\parallel,\,^1P_1}$ and the upper (lower) sign is for H_1^+ (H_5^+).

M_1M_2	$H_{1,5}^-$	H_6^-	$H_{1,5}^+$
$V_1\,V_2$	$9(X_H^- - 1)$	9	0
$V\,{}^3P_1$	$9(X_H^- - 1)$	0	0
${}^3P_1\,V$	$27\alpha(X_H^- - 2)$	9	0
$V\,{}^1P_1$	$-3\beta(X_H^- - 1)$	9	-3β
${}^1P_1\,V$	$9(X_H^- - 1)$	3β	$\mp 3\beta$
${}^3P_1\,{}^1P_1$	$-9\alpha\beta(X_H^- - 2)$	9	-3β
${}^1P_1\,{}^3P_1$	$9(X_H^- - 1)$	0	$\mp 3\beta$
${}^3P_1\,{}^3P_1$	$27\alpha(X_H^- - 2)$	0	0
${}^1P_1\,{}^1P_1$	$-3\beta(X_H^- - 1)$	3β	$-6\beta^2$

[1] H.Y. Cheng and K.C. Yang, Phys. Rev. D **76**, 114020 (2007).

[2] K.C. Yang, Phys. Rev. D **76**, 094002 (2007).

[3] B. Aubert *et al.* (BaBar Collaboration), Phys. Rev. Lett. **91**, 171802 (2003).

[4] K.F. Chen *et al.* (Belle Collaboration), Phys. Rev. Lett. **91**, 201801 (2003).

[5] M. Beneke, G. Buchalla, M. Neubert, and C.T. Sachrajda, Phys. Rev. Lett. **83**, 1914 (1999); Nucl. Phys. B **591**, 313 (2000); Nucl. Phys. B **606**, 245 (2001).

[6] M. Beneke and M. Neubert, Nucl. Phys. B **675**, 333 (2003).

[7] H. Y. Cheng and K.C. Yang, Phys. Lett. B **511**, 40 (2001).

[8] X.Q. Li, G.R. Lu, and Y.D. Yang, Phys. Rev. D **68**, 114015 (2003).

[9] Y.D. Yang, R.M. Wang, and G.R. Lu, Phys. Rev. D **72**, 015009 (2005).

[10] X.Q. Li, G.R. Lu, and Y.D. Yang, Phys. Rev. D **68**, 114015 (2003); W.J. Zou and Z.J. Xiao, Phys. Rev. D **72**, 094026 (2005); C. S. Huang, P. Ko, X. H. Wu and Y. D. Yang, Phys. Rev. D **73**, 034026 (2006).

[11] A. L. Kagan, Phys. Lett. B **601**, 151 (2004).

[12] P.K. Das and K.C. Yang, Phys. Rev. D **71**, 094002 (2005).

[13] M. Beneke, J. Rohrer, and D.S. Yang, Nucl. Phys. B **774**, 64 (2007).

[14] H. n. Li and S. Mishima, Phys. Rev. D **71**, 054025 (2005).

[15] C.W. Bauer, D. Pirjol, I.Z. Rothstein, and I.W. Stewart, Phys. Rev. D **70**, 054015 (2004).

[16] P. Colangelo, F. De Fazio and T. N. Pham, Phys. Lett. B **597**, 291 (2004).

[17] M. Ladisa, V. Laporta, G. Nardulli and P. Santorelli, Phys. Rev. D **70**, 114025 (2004).

[18] H.Y. Cheng, C.K. Chua, and A. Soni, Phys. Rev. D **71**, 014030 (2005).

[19] K.C. Yang, Phys. Rev. D **72**, 034009 (2005); D **72**, (E)059901 (2005).

[20] C.H. Chen, C.Q. Geng, Y.K. Hsiao, and Z.T. Wei, Phys. Rev. D **72**, 054011 (2005).

[21] G. Calderón, J.H. Muñoz, and C.E. Vera, Phys. Rev. D **76**, 094019 (2007).
[22] K.C. Yang, Nucl. Phys. B **776**, 187 (2007) [arXiv:0705.0692 [hep-ph]].
[23] H.Y. Cheng, Phys. Rev. D **67**, 094007 (2003).
[24] H. Hatanaka and K. C. Yang, Phys. Rev. D **77**, 094023 (2008) [arXiv:0804.3198 [hep-ph]].
[25] Particle Data Group, Y.M. Yao *et al.,* J. Phys. G **33**, 1 (2006).
[26] F.E. Close, *An Introduction to Quarks and Partons* (Academic Press Inc. Ltd., London, 1979).
[27] H.Y. Cheng, C.K. Chua, and C.W. Hwang, Phys. Rev. D **69**, 074025 (2004).
[28] K. C. Yang, Phys. Rev. D **78**, 034018 (2008) [arXiv:0807.1171 [hep-ph]].
[29] W. Wang, R.H. Li, and C.D. Lü, arXiv:0711.0432 [hep-ph].
[30] N. Isgur, D. Scora, B. Grinstein, and M.B. Wise, Phys. Rev. D **39**, 799 (1989).
[31] D. Scora and N. Isgur, Phys. Rev. D **52**, 2783 (1995).
[32] P. Ball and R. Zwicky, Phys. Rev. D **71**, 014029 (2005) [arXiv:hep-ph/0412079].
[33] P. Ball, V. M. Braun and A. Lenz, JHEP **0605**, 004 (2006) [arXiv:hep-ph/0603063].
[34] M. Beneke and T. Feldmann, Nucl. Phys. B **592**, 3 (2001).
[35] S. T'Jampens, BaBar Note No.515 (2000).
[36] CKMfitter Group, J. Charles *et al.,* Eur. Phys. J. C **41**, 1 (2005) and updated results from http://ckmfitter.in2p3.fr; UTfit Collaboration, M. Bona *et al.,* JHEP **0507**, 028 (2005) and updated results from http://utfit.roma1.infn.it.
[37] Z. Z. Xing, H. Zhang and S. Zhou, Phys. Rev. D **77**, 113016 (2008).
[38] X. Q. Li and Y. D. Yang, Phys. Rev. D **73**, 114027 (2006) [arXiv:hep-ph/0602224].
[39] P. Ball, G.W. Jones, and R. Zwicky, Phys. Rev. D **75**, 054004 (2007).
[40] P. Ball and G.W. Jones, JHEP **0703**, 069 (2007).
[41] N. de Groot, W. N. Cottingham and I. B. Whittingham, Phys. Rev. D **68**, 113005 (2003).
[42] M. Beneke, J. Rohrer, and D.S. Yang, Phys. Rev. Lett. **96**, 141801 (2006).
[43] H.-n. Li, Phys. Lett. B **622**, 63 (2005).
[44] C. S. Kim and Y. D. Yang, hep-ph/0412364; C. H. Chen and C. Q. Geng, Phys. Rev. D **71**, 115004 (2005); S. Baek, A. Datta, P. Hamel, O. F. Hernandez and D. London, Phys. Rev. D **72**, 094008 (2005); Q. Chang, X. Q. Li and Y. D. Yang, JHEP **0706**, 038 (2007).
[45] W. S. Hou and M. Nagashima, hep-ph/0408007; A. K. Giri and R. Mohanta, arXiv:hep-ph/0412107; E. Alvarez, L. N. Epele, D. G. Dumm and A. Szynkman, Phys. Rev. D **70**, 115014 (2004); W. J. Zou and Z. J. Xiao, Phys. Rev. D **72**, 094026 (2005).
[46] H. Hatanaka and K. C. Yang, Phys. Rev. D **77**, 035013 (2008) (arXiv:0711.3086 [hep-ph]).
[47] B. Aubert *et al.* (BaBar Collaboration), Phys. Rev. Lett. **97**, 201801 (2006).
[48] J. Zhang *et al.* (Belle Collaboration), Phys. Rev. Lett. **95**, 141801 (2005).
[49] B. Aubert *et al.* (BaBar Collaboration), Phys. Rev. Lett. **99**, 201802 (2007).
[50] B. Aubert *et al.* (BaBar Collaboration), Phys. Rev. Lett. **98**, 051801 (2007).
[51] K.F. Chen *et al.* (Belle Collaboration), Phys. Rev. Lett. **94**, 221804 (2005).
[52] B. Aubert *et al.* (BaBar Collaboration), Phys. Rev. Lett. **97**, 261801 (2006).
[53] J. Zhang *et al.* (Belle Collaboration), Phys. Rev. Lett. **91**, 221801 (2003).
[54] B. Aubert *et al.* (BaBar Collaboration), arXiv:0708.1630 [hep-ex].
[55] C.C. Chiang (for Belle Collaboration), talk presented at Les Rencontres de Physique de la

Vallee d'Aoste, February 24 - March 1, 2008.
[56] B. Aubert *et al.* (BaBar Collaboration), Phys. Rev. D **76**, 052007 (2007).
[57] A. Somov *et al.* (Belle Collaboration), Phys. Rev. Lett. **96**, 171801 (2006).
[58] B. Aubert *et al.* (BaBar Collaboration), Phys. Rev. D **74**, 051102 (2006).
[59] B. Aubert *et al.* (BaBar Collaboration), Phys. Rev. Lett. **100**, 081801 (2008).
[60] R. Godang *et al.* (CLEO Collaboration), Phys. Rev. Lett. **88**, 021802 (2002).
[61] K. Abe *et al.* (Belle Collaboration), arXiv:0707.2462 [hep-ex].
[62] Heavy Flavor Averaging Group, E. Barberio *et al.,* arXiv:0704.3575 [hep-ex] and online update at http://www.slac.stanford.edu/xorg/hfag.
[63] A. Datta, D. London, J. Matias, M. Nagashima and A. Szynkman, Phys. Rev. D **76**, 034015 (2007); arXiv:0802.0897 [hep-ph].
[64] B. Aubert *et al.* (BaBar Collaboration), Phys. Rev. D **74**, 031104 (2006).